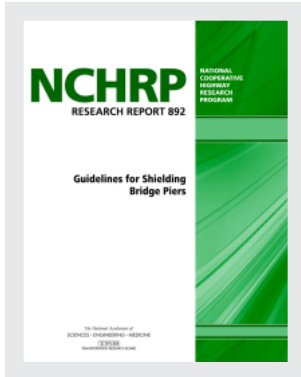


This PDF is available at <http://nap.edu/25313>

SHARE    



Guidelines for Shielding Bridge Piers (2018)

DETAILS

116 pages | 8.5 x 11 | PAPERBACK
ISBN 978-0-309-47995-0 | DOI 10.17226/25313

CONTRIBUTORS

Malcolm H. Ray, Christine E. Carrigan, and Chuck A. Plaxico; National Cooperative Highway Research Program; Transportation Research Board; National Academies of Sciences, Engineering, and Medicine

SUGGESTED CITATION

National Academies of Sciences, Engineering, and Medicine 2018. *Guidelines for Shielding Bridge Piers*. Washington, DC: The National Academies Press. <https://doi.org/10.17226/25313>.

GET THIS BOOK

FIND RELATED TITLES

Visit the National Academies Press at NAP.edu and login or register to get:

- Access to free PDF downloads of thousands of scientific reports
- 10% off the price of print titles
- Email or social media notifications of new titles related to your interests
- Special offers and discounts



Distribution, posting, or copying of this PDF is strictly prohibited without written permission of the National Academies Press. (Request Permission) Unless otherwise indicated, all materials in this PDF are copyrighted by the National Academy of Sciences.

Copyright © National Academy of Sciences. All rights reserved.

NATIONAL COOPERATIVE HIGHWAY RESEARCH PROGRAM

NCHRP RESEARCH REPORT 892

**Guidelines for Shielding
Bridge Piers**

Malcolm H. Ray
Christine E. Carrigan
Chuck A. Plaxico
ROADSAFE LLC
Canton, ME

Subscriber Categories

Bridges and Other Structures • Design

Research sponsored by the American Association of State Highway and Transportation Officials
in cooperation with the Federal Highway Administration

The National Academies of
SCIENCES • ENGINEERING • MEDICINE



TRANSPORTATION RESEARCH BOARD

2018

NATIONAL COOPERATIVE HIGHWAY RESEARCH PROGRAM

Systematic, well-designed research is the most effective way to solve many problems facing highway administrators and engineers. Often, highway problems are of local interest and can best be studied by highway departments individually or in cooperation with their state universities and others. However, the accelerating growth of highway transportation results in increasingly complex problems of wide interest to highway authorities. These problems are best studied through a coordinated program of cooperative research.

Recognizing this need, the leadership of the American Association of State Highway and Transportation Officials (AASHTO) in 1962 initiated an objective national highway research program using modern scientific techniques—the National Cooperative Highway Research Program (NCHRP). NCHRP is supported on a continuing basis by funds from participating member states of AASHTO and receives the full cooperation and support of the Federal Highway Administration, United States Department of Transportation.

The Transportation Research Board (TRB) of the National Academies of Sciences, Engineering, and Medicine was requested by AASHTO to administer the research program because of TRB's recognized objectivity and understanding of modern research practices. TRB is uniquely suited for this purpose for many reasons: TRB maintains an extensive committee structure from which authorities on any highway transportation subject may be drawn; TRB possesses avenues of communications and cooperation with federal, state, and local governmental agencies, universities, and industry; TRB's relationship to the National Academies is an insurance of objectivity; and TRB maintains a full-time staff of specialists in highway transportation matters to bring the findings of research directly to those in a position to use them.

The program is developed on the basis of research needs identified by chief administrators and other staff of the highway and transportation departments, by committees of AASHTO, and by the Federal Highway Administration. Topics of the highest merit are selected by the AASHTO Special Committee on Research and Innovation (R&I), and each year R&I's recommendations are proposed to the AASHTO Board of Directors and the National Academies. Research projects to address these topics are defined by NCHRP, and qualified research agencies are selected from submitted proposals. Administration and surveillance of research contracts are the responsibilities of the National Academies and TRB.

The needs for highway research are many, and NCHRP can make significant contributions to solving highway transportation problems of mutual concern to many responsible groups. The program, however, is intended to complement, rather than to substitute for or duplicate, other highway research programs.

NCHRP RESEARCH REPORT 892

Project 12-90
ISSN 2572-3766 (Print)
ISSN 2572-3774 (Online)
ISBN 978-0-309-47995-0
Library of Congress Control Number 2018960155

© 2018 National Academy of Sciences. All rights reserved.

COPYRIGHT INFORMATION

Authors herein are responsible for the authenticity of their materials and for obtaining written permissions from publishers or persons who own the copyright to any previously published or copyrighted material used herein.

Cooperative Research Programs (CRP) grants permission to reproduce material in this publication for classroom and not-for-profit purposes. Permission is given with the understanding that none of the material will be used to imply TRB, AASHTO, FAA, FHWA, FMCSA, FRA, FTA, Office of the Assistant Secretary for Research and Technology, PHMSA, or TDC endorsement of a particular product, method, or practice. It is expected that those reproducing the material in this document for educational and not-for-profit uses will give appropriate acknowledgment of the source of any reprinted or reproduced material. For other uses of the material, request permission from CRP.

NOTICE

The research report was reviewed by the technical panel and accepted for publication according to procedures established and overseen by the Transportation Research Board and approved by the National Academies of Sciences, Engineering, and Medicine.

The opinions and conclusions expressed or implied in this report are those of the researchers who performed the research and are not necessarily those of the Transportation Research Board; the National Academies of Sciences, Engineering, and Medicine; or the program sponsors.

The Transportation Research Board; the National Academies of Sciences, Engineering, and Medicine; and the sponsors of the National Cooperative Highway Research Program do not endorse products or manufacturers. Trade or manufacturers' names appear herein solely because they are considered essential to the object of the report.

Published research reports of the

NATIONAL COOPERATIVE HIGHWAY RESEARCH PROGRAM

are available from

Transportation Research Board
Business Office
500 Fifth Street, NW
Washington, DC 20001

and can be ordered through the Internet by going to

<http://www.national-academies.org>

and then searching for TRB

Printed in the United States of America

The National Academies of **SCIENCES • ENGINEERING • MEDICINE**

The **National Academy of Sciences** was established in 1863 by an Act of Congress, signed by President Lincoln, as a private, non-governmental institution to advise the nation on issues related to science and technology. Members are elected by their peers for outstanding contributions to research. Dr. Marcia McNutt is president.

The **National Academy of Engineering** was established in 1964 under the charter of the National Academy of Sciences to bring the practices of engineering to advising the nation. Members are elected by their peers for extraordinary contributions to engineering. Dr. C. D. Mote, Jr., is president.

The **National Academy of Medicine** (formerly the Institute of Medicine) was established in 1970 under the charter of the National Academy of Sciences to advise the nation on medical and health issues. Members are elected by their peers for distinguished contributions to medicine and health. Dr. Victor J. Dzau is president.

The three Academies work together as the **National Academies of Sciences, Engineering, and Medicine** to provide independent, objective analysis and advice to the nation and conduct other activities to solve complex problems and inform public policy decisions. The National Academies also encourage education and research, recognize outstanding contributions to knowledge, and increase public understanding in matters of science, engineering, and medicine.

Learn more about the National Academies of Sciences, Engineering, and Medicine at www.national-academies.org.

The **Transportation Research Board** is one of seven major programs of the National Academies of Sciences, Engineering, and Medicine. The mission of the Transportation Research Board is to increase the benefits that transportation contributes to society by providing leadership in transportation innovation and progress through research and information exchange, conducted within a setting that is objective, interdisciplinary, and multimodal. The Board's varied committees, task forces, and panels annually engage about 7,000 engineers, scientists, and other transportation researchers and practitioners from the public and private sectors and academia, all of whom contribute their expertise in the public interest. The program is supported by state transportation departments, federal agencies including the component administrations of the U.S. Department of Transportation, and other organizations and individuals interested in the development of transportation.

Learn more about the Transportation Research Board at www.TRB.org.

COOPERATIVE RESEARCH PROGRAMS

CRP STAFF FOR NCHRP RESEARCH REPORT 892

Christopher J. Hedges, *Director, Cooperative Research Programs*
Lori L. Sundstrom, *Deputy Director, Cooperative Research Programs*
Waseem Dekelbab, *Senior Program Officer*
Megan Chamberlain, *Senior Program Assistant*
Eileen P. Delaney, *Director of Publications*
Natalie Barnes, *Associate Director of Publications*
Doug English, *Senior Editor*

NCHRP PROJECT 12-90 PANEL Field of Design—Area of Bridges

Keith R. Fulton, *Wyoming DOT, Cheyenne, WY (Chair)*
Arielle L.G. Ehrlich, *Minnesota DOT, Oakdale, MN*
Paul B. Fossier, *Louisiana DOTD (retired), Baton Rouge, LA*
Don J. Grippe, *Trinity Highway Products, LLC, Olympia, WA*
Rodney D. Lacy, *Burns & McDonell, Kansas City, MO*
Peter C. McCowan, *New York State DOT, Albany, NY*
Richard G. Sarchet, *DiExSys, LLC, Fruita, CO*
William P. Longstreet, *FHWA Liaison*
Stephen F. Maher, *TRB Liaison*

F O R E W O R D

By **Waseem Dekelbab**

Staff Officer

Transportation Research Board

This report provides proposed load and resistance factor design (LRFD) bridge design pier protection specifications and proposed occupant protection guidelines to update the *AASHTO LRFD Bridge Design Specifications* and *AASHTO Roadside Design Guide*, respectively. The proposed specifications and guidelines are based on a comprehensive analytical program that used a risk-based approach for investigating the effects of a heavy truck hitting one or more bridge columns or piers. The report also includes four examples that illustrate the use of the proposed specifications and guidelines for shielding bridge piers. The material in this report will be of immediate interest to bridge and safety engineers.

Bridge piers are generally close to the travelway to minimize bridge lengths. As a consequence, barriers are normally placed around piers to reduce the potential of vehicle crashes damaging the piers. However, the design and placement of the barriers may not have taken into consideration the possibility that vehicles, particularly large trucks, might still impact the pier. The *AASHTO LRFD Bridge Design Specifications* require piers that were not designed to withstand large impact loads to be protected by a 54-in.-high structurally independent barrier if the barrier is within 10 ft of the pier. If the barrier is more than 10 ft from the pier, a 42-in.-high barrier is specified. There is no consideration of the risk of a high-speed impact, traffic volume, truck usage, operating speeds, facility type, or other factors in the bridge specifications. In addition, while the bridge specifications specify a barrier height, they do not specify a barrier length in advance of the pier. The specifications also do not specify the transition that might be appropriate.

The requirement for protecting bridge piers from truck impacts may have a significant effect on passenger car safety. Rigid barriers are generally believed to cause more injuries and fatalities than semi-rigid and flexible barrier systems. In addition, having barriers close to the travelway may significantly increase the number of passenger car crashes. Crashes involving heavy trucks hitting bridge piers are rare, and a barrier designed to protect a bridge pier from impact may create a new hazard especially for passenger vehicles. In the aggregate, the personal cost in lives and property to drivers who hit barriers is more than the cost of repairing bridge piers damaged by heavy trucks.

Further, there are operational concerns associated with the use of tall concrete barriers near the travelway. Concrete barriers are much more likely to produce deep snow drifts than are other more open barriers. Drifting is also a problem during severe sand storms. The increase in snow and sand drifting will increase operational costs since highway agencies are forced to make more frequent passes with snow-plowing equipment to keep highways open. Also, tall concrete barriers placed near interchanges can adversely affect sight distances.

In fact, most of the issues mentioned here result from following a one-size-fits-all approach in protecting bridge piers without quantifying when and how the bridge pier protection should be applied. States are spending significant funding on projects that may not provide the expected benefits, particularly on lower traffic volume or functional class bridges.

Under NCHRP Project 12-90, Roadsafe LLC was asked to develop (1) risk-based guidelines that quantify when bridge piers should be investigated for vehicular collision forces per *AASHTO LRFD Bridge Design Specifications* or be shielded with a longitudinal barrier, considering as a minimum: site condition, traffic, bridge design configurations, geometry of the roadway section passing beneath a bridge, operation characteristics, and benefit/cost and (2) guidelines for barrier selection, length-of-need, and placement for shielding bridge piers and protecting the traveling public.

A number of deliverables, provided as appendices, are not published in this report but are available at the NCHRP Project 12-90 web page (<https://apps.trb.org/cmsfeed/TRBNetProjectDisplay.asp?ProjectID=3170>):

- Appendix A: Proposed LRFD Bridge Design Pier Protection Specifications
- Appendix B: Proposed RDG Occupant Protection Guidelines
- Appendix C: Survey of Practice
- Appendix D: Lateral Impact Loads on Pier Columns
- Appendix E: Nominal Resistance to Lateral Impact Loads on Pier Columns
- Appendix F: Heavy-Vehicle Traffic Mix and Properties

CONTENTS

1	Chapter 1	Introduction
3	Chapter 2	Literature Review
3	2.1	Guidelines and Specifications
6	2.2	Capacity, Design, and Impact Loading of Bridge Piers
9	2.3	Barrier Crash-Testing Guidelines
10	2.4	Crash Data Studies
10	2.5	Exemplar Bridge Pier Crashes
18	2.6	Bridge Pier Risk Analysis
20	2.7	Benefit/Cost Versus Risk
21	2.8	Summary
22	Chapter 3	Discussion of Proposed LRFD Bridge Design Pier Protection Guidelines
22	3.1	Defining Bridge Collapse
29	3.2	Design Choice Is Structural Resistance
37	3.3	Design Choice Is Shielding with a Barrier
54	Chapter 4	Discussion of Proposed RDG Occupant Protection Guidelines
54	4.1	Proposed RDG Guidelines
54	4.2	Proposed Preliminary RDG Guideline Development
68	Chapter 5	Verification and Validation
68	5.1	Example #1: Two-Lane Undivided Rural Collector with Three Pier Columns
74	5.2	Example #2: Four-Lane Divided Rural Primary with Three Pier Columns on a Skew in the Median
78	5.3	Example #3: Six-Lane Divided Urban Primary with Four Pier Columns Offset in the Median
83	5.4	Example #4: Six-Lane Rural Primary with Two Columns in a Gore of an Off-Ramp
90	Chapter 6	Implementation Strategy
90	6.1	Products
90	6.2	Audience
90	6.3	Impediments
90	6.4	Leadership
90	6.5	Activities
91	6.6	Criteria

92	Chapter 7 Conclusion
93	References
97	Appendices

Note: Photographs, figures, and tables in this report may have been converted from color to grayscale for printing. The electronic version of the report (posted on the web at www.trb.org) retains the color versions.

CHAPTER 1

Introduction

While large trucks do not often strike the pier systems of highway bridges, the potential for catastrophic bridge collapse in such collisions makes the design of pier systems and their protection important considerations for highway and bridge designers. Avoiding bridge collapse is of paramount importance because, in addition to the immediate safety consequences, a bridge collapse causes major disruptions to the operation of transportation networks, and repairs are both costly and time consuming. Although the potential for a heavy truck impact with one or more bridge columns or piers to produce catastrophic collapse of a bridge has always been a concern for bridge engineers, only within the last 25 years have the AASHTO bridge design specifications begun requiring that piers either be designed to withstand heavy truck impacts or that high-capacity barriers be installed to prevent heavy trucks from striking the columns. The *AASHTO Roadside Design Guide* (RDG) has generally considered bridge piers the same way as any other roadside fixed objects. This report documents the development of risk-based guidelines for shielding bridge piers and presents the proposed guidance for consideration in the *AASHTO LRFD Bridge Design Specifications* and the RDG. These approaches proposed for the *LRFD Bridge Design Specifications* and RDG have been coordinated in this research. These guidelines satisfy the objectives of this project, which include:

1. Developing risk-based guidelines that quantify when bridge piers should be investigated for vehicular collision forces per the *AASHTO LRFD Bridge Design Specifications* or be shielded with a longitudinal barrier, considering, at a minimum, site conditions, traffic, bridge design configurations, geometry of the roadway section passing beneath a bridge, operations characteristics, and benefit/cost, and
2. Developing guidelines for barrier selection, length-of-need, and placement for shielding bridge piers and protecting the traveling public.

A highway bridge is composed of two major structures: the superstructure, which supports the live load of moving vehicles and pedestrians, and the substructure, which supports the vertical loads of the superstructure. The substructure components that transfer the live and dead load from the superstructure to the foundation along the span of the bridge constitute the pier system. There are four general types of bridge piers typically used in highway bridges that cross other highways. There are a variety of other more complex pier designs that are more commonly used in waterway crossings, but since the focus of this project is pier protection from heavy vehicle and passenger vehicle traffic, this research is concerned only with bridges that cross over roadways.

The term “bridge pier,” as used in this report, is taken to mean the vertical support system of a bridge between the abutments. The Ohio Department of Transportation (ODOT) uses a fairly typical method for categorizing bridge piers, as shown in the following and in Figure 1 [ODOT 2014]. This terminology has been adopted herein:

- Pier walls are “a full height, rectangular pier extending from the ground line or streambed up to the bearing elevation. The pier extends the full width of the bridge, supporting all beam members” [ODOT 2014].
- Tee-type or hammerhead piers are “rectangular stem capped with a cantilever-type cap” [ODOT 2014].
- Cap (or bent) and column are a type of pier system that has a series of two or more rectangular or circular columns capped with a bent.
- Multiple-column piers use rectangular or circular columns that directly support bridge girders without a cap or bent.

Within these broad categories are numerous possible configurations. Configurations like the pier system shown in Figure 2 are particularly vulnerable to vehicle impacts since the pier is unshielded and contains only a single pier column such that the pier system is not redundant.



(a) Pier wall



(b) Cap and column



(c) Tee or hammerhead



(d) Multicolumn with no cap

Figure 1. ODOT bridge pier types [after ODOT 2014].



Figure 2. Single-column bridge pier system [ODOT 2014].

CHAPTER 2

Literature Review

2.1 Guidelines and Specifications**2.1.1 AASHTO Bridge Design Specifications**

The guidance for protecting structures from vehicle impacts has evolved over the past several decades, as reflected in AASHTO bridge design specifications. The first edition of the *AASHTO LRFD Specifications for the Design of Highway Bridges* was published in 1994. The AASHTO Subcommittee on Bridges and Structures (SCOBS) voted to stop maintaining the *Standard Specifications for Highway Bridges* in 1999. Subsequently, AASHTO and the FHWA set a transition date of October 1, 2007, after which all new bridges were to be designed using the *LRFD Bridge Design Specifications*. Furthermore, by October 2006, the LRFD Specifications were to be used exclusively in the design of all replacement structures [FHWA 2013].

Twenty years of excerpts related to bridge piers from the Standard Specifications and LRFD Specifications are summarized in the following. These excerpts show the evolution of the design and protection of piers for vehicle impacts. (The 1992 and 2002 quotations are from the Standard Specifications, while the 1998 and 2007 are from the LRFD Specifications.)

1992 Standard Specifications: “When the possibility of collision exists from highway or river traffic, an appropriate risk analysis should be made to determine the degree of impact resistance to be provided and/or the appropriate protection system” [AASHTO 1992].

1994 LRFD: “Abutments and piers located within a distance of 30.0 ft to the edge of roadway, or within a distance of 50.0 ft to the centerline of a railway track, shall be designed for an equivalent static force of 400 kip” [AASHTO 1994b].

1998 LRFD: “Pier columns or walls for grade separation structures should be located in conformance with the clear zone concept as contained in Chapter 3 of the *AASHTO Roadside Design Guide*, 1996. Where the practical limits

of structure cost, type of structure, volume and design speed of through traffic, span arrangement, skew, and terrain make conformance for the *Roadside Design Guide* impractical, the pier or wall should be protected by the use of guardrail or other barrier devices. The guardrail or other device should, if practical, be independently supported, with its roadway face at least 600 mm from the face of pier or abutment, unless a rigid barrier is provided. The face of the guardrail or other device should be at least 600 mm outside the normal shoulder line” [AASHTO 1998].

2002 Standard Specifications: “Pier columns or walls for grade separation structures shall generally be located a minimum of 30 ft from the edges of the through-traffic lanes. Where the practical limits of structure cost, type of structure, volume and design speed of through traffic, span arrangement, skew, and terrain make the 30-ft offset impractical, the pier or wall may be placed closer than 30 ft and protected by the use of guardrail or other barrier devices. The guardrail or other device shall be independently supported with the roadway face at least 2 ft 0 in. from the face of pier or abutment.”

The face of the guardrail or other device should be at least 2 ft 0 in. outside the normal shoulder line” [AASHTO 2002b].

2007 and 2010 LRFD: “Unless protected . . . abutments and piers located within a distance of 30.0 ft. to the edge of roadway . . . shall be designed for an equivalent static force of 400 kips, which is assumed to act in any direction in a horizontal plane, at a distance of 4.0 ft. above ground” [AASHTO 2007]. “In order to qualify for this exemption, such barrier shall be structurally and geometrically capable of surviving the crash test for Test Level 5. . . .” [AASHTO 2010].

Although a risk analysis was suggested in 1992, the nature of that analysis was not specified. The suggestion to perform

a risk analysis, however, implies that quantifying the likelihood of a catastrophic impact is a key consideration, and that consideration would certainly depend on the particular site conditions.

The 400-kip design load that first appeared in 2007 was based on information from crash tests with an 80,000-lb tractor-trailer truck and load estimates for train impacts developed by Hirsch [Hirsch 1985]. The specification also suggested that the pier should be at least 10 ft behind a shielding barrier to prevent vehicles that lean or roll over the barrier from striking the pier. The fifth edition of the *AASHTO LRFD Bridge Design Specifications* retained this same language [AASHTO 2010].

In March 2012, the sixth edition of the *AASHTO LRFD Bridge Design Specifications* made significant changes to the design for impact resistance of bridge piers, largely based on work by Buth et al. at the Texas Transportation Institute [AASHTO 2012, Buth 2010, Buth 2011]. For example, the design load for pier components was increased from 400 kips to an equivalent static force of 600 kips, and the height of load application was increased from 4 to 5 ft above the ground. The impact load was changed from any direction in the fourth and fifth editions to between 0 and 15 degrees from the traveled way in the sixth edition. The requirement to design for train collisions was removed in the sixth edition, although at least one state (Massachusetts) was considering keeping the train provision. The pier protection provisions of the eighth edition [AASHTO 2017] have not been changed since the sixth edition.

Prior to the sixth edition, designing for structural resistance to collision forces was not necessary if a MASH Test Level 5 (TL-5) barrier was provided to protect the pier system. A new provision was added in the sixth edition that allows for the consideration of the annual probability of the bridge pier to be hit by a heavy vehicle [AASHTO 2012]. When the annual frequency of a heavy-vehicle collision is less than 0.0001, the pier does not need to be protected or designed for impact resistance. The sixth edition includes a method for assessing the annual frequency of a heavy-vehicle impact (i.e., AF_{HBP}) [AASHTO 2012]:

$$AF_{\text{HBP}} = 2 \cdot \text{ADTT} \cdot P_{\text{HBP}} \cdot 365$$

where

AF_{HBP} = Annual frequency for a bridge pier to be struck by a heavy vehicle;

ADTT = One-way volume of trucks per day, where the percent trucks is assumed to be 10% of the total average daily traffic (ADT); and

P_{HBP} = Probability of a bridge pier being struck by a heavy vehicle.

A table is provided in the commentary of Article 3.6.5 that contains values of the P_{HBP} listed by ADTT and highway type. The probability P_{HBP} is constant for each type of highway. For example, the P_{HBP} for a divided tangent highway is 1.09E-09, and for an undivided tangent highway is 3.457E-09. The tabulated values do not account for the position of the pier with respect to the roadway or characteristics of the highway that are expected to affect the frequency of encroachments (e.g., grade, horizontal curvature, lane width), so the method does not adequately account for traffic conditions and site layout. In addition, the sixth edition method does not account for any potential redundancy in the pier system or continuity of the bridge superstructure that would affect the likelihood of a bridge collapsing in a heavy-vehicle impact.

The changes in the design loading in the sixth edition (i.e., 400 kips at 4 ft above the ground from any direction to 600 kips at 5 ft above the ground at an impact angle of between 0 and 15 degrees) were based on two full-scale crash tests performed at the Texas Transportation Institute (TTI) that showed that an 80,000-lb tractor-trailer truck striking an instrumented bridge column at 0 degrees and 50 mph produced forces just slightly over 600 kips [Buth 2011, AASHTO 2012].

In the past 25 years, the LRFD Bridge Design Specifications have evolved toward a more probabilistic approach to dealing with heavy-vehicle impacts with bridge piers, but the current method does not consider many important characteristics that are likely to affect the frequency and severity of pier collisions. Traffic volume, traffic mix, and speed are important predictors, as are highway geometrics such as grade and horizontal curvature. The position of the pier components with respect to the travel lanes is also a notable feature that will affect the likelihood of a pier crash. While the probabilistic method in the sixth edition was a significant step forward, it still is relatively simple with respect to what is known about how and when vehicles encroach on the roadside and the effects of site, traffic, and roadway conditions on the likelihood of vehicles striking the piers.

2.1.2 The States

The states have adopted a variety of approaches to protecting bridge abutments and piers, as documented in state bridge design manuals. A survey of bridge design engineers included in Appendix C: Survey of Practice indicated that approximately 60% of the respondents used the *AASHTO LRFD Bridge Design Specifications* procedures of Article 3.6.5 for pier protection guidance, and 22% stated that they used something else (note: some of the respondents were international). The current guidelines, therefore, are widely if not universally applied. A review of several state guidelines provides some understanding of the different approaches

currently employed and the material referenced in the development of these approaches.

Chapter 13 of the *Wisconsin Department of Transportation Bridge Design Manual* states that piers shall resist loads applied directly to them, including vehicle impact loads [WIDOT 2013a]. For new structures, the *Wisconsin Department of Transportation Bridge Design Manual* states that it is preferred that the required clear zone be provided so that a barrier is not needed. W-beam barriers may only be used for passenger-vehicle occupant protection (i.e., not structure protection) and must be offset a minimum of 4.5 ft from the pier. Concrete safety shaped barriers may be used for passenger-vehicle occupant or structural pier protection and must be offset 4.5 ft from the pier. If used for structural pier protection, barriers must be a minimum of 54 in. tall; if used for vehicle occupant protection, barriers must be a minimum of 42 in. tall. A 51-in. vertical wall may be used for passenger-vehicle occupant protection with zero offset from the pier [WIDOT 2013b].

The Florida DOT design manual references the AASHTO LRFD specifications when a pier or bent is less than 30 ft from the edge of a traffic lane (i.e., within the clear zone). A TL-5 concrete safety shaped barrier is installed for a minimum of 50 ft parallel to the roadway upstream of the leading edge of the pier. The barrier must be 54 in. tall, and there must be a minimum offset of 2 ft from the face of the barrier to the face of pier column or pile [FDOT 2013a]. Allowances are made in FDOT index 410 when the minimum offset from the barrier to the pier cannot be achieved [FDOT 2013b].

The Ohio DOT design manual states that abutments and piers located within 30 ft of the edge of the roadway should be designed for impact from a vehicle through an equivalent static force of 400 kips applied at 4 ft above the ground, unless the pier system is redundant, protected by an embankment, or protected by a structurally independent TL-5 barrier. When the barrier is within 10 ft of the abutment or pier, the barrier must be 54 in. tall, while it may be 42 in. tall if the barrier is located more than 10 ft from the abutment or pier. Redundant pier systems should be shielded to protect passenger vehicle occupants when within the clear zone [ODOT 2013].

Minnesota distributed a memo in 2007 to bridge engineers explaining that MNDOT “considers Section 3.6.5 of the 2012 *LRFD Bridge Design Specifications* to be overly restrictive because . . .” consideration is not given to the probability of vehicle collision, the vehicle mix, or the travel speed [MNDOT 2007a, AASHTO 2012]. MNDOT exempted designers from protecting piers with a minimum of three columns, with design speeds less than or equal to 40 mph, or with design speeds over 40 mph but with ADTT of less than or equal to 250 per day. Designers were instructed to assume, when vehicle mix is not available, that ADTT is 10% of ADT. For non-exempt bridges, options were provided for

piers with one, two, or three or more columns. The options included (1) protecting the piers with a 54-in.-tall TL-5 barrier if the distance between the pier and the barrier is 10 ft or less, or a 42-in.-tall TL-5 barrier if the face of the pier is more than 10 ft from the barrier; (2) design the columns to have an area greater than 30 ft² and for a 400-kip collision load; or (3) provide a “crash strut” between pier columns, and design the strut for a 400-kip collision load. When the piers have three or more columns and are considered redundant, the preference of MNDOT was to provide a crash strut designed for a 400-kip collision load. The next preference was to design each column for impact or protect the piers with TL-5 barriers. Designers could have also verified that the structure would not collapse if any single column was removed [MNDOT 2007a; MNDOT 2013]. MNDOT updated this guidance in 2016 [MNDOT 2016].

The state of New Jersey designates the type of longitudinal barrier warranted based on median width. Provided that the median protection warrant is met, for median widths of up to 12 ft, a TL-4 concrete barrier may be used. A TL-4 concrete barrier is the preferred treatment for median widths ranging from 13 to 26 ft, but w-beam or thrie-beam barriers may also be used. For median widths above 26 ft, w-beam or thrie-beam barriers are preferred. When a guardrail is used and piers are present but vertical curbs are not, the minimum pier offset from the edge of roadway, regardless of shoulder width, should be 8.25 ft, with 4 ft from the back of the guardrail to the pier, or 4.75 ft if the rail is attached to the pier. When the TL-4 concrete barrier is warranted and piers are present, a minimum 3.25-ft offset from the face of the barrier to the face of the pier should be observed to prevent vehicles that roll over from striking the pier [NJDOT 2013].

Most DOTs treat bridge piers as they would any other fixed object (e.g., trees, utility poles, high-mast lighting) in the clear zone, stating that piers within the clear zone should be shielded by a barrier. Iowa DOT suggests that on high-speed, multilane facilities, piers located outside of the clear zone should also be considered for shielding [IDOT 2013]. South Dakota DOT provides specific barrier warrants for all fixed objects within the clear zone on roadways of various traffic volumes and speeds [SDDOT 2013]. The New York State DOT also uses the clear zone as the determining factor for installing longitudinal barriers but notes that the LRFD guidance for protecting piers from truck impacts was anticipated at the time the document was published [NYDOT 2013].

2.1.3 Summary

There is some variation among the states in addressing the need for protection of bridge piers, although much of the variation appears to be related to which edition of the

AASHTO LRFD Bridge Design Specifications has been used as the basis for the state bridge design standards. A few states provide different test-level barriers for different offsets of the piers and travel lanes. No specific guidance was found for the treatment of bridge piers on existing structures that cannot be designed for impact with heavy vehicles since they are already constructed.

All states consider bridge piers as hazardous fixed objects that require shielding when they are located within the clear zone and address such situations with the guidance contained in the *AASHTO RDG*. The *RDG* in this context is focused on protecting vehicle occupants from the piers. Less attention has been given to protecting the piers from impacts with vehicles, particularly heavy vehicles traveling at high speeds. Examples of efforts used to protect piers from vehicles are designing piers for direct impact forces and using offsetting barriers in front of piers to allow for vehicle roll rotation.

2.2 Capacity, Design, and Impact Loading of Bridge Piers

2.2.1 Pier Component Capacity

A bridge pier can be composed of a variety of structural components. The pier could be a simple wall that supports the bridge superstructure, or it could be a series of columns that support a pier cap in a bent arrangement that in turn supports the bridge superstructure. Failure or collapse of the pier system, then, is dependent on the strength of the component that is struck in an impact, the redundancy of the pier system, and the continuity of the superstructure. For example, a three-column bent system might be designed such that the pier is still stable even if one of the columns collapses.

On the other hand, a two-column bent system will generally not be stable if one column collapses.

Buth et al. calculated the shear capacity of a variety of circular pier columns using the fourth edition of the *LRFD Bridge Design Specifications*; these are summarized in Figure 3. Buth et al. also estimated the shear capacity of the pier columns for each of the 19 crashes summarized later in Table 2. Most of the real-world crashes investigated by Buth et al. involved circular, 30-in.-diameter columns with eight #9 longitudinal bars and #2 spiral stirrups with a 6-in. pitch using Grade 60 steel and 4 ksi concrete. These columns had an estimated unfactored lateral capacity of about 88 kips, far below the 400-kip recommendation of the fourth edition or the 600-kip recommendation of the sixth edition.

2.2.2 Pier Impact Loading

El-Tawil examined the impact forces experienced by two types of bridge columns commonly used in Florida: (1) a 54-in. square column with 24 #11 longitudinal bars and #5 stirrups spaced at 5 in., and (2) a 43-in.-diameter circular bridge column with 14 #11 longitudinal bars and #5 stirrups spaced at 5 in. [El-Tawil 2004]. Unfortunately, El-Tawil did not calculate the capacity as per the LRFD Specifications but rather compared the dynamic forces to the equivalent static force (ESF), which he defined as the static force that results in the same deformation of the structure at the point of load application. El-Tawil found that the computed equivalent static force varied linearly with the approach speed of pickup trucks and single-unit vehicles in a 2004 study of vehicle collisions with bridge piers using the nonlinear dynamic finite element code LSDYNA (see Figure 4). El-Tawil concluded

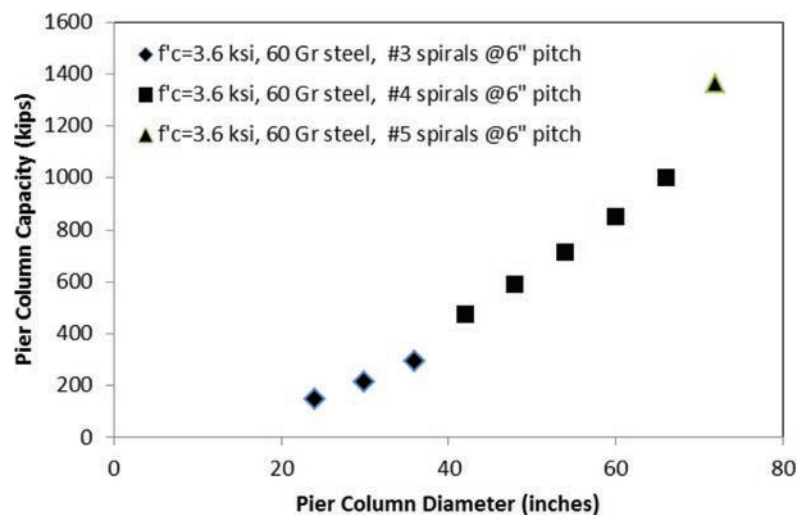


Figure 3. Pier column capacity as a function of column diameter [after Buth 2010].

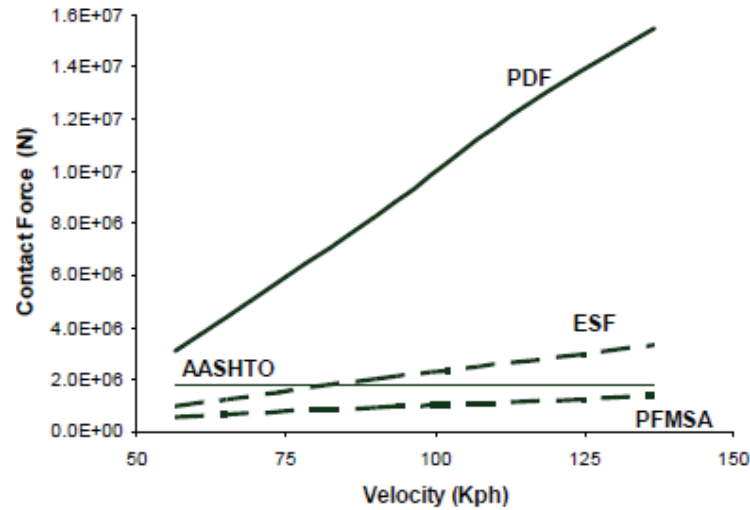


Figure 4. Forces from a 14-kN pickup truck striking a 54-in. square pier [El-Tawil 2004].

that the AASHTO vehicle collision provisions were not adequate because the peak dynamic force (PDF) is always more than the AASHTO collision provisions, and the ESF exceeds the AASHTO provisions between impact speeds of 75 and 100 km/h.

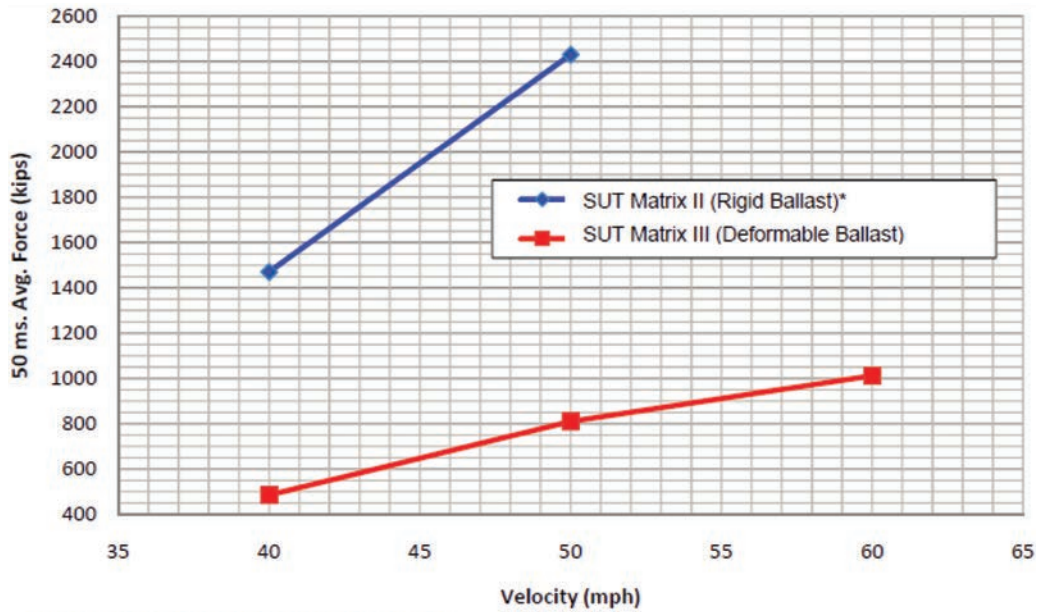
The PDF, however, is not a suitable force for comparison to the quasi-static force used in design since it is of extremely short duration. Most impact researchers prefer to use a force based on the 50-ms average acceleration (i.e., PFMSA in Figure 4 and El-Tawil) to estimate the quasi-static forces. The line labeled “AASHTO” in Figure 4 corresponds to the 400-kip recommendation of the fourth edition of the LRFD Specifications. El-Tawil concludes that the 400-kip design load is not adequate since the ESL exceeds this value at velocities over about 80 km/h (50 mph), but it is significant that the peak 50-ms average force remains below 1,800 kN (i.e., 400 kips) even at a velocity of 85 mph (135 km/h). The loads shown in Figure 4 are based on a standard pickup truck, so they suggest relatively little about the impact loads associated with heavier vehicles.

Buth et al. conducted finite element analyses of heavy-vehicle impacts with bridge piers, concluding that the “impact force experienced by the pier is much larger than that stated in the AASHTO LRFD vehicle collision provisions. The values of the imparted force from the engine block impact ranges from 480 kip to 600 kip, while the values of the imparted force from the ballast impact (albeit through the squeezing of the cab) ranges from 480 kip to more than 2,000 kip” [Buth 2010]. Buth et al. also concluded that the forces vary with speed, as shown in Figure 5 and Figure 6. Buth, like El-Tawil, concluded that the 400-kip design force was probably lower than some reasonably likely vehicle impact forces.

Buth’s analysis also shows that the forces are affected by the character of the ballast in the truck. Rigid ballast resulted in 50-ms-average forces that were on the order of three times higher than the forces observed when the ballast was deformable. This shows that the forces experienced by a bridge pier in an impact are not only determined by the mass, speed, and impact angle of the vehicle but are also dependent on the rigidity of the cargo and its ability to deform or shift in the trailer. A heavy-vehicle impact is not one impact but a sequence of impacts with the truck tractor, the trailer, and the trailer’s load.

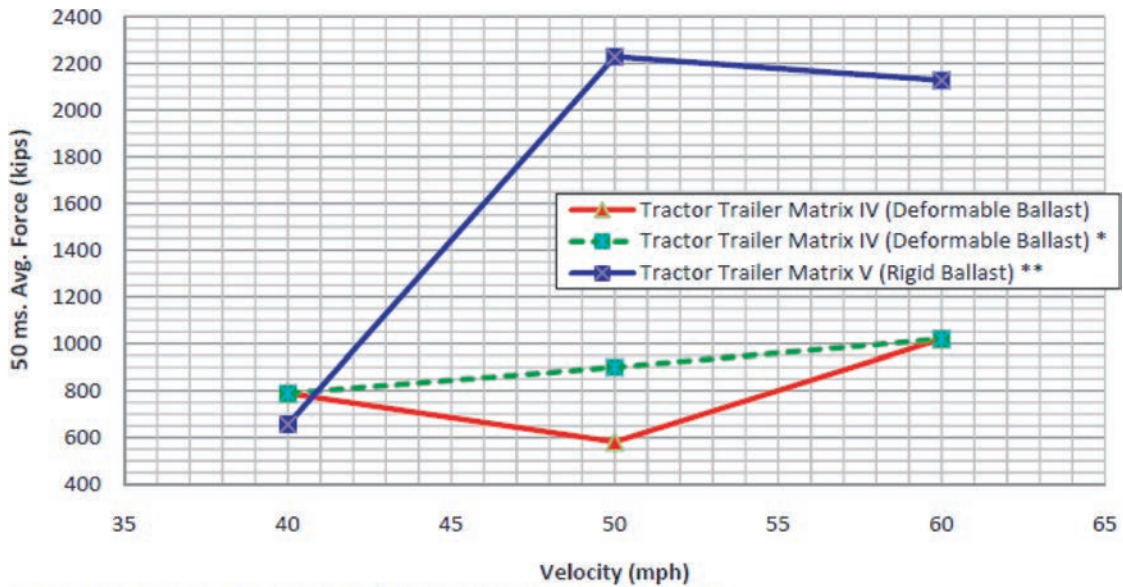
Buth et al. also were able to perform two full-scale crash tests using a 36-in.-diameter rigid instrumented bridge column [Buth 2011]. The instrumented column was struck by an 80,000-lb tractor-trailer truck traveling at 50 mph. In the first test, the truck struck the column with its centerline misaligned by about 2 ft, so a second test was run where the centerline of the truck corresponded with the center of the instrumented column. As shown in the force–time history for the second test in Figure 7, the force exceeded 600 kips for a very short time at two times early in the impact event. Based on these results, Buth et al. recommended that the 400-kip design load used in the fourth edition of the LRFD Specifications be increased, and this was the basis for the change in the sixth edition to the current 600-kip design lateral capacity [Buth 2011, AASHTO 2012]. Buth et al. also found that the height of load application in the crash test was at 5 ft, which formed the basis for the force application recommendation in the sixth edition.

Referring back to the unfactored design capacities shown in Figure 3, Buth’s results would indicate that typical circular columns smaller than 50 in. may fail when struck by an 80,000-lb tractor-trailer truck traveling at 50 mph. El-Tawil’s



* 60 mph case yielded unreliable results

Figure 5. Force velocity relationship for single-unit trucks (SUTs) [Buth 2010].



** The rigid ballast case became unstable beyond the data shown

* Projected force at 50 mph without slipping action between the engine and trailer structure as described previously

Figure 6. Force velocity relationship for tractor-trailer trucks [Buth 2010].

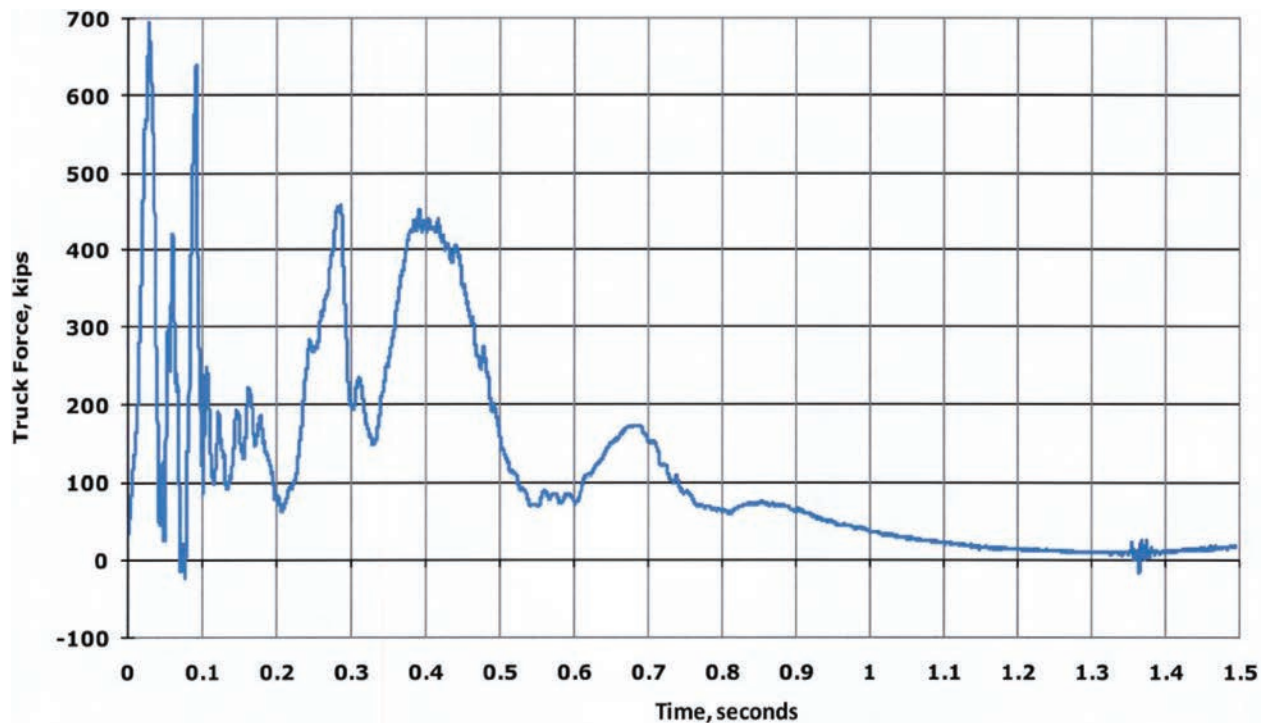


Figure 7. Impact force–time history for an 80,000-lb tractor-trailer truck striking an instrumented bridge column [Buth 2011].

work suggests that even pickup trucks might pose a risk of bridge column collapse if the pickup truck is traveling very fast (i.e., 85 mph or more) and strikes a circular column less than about 40 in. in diameter.

2.3 Barrier Crash-Testing Guidelines

In 1993, *NCHRP Report 350* was published [Ross 1993], superseding the previous crash-testing guidelines contained in *NCHRP Report 230* [Michie 1981]. One major change in *NCHRP Report 350* was that six different test levels for roadside hardware were added for longitudinal barriers. The intent was to provide test guidelines for developing a range of barriers that could be used in different situations. Test Levels 1 through 3 related to containment of passenger vehicles (e.g., small passenger cars and pickup trucks) and varied by impact speed, with increasing impact speeds defined for increasing test levels. The “basic” test level for longitudinal barriers was TL-3. The structural adequacy test for this test level consisted of a 2,000-kg (4,409-lb) pickup truck striking a barrier at 100 km/h (62 mph) and 25 degrees. At a minimum, all barriers on high-speed roadways on the National Highway System are required to meet at least TL-3 requirements.

Test Levels 4 through 6 also included consideration of passenger vehicles, but additionally incorporated consideration of assorted sizes of heavy vehicles. For example, many state

transportation departments require that bridge railings meet at least TL-4, and TL-5 median barriers are becoming more common, especially on routes with higher percentages of trucks in the vehicle mix.

The AASHTO LRFD Bridge Specifications require that TL-5 barriers be used when heavy-vehicle and railway static collision forces are not accounted for in the design of piers. A TL-5 test involves an 80,000-lb van-type tractor-trailer truck (TT) striking the barrier at a speed of 50 mph and an angle of 15 degrees. TL-6 uses the same impact conditions but incorporates an 80,000-lb tractor-tanker trailer. Barriers meeting these higher containment levels are sometimes used when site and traffic conditions warrant. Site-specific factors that might justify use of a high-containment barrier include a high percentage of heavy truck traffic or truck-related crashes or an unusually high risk associated with barrier penetration. Such barriers are necessarily taller, stronger, and more expensive to construct.

The higher test levels were intended for locations with a higher percentage of trucks and where the consequences of trucks penetrating or rolling over a barrier would be more severe. While *NCHRP Report 350* provided the testing suggestions, no specific guidance was provided about what field conditions would indicate the need for a higher test-level railing.

Since the publication of *NCHRP Report 350* in 1993, changes have occurred in vehicle fleet characteristics,

operating conditions, technology, and so forth. NCHRP Project 22-14(2), “Improvement of Procedures for the Safety-Performance Evaluation of Roadside Features,” was initiated to take the next step in the continued advancement and evolution of roadside safety testing and evaluation. The results of this research effort culminated in 2009 with the first edition of the AASHTO *Manual for Assessing Safety Hardware* (MASH) [AASHTO 2009].

MASH was updated in 2016, superseding *NCHRP Report 350* as the industry-standard crash test and evaluation procedure [AASHTO 2009]. MASH includes essentially the same test-level approach, with some modifications to the impact conditions for the higher-capacity longitudinal barrier test levels [AASHTO 2009; Ross 1993]. These modifications were primarily related to the size of the test vehicles. Impact conditions associated with the six test levels tend to be calibrated from impact conditions associated with TL-3 impact conditions. TL-3 is intended to represent barrier applications on typical high-speed, high-volume roadways. Impact speeds and angles for TL-3 have traditionally been selected to be equal to the 85th percentile impact speed and 85th percentile impact angle of run-off-road (ROR) crashes. Further, vehicle masses are normally selected to be equal to the 95th and 5th percentile values from the passenger car fleet. However, in recognition of the recent increase in the size of passenger vehicles and the expectation that then-high gasoline prices might push vehicle masses down, the light truck vehicle mass was reduced to the 90th percentile, and the small car mass was reduced to the 2nd percentile of the 2002 new vehicle fleet [AASHTO 2009].

Even with these adjustments, the severity of the TL-3 test condition was increased significantly. The weight and body style of the pickup truck test vehicle changed from a 4,409-lb, ¾-ton, standard-cab pickup to a 5,000-lb, ½-ton, four-door pickup. This change in vehicle mass of approximately 15% was deemed to produce an impact severity that was more severe than the *NCHRP Report 350* TL-4 single-unit truck test. The primary concern was that if TL-3 and TL-4 converged, highway agencies would lose one of the longitudinal barrier options. It was decided to increase the impact energy associated with TL-4 test 4–12 conditions by increasing the single-unit truck mass from 17,637 lb to 22,000 lb and the speed of the test vehicle from 50 mph to 56 mph. The 57% increase in impact severity for MASH TL-4 has resulted in a larger design impact load for TL-4, which will require stronger barriers and an increased overturning moment, leading to increased barrier height to prevent the single-unit truck (SUT) from rolling over the top of the barrier. The impact conditions for TL-5 and TL-6 involving the tractor-trailer and tractor-tanker trucks remained essentially unchanged from *NCHRP Report 350* to MASH.

2.4 Crash Data Studies

2.4.1 Crash Data

McDonald et al. analyzed the crash history at bridges over state-maintained, high-speed, multilane divided roadways in Iowa [McDonald 2009]. The crashes were categorized into bridge piers that were protected, partially protected, and unprotected. The severity of these crashes is summarized in Table 1, where crash severity is represented using the KABCO scale. In that scale, K is taken to equal a fatal crash, A is an incapacitating injury crash, B is a non-incapacitating injury crash, C is a possible injury crash, and O is a property-damage-only crash. As shown in Table 1, the highest crash severity percentage was found for unprotected piers, where more than 26% of the crashes involved severe or fatal injuries. The lowest crash severity was for fully protected piers, where 8.5% of the crashes involved severe or fatal injuries, indicating that shielding the piers resulted in a substantial reduction in crash severity. These results are also interesting because only unprotected piers in Iowa would be located outside the clear zone according to Iowa DOT policy.

Perhaps the most comprehensive review of bridge pier collapses was performed by Buth et al. [Buth 2010], who collected pier crash data while conducting a study for TXDOT and FHWA. Table 2 shows the distribution of heavy vehicles which struck the piers in the state of Texas during 1998 through 2001. Buth et al. did not separate piers by their protection characteristics, but the data from both Iowa and Texas clearly show that impacts with piers are very hazardous collisions for vehicle occupants. Buth’s data also includes several complete bridge-pier component failures as well as some bridge collapses due to heavy-vehicle impacts. The cases collected by Buth et al. will be discussed in more detail in Section 2.5.3.

2.5 Exemplar Bridge Pier Crashes

Although not useful from a statistical standpoint, bridge pier crashes reported in the media, investigated by the NTSB, or found in the literature help illustrate the outcome of these

Table 1. Crash history at Iowa bridges over high-speed, multilane divided roadways [after McDonald 2009].

Severity	Full Protection		Unprotected		Partial Protection	
	Crashes	Percent	Crashes	Percent	Crashes	Percent
K	1	0.5	2	10.5	2	1.3
A	17	8.0	3	15.7	15	9.7
B	23	10.8	4	21.1	21	13.6
C	40	18.9	2	10.5	36	23.4
O	131	61.8	8	42.1	80	51.9
Total	212	100	19	100	154	100

Table 2. Heavy-vehicle crashes with piers [after Buth 2010].

Severity	Undivided Tangent	Undivided Horizontal Curve	Divided Tangent	Divided Horizontal Curve	Total Events	Percent
K	0	0	5	1	6	6.2
A	0	0	8	9	17	17.5
B	1	0	6	17	24	24.7
C	0	0	16	9	25	25.7
O	1	0	11	13	25	25.7
Total	2	0	46	49	97	100

exceptional events and provide anecdotal information that is useful in developing an improved understanding of the factors that influence catastrophic failure and the development of the guidelines. Cases from a variety of sources will be examined in the following sections.

2.5.1 Crashes in the Media

2.5.1.1 Worthington, Minnesota

During the early morning of June 2, 2003, a truck crashed into a pier column of the bridge that carries Nobles County Road 9 over I-90 just west of Worthington, Minnesota, after a tire blowout caused the driver to lose control of the truck. The driver and his passenger suffered minor injuries. MNDOT officials already had the bridge closed for scheduled rehabilitation; however, the I-90 detour was in place for more than 2 weeks. Figure 8 shows that the truck was able to get behind the guardrail, indicating that the length of need of the guardrail protecting the pier may not have been adequate, allowing the truck to strike one of the pier columns. It appears that the guardrail was not struck during the crash and that the



Figure 8. Truck crash near Worthington, Minnesota [MNDOT 2003].

truck traveled behind the guardrail, striking the pier system [MNDOT 2003].

2.5.1.2 Litchfield, Illinois

A bus carrying 72 passengers and two drivers ran off the left side of the road after a tire blowout and entered the median on Thursday, August 2, 2012, at 1:20 p.m. The bus struck a rectangular bridge-pier column in the median and came to rest in contact with the leading pier column. One passenger was fatally injured, 47 passengers were taken from the scene to hospitals, and several others were treated for minor injuries [Stone 2012; Blakley 2012]. The pier had limited guardrail protection that was not sufficient to redirect the bus or prevent it from striking the pier. The pier and bridge do not appear to have been seriously damaged in the collision, although the potential for a catastrophic failure is apparent.

2.5.1.3 East Dallas, Texas

A tractor trailer ran off the road while traveling on I-30, vaulting a concrete safety shaped barrier and striking a rectangular bridge-pier column on Sunday, June 10, 2012, at 4:45 p.m. The driver was fatally injured. There were no other reported injuries, but one of the pier columns was seriously damaged in the impact [Hardwick 2012].

2.5.1.4 Hamilton County, Ohio

On the evening of May 20, 2008, a flatbed trailer hauling a locomotive broke free from its hitch, ultimately crashing into a pier supporting I-74 eastbound over I-275. Two of the three columns were destroyed during the impacts with the trailer and the locomotive. The bridge did not collapse, and ODOT reopened the bridge within 2 months at a cost of \$600,000 [WLWT 2008]. One of the interesting aspects of this crash was that the locomotive being hauled on the trailer was a very heavy, essentially rigid object and, as shown earlier by Buth et al., the rigidity of the cargo can increase the load experienced by the pier significantly in a collision [Buth 2010].

2.5.2 Crashes Investigated by the National Transportation Safety Board

The NTSB investigates and determines the probable cause of significant crashes on highways and in other modes of transportation, with the goal of promoting transportation safety and preventing future similar crashes. In total, the NTSB investigates approximately six highway crashes per year, with each investigation lasting approximately 20 months. The following sections contain brief summaries of crashes involving bridge piers that have been investigated by the NTSB in the last 30 years.

2.5.2.1 Indianapolis, Indiana

On October 22, 2009, at 10:38 a.m., a tanker truck hauling approximately 9,000 gal of petroleum rolled over on I-69 in Indianapolis, Indiana. The driver was exiting I-69 southbound in the right lane of a two-lane ramp that curved to the left toward I-465. The truck engaged in a series of erratic movements after entering the left lane, which was occupied by a Volvo. Ultimately, the tank trailer became decoupled from the truck, penetrated a steel w-beam guardrail, and struck the concrete pier that supported the southbound I-465 overpass. A fire started. The truck driver and vehicle driver sustained serious injuries as a result of the crash, and three occupants of a passenger vehicle traveling on I-465 received minor injuries from the fire. The bridge pier was completely displaced as a result of the crash.

The NTSB “determined that the probable cause of this accident was the excessive, rapid, evasive steering maneuver that the truck driver executed after the combination unit began to encroach upon the occupied left lane.” The bridge design, “. . . including the elements of continuity and redundancy,” mitigated the outcome of the crash and prevented the structure from collapsing [NTSB 2011].

NTSB had the following recommendations for the FHWA and AASTHO:

To the Federal Highway Administration: Work with the American Association of State Highway and Transportation Officials to develop guidance for a bridge pier protection program that will allow state transportation agencies to conduct risk-based assessments of bridges located within highway interchanges. At a minimum, the program should consider each structure’s redundancy, continuity, and the distance of bridge pier columns from the edge of traveled ways. Additionally, consider traffic volumes, traffic type, and the percentage of commercial vehicles transporting bulk liquid hazardous materials in identifying and prioritizing initiatives for preventing vulnerable bridges at high-risk interchanges from collapsing if struck or otherwise damaged by a heavy vehicle [NTSB 2011].

To the Federal Highway Administration: Once the guidance for a bridge pier protection program as described in Safety

Recommendation H-11-16 has been developed, require that it be applied to bridges that are vulnerable to collapse if struck by a heavy vehicle [NTSB 2011].

2.5.2.2 Evergreen, Alabama

A tractor hauling a trailer with a bulk cement tank was traveling southbound on I-65 on May 19, 1993, at 1:35 a.m. when it left the paved road, vaulted a guardrail, and struck a bridge pier supporting County Road 22. The driver suffered serious injuries. Two spans of the overpass collapsed, leading to a car and tractor trailer striking the collapsed bridge. Both drivers of the subsequent crashes were killed.

The NTSB determined that the cement truck driver may have fallen asleep and had been operating under the influence of marijuana, both of which contributed to the original crash. The “. . . nonredundant bridge design, the close proximity of the column bent to the road, and the lack of protection for the column bent from high-speed heavy-vehicle collision” contributed to the second collision [NTSB 1993].

NTSB had the following recommendations for the FHWA and AASTHO:

To the Federal Highway Administration: Request states to identify and assess bridges that are vulnerable to collapse from a high-speed heavy-vehicle collision with their bridge columns and develop and implement countermeasures to protect the structures (Class II, Priority Action) (H-94-5). In cooperation with the American Association of State Highway Transportation Officials, ensure that the bridge management program guidelines include information on evaluating which bridges are vulnerable to high-speed heavy-vehicle collision and subsequent collapse (Class II, Priority Action) (H-94-6) [NTSB 1993].

To the American Association of State Highway Transportation Officials: In cooperation with the Federal Highway Administration, ensure that the bridge management program guidelines include information on evaluating which bridges are vulnerable to high-speed heavy-vehicle collision and subsequent collapse (Class II, Priority Action) (H-94-7) [NTSB 1993].

2.5.2.3 Sacramento, California

A Greyhound bus collided with a concrete overpass support column on I-880 on November 3, 1973. The highway was a relatively flat, straight, six-lane divided highway. The lanes were 12 ft wide, and the paved shoulders were 10 ft wide. The piers were protected by a w-beam guardrail with wooden posts installed on a curbed median. The top of the guardrail was 21 to 23 in. above the height of the curbing. The bus penetrated the guardrail and struck the piers. NTSB made the following recommendation to the FHWA.

To the Federal Highway Administration: Promulgate mandatory national performance standards for traffic barrier systems. Those standards should contain criteria for dynamic testing or



analytical procedures substantiated by such test for each design to increase the compatibility of barriers with both light and heavy vehicles. The standard should also contain requirements regarding the placement of the barriers in the field to assure that compatibility of the vehicle/barrier is not compromised by adjacent environment [NTSB 1973].

2.5.3 Crashes in the Literature

Buth et al. reviewed 19 heavy-vehicle crashes with bridge piers or at locations near piers and the outcome of those crashes [Buth 2010]. Crashes 13 and 14 identified by Buth

et al. were actually not pier crashes. Crash 13 occurred near a pier, and crash 14 occurred on an overpass. Both involved tanker trucks that caught fire and damaged the bridges, but neither involved an impact with a bridge pier. The remaining 17 crashes investigated by Buth et al. are summarized in Table 3. Table 3 also includes a summary of crashes reported by El-Tawil and summarizes the crashes discussed earlier and investigated by the NTSB. The last column in the table includes a literature reference for the crash. When the crash was reviewed by multiple sources, multiple references are reported.

Table 3. Summary of pier crashes found in the literature.

Year/ Location	Events	Injuries	Image	Ref/ Source
1965/bridge over I-45, Dallas County, Texas	A tractor trailer with an unknown load entered the median and struck the first column of a two-column pier. The column failed, and the bridge collapsed as a result of the impact.	Unknown	No photograph available	Buth #6 [Buth 2010]
1973/I-880 overpass, Sacramento, California	A passenger bus penetrated a 23-in.-tall w-beam guardrail and struck a pier. The pier was damaged; the bridge did not collapse.	The driver and 12 passengers were killed, and 33 others were injured.	No photograph available	[NTSB 1973]
1989/Murphy Hollow Road over I-24, Marion County, Tennessee	A box truck entered the median and struck a two-column pier. The column failed; however, the bridge did not collapse as a result of the impact.	Unknown	No photograph available	Buth #16 [Buth 2010]
1993/County Road 22 over I-65, Evergreen Alabama	A cement truck vaulted a guardrail and struck a pier. Two spans of the bridge collapsed. A car and tractor trailer struck the collapsed bridge.	Two were fatally injured.	No photograph available	El-Tawil #1 [El-Tawil 2004] [NTSB 1993]
1994/FM 2110 over I-30, Texarkana, Texas	An 80,000-lb tractor trailer traveling about 60 mph carrying coils of steel crashed into the easternmost column of a two-column pier. The collision caused two spans of the bridge to collapse.	The truck driver and passenger were fatally injured.		Buth #1 [Buth 2010]
2002/SH 14 over I-45, Corsicana, Texas	A tractor trailer carrying paper struck the southernmost column of the median two-column pier. The column failed, and the bridge collapsed.	The collision killed the driver.		Buth #8 [Buth 2010] El-Tawil #2 [El-Tawil 2004]

(continued on next page)

Table 3. (Continued).












Year/ Location	Events	Injuries	Image	Ref/ Source
2003/I-275 north ramp bridge at I-40 east, Knoxville, Tennessee	A tractor trailer overturned on the I-275 north ramp toward I-40 east. The vehicle fell to the roadway below, striking a ramp support. The support was slightly damaged.	Unknown	No photograph available	Buth #12 [Buth 2010]
2003/I-80 Bridge, Big Spring, Nebraska	A tractor trailer struck the columns protected by a guardrail. The pier and bridge failed.	Unknown	 A photograph showing a white tractor trailer that has struck a concrete bridge pier. The pier is heavily damaged and partially collapsed. A guardrail is visible in the foreground, and the bridge deck is above.	El-Tawil #3 [El-Tawil 2004]
2003/I-90 bridge, #53812, Worthington, Minnesota	A single-unit truck struck a column, causing the column to fail. The bridge did not collapse as a result of impact.	Unknown	 A close-up photograph of a concrete bridge column that has been severely damaged. The concrete is cracked and crumbling, with a large section missing from the base. The column is supported by a foundation.	Buth #17 [Buth 2010] [MNDOT 2003]
2004/ Tancahua Street over I-37, Corpus Christi, Texas	A tanker loaded with compressed gas crashed into the easternmost 30-in.-diameter column of the center three-column pier located in the median of I-37. The easternmost column failed; however, the bridge did not collapse as a result of impact.	The driver was fatally injured.	 A photograph showing a white tanker truck that has crashed into a concrete bridge pier. The truck is tilted and partially crushed. The bridge deck is above, and the surrounding area is a highway median.	Buth #3 [Buth 2010]
2004/Pyke Road over I-10, Sealy, Texas	A tractor trailer carrying steel sheet piling struck the westernmost column of the median two-column pier. The bridge did not collapse.	The driver was fatally injured.	 A close-up photograph of a concrete bridge column that has been severely damaged. The concrete is cracked and crumbling, with a large section missing from the base. The column is supported by a foundation.	Buth #7 [Buth 2010]
2005/bridge at I-35 and U.S. 77, Red Oak, Texas	A tractor trailer with an unknown cargo entered the I-35 median and struck the northernmost column of a three-column pier. The collision caused the column to fail; however, the bridge did not collapse.	The driver was fatally injured.	 A close-up photograph of a concrete bridge column that has been severely damaged. The concrete is cracked and crumbling, with a large section missing from the base. The column is supported by a foundation.	Buth #4 [Buth 2010]

Table 3. (Continued).

Year/ Location	Events	Injuries	Image	Ref/ Source
2007/ Chatfield Road over I-35, Navarro County, Texas	A tractor trailer carrying home construction materials struck the northernmost 30-in.-diameter column of the two-column pier after the driver fell asleep and drifted into the median. The bridge did not collapse; however, the collision caused severe cracking of the column.	The driver was fatally injured.		Buth #2 [Buth 2010]
2007/bridge over I-70, Grand Junction, Colorado	A tractor trailer carrying barrels of a flammable liquid struck a median bridge-pier column. The cause of the crash is unknown.	Unknown		Buth #9 [Buth 2010]
2007/I-20 over Rabbit Creek, Longview, Texas	A tractor trailer with an unknown load struck an exterior column of an interior three-column pier. The column failed; however, the bridge did not collapse as a result of the impact.	Unknown		Buth #10 [Buth 2010]
2007/bridge I-240 over I-40, Memphis, Tennessee	A truck tractor trailer loaded with produce struck an exterior pier.	Unknown	No photograph available	Buth #11 [Buth 2010]
2008/FM 1401 bridge over I-30, Mount Pleasant, Texas	A truck tractor trailer loaded with car parts struck a pier of the bridge carrying FM 1401 over I-30. The westernmost 30-in.-diameter pier of the three-pier bent located on the shoulder of the eastbound lanes of I-30 was struck. The pier failed; the bridge did not.	The collision killed the driver.		Buth #18 [Buth 2010]

(continued on next page)

Table 3. (Continued).

Year/ Location	Events	Injuries	Image	Ref/ Source
2008/ Milepost 519 bridge over I-20, Canton, Texas	An unloaded tractor trailer struck the westernmost column of the two-column pier located in the shoulder of I-20 eastbound. The column failed; however, the bridge did not.	Unknown		Buth #19 [Buth 2010]
2008/Exit 111 bridge over I-24, Manchester, Tennessee	A tractor trailer carrying pies struck the pier. Damage to the pier was minor.	Unknown	No photograph available	Buth #15 [Buth 2010]
2008/I-74 over I-275, Hamilton County, Ohio	A flatbed trailer hauling a locomotive broke free from its hitch and struck a pier. Two of the three columns were destroyed. The bridge did not collapse.	Unknown	No photograph available	[WLWT 2008]
2009/I-465 over I-69, Indianapolis, Indiana	After a series of erratic movements, a tanker truck hauling petroleum penetrated a w-beam guardrail and struck a concrete pier. A fire was started. The bridge pier was completely displaced.	There were two serious injuries and three minor injuries.	No photograph available	[NTSB 2011]
2012/ Litchfield, Illinois	A passenger bus entered the median, penetrated a w-beam guardrail, and struck a pier. The pier and bridge do not appear to have been seriously damaged in the collision.	One passenger was fatally injured, 47 were seriously injured, and several others had minor injuries.	No photograph available	[Stone 2012]
2012/ Dolphin Road over I-30, East Dallas, Texas	A tractor trailer vaulted a concrete safety shaped barrier and struck a rectangular column. The column was seriously damaged. The bridge did not collapse.	The driver was fatally injured.	No photograph available	[Hardwick 2012]
Year unknown/ FM 2207 over I-20, Tyler, Texas	A tractor trailer carrying structural steel struck the easternmost 30-in.-diameter column of a two-column pier located on the shoulder of the westbound lanes of I-20. The collision caused failure in the 30-in.-diameter column. The bridge did not collapse as a result of impact.	Unknown		Buth #5 [Buth 2010]

Notes: Numbers in the source column refer to crashes in Buth 2010. For example, Buth #6 is the sixth crash listed in Buth 2010. FM = farm-to-market road, SH = state highway.

2.5.4 Summary

These crashes illustrate that heavy vehicles have more than sufficient energy to cause considerable damage to bridge piers that can result in the structural failure of pier components and, in some cases, the catastrophic collapse of a bridge. Protecting the bridge structures from heavy-vehicle, high-energy crashes is essential for maintaining the structural integrity of a bridge, especially for bridges with nonredundant pier systems or noncontinuous superstructures. The crashes in Table 3 are further summarized in Table 4 with respect to the approximate impact conditions and pier column structural details. Five of the cases described by Buth et al. summarized in Table 3 and Table 4 involved collapse of the bridge. Interestingly, all five of these cases involved two-column pier systems on bridges that were apparently not continuous [Buth 2010]. Three of the five cases reported by Buth where the bridge collapsed involved 30-in. piers with #9 longitudinal reinforcing steel and #2 spiral stirrups; the structural details of the other

two cases are unknown [Buth 2010]. Buth estimated the unfactored design capacity of the columns where the bridge collapsed to be between 80 and 88 kips and, as shown earlier in Figure 6, the impact load measured in a crash test of an 80,000-lb tractor-trailer truck striking an instrumented column at 50 mph was just over 600 kips. While the impact conditions for most of the cases in Table 4 are unknown, it is interesting that many of the cases involved 80,000-lb tractor-trailer trucks traveling at speeds of between 50 and 60 mph. Roughly speaking, the cases in Table 4 where the bridge collapsed and the structural details are known appear to have experienced impact loadings almost seven times higher than their unfactored quasi-static design load.

These cases also show that vehicle impacts with bridge piers can result in serious crashes that cause severe injuries and death to vehicle occupants. Of the 23 cases reported in Table 4 by Buth and El-Tawil, nine (i.e., 40%) involved at least one fatality. Many of the cases in Table 4 also illustrate

Table 4. Pier details and impact conditions in crashes found in the literature [Buth 2010, El-Tawil 2004].

Crash Reference	Vehicle	Approximate Vehicle Weight	Approximate Impact Speed	Approximate Impact Energy	Approximate Momentum	Occupant Crash Severity	Column Shape	Column Size	Number of Columns in Pier	Reinforcement Details	Pier Column Failure?	Bridge Failure?
		lb.	mi/h	ft-kips	lb.-sec.							
Buth #1	TT	80,000	60	9,620	218,634	Circ	2K	30	2	#9 long. Bars and #2 spiral	Yes	Yes
Buth #2	TT	80,000	60	9,620	218,634	Circ	1C	30	2	#9 long. Bars and #2 spiral	Cracking	No
Buth #3	TT	72,000	55	7,275	180,373	Circ	1K	30	3	#9 long. Bars and #2 spiral	Yes	No
Buth #4	TT	40,000	60	4,810	180,373	Circ	1K	30	3	#9 long. Bars and #2 spiral	Yes	No
Buth #5	TT	-	-	-	-	Circ	-	30	2	#9 long. Bars and #2 spiral	Yes	No
Buth #6	TT	-	-	-	-	Circ	-	30	2	Unk	Yes	Yes
Buth #7	TT	80,000	50	6,680	109,317	Circ	1K	30	2	#9 long. Bars and #2 spiral	Yes	No
Buth #8	TT	80,000	-	-	-	Circ	1K	30	2	#9 long. Bars and #2 spiral	Yes	Yes
Buth #9	TT	-	-	-	-	Circ	-	Unk	2	Unk	Yes	Yes
Buth #10	TT	80,000	75	15,031	273,292	Circ	-	24	3	#7 long. Bars and #2 spiral	Yes	No
Buth #11	TT	-	-	-	-	Circ	O	30	Unk	Unk	No	No
Buth #12	TT	-	-	-	-	Unk	-	Unk	Unk	Unk	No	No
Buth #13	TT	-	25	-	-	Circ	-	36	Unk	Unk	No	No
Buth #14	TT	-	-	-	-	Unk	-	Unk	Unk	Unk	Unk	Unk
Buth #15	TT	-	-	-	-	Unk	-	Unk	Unk	Unk	No	No
Buth #16	TT	-	-	-	-	Sqr	-	24	2	#10 long. Bars and #4 spiral	Yes	No
Buth #17	SUT	-	-	-	-	Circ	-	32	Unk	#9 long. Bars and #4 spiral	Yes	No
Buth #18	TT	80,000	-	-	-	Circ	1K	30	2	#9 long. Bars and #3 spiral	Yes	Yes
Buth #19	TT	-	-	-	-	Circ	-	30	2	#9 long. Bars and #3 spiral	Yes	No
El-Tawil #1	TT	-	-	-	-	Unk	2K	Unk	Unk	Unk	Yes	Partial
El-Tawil #2	TT	-	-	-	-	Unk	1K	Unk	Unk	Unk	Yes	Yes
El-Tawil #3	TT	-	-	-	-	Unk	1K	Unk	Unk	Unk	Yes	Yes

Note: TT = tractor-trailer truck; PDO = property damage only; Unk = unknown; Circ = circular; Sqr = square.

insufficient barrier shielding, where the length of need was too short or a TL-3 barrier was not adequate for a truck impact. Details of barrier selection, length of need, and barrier placement are important considerations when designing a bridge pier protection strategy that will not only protect the bridge but protect the motoring public.

2.6 Bridge Pier Risk Analysis

In Section C3.14.5 of the *LRFD Bridge Design Specifications*, in the discussion on collisions with ships and barges, risk is defined as “the potential realization of unwanted consequences of an event. Both a probability of occurrence of an event and the magnitude of its consequences are involved. Defining an acceptable level or risk is a value-oriented process and is by nature subjective” [AASHTO 2012]. Risk, then, involves estimating the probability of an undesirable event like a bridge collapse occurring. While the choice of selecting an acceptable level of risk is a subjective, “value-oriented process,” the calculation of the risk itself is based on a conditional probability. The acceptable level is easily modified based on the quantifiable assessment of the probability of a catastrophic failure.

2.6.1 LRFD Bridge Specifications Probabilistic Method

Buth et al. estimated the risk of heavy-vehicle collisions with bridge piers in the states of Texas and Minnesota. The study focused on principal arterials and collectors because the researchers believed there are higher risks of catastrophic failure at greater speeds [Buth 2010]. The crash risk for individual piers was modeled as well as the crash risk as a function of the roadway characteristics. There was no distinction made as to whether the piers were protected or unprotected from errant vehicles on the undivided roadways or where the pier was located (i.e., median or roadside or offset from the roadway). Specifically, Buth et al. found that the probability of a bridge pier to be hit by a heavy vehicle (P_{HBP}) is equal to:

- 1.09×10^{-9} for divided highways in Texas,
- 2.18×10^{-9} for curves on divided highways in Texas,
- 1.35×10^{-8} for undivided roads in Minnesota, and
- 2.19×10^{-8} for divided roads in Minnesota.

It is notable that there is an order of magnitude difference between the coefficients for Texas and Minnesota, so it is unclear what value a state might use most appropriately or what the reason for the difference might be. Given the appropriate value chosen for P_{HBP} , the annual frequency of bridge pier crashes can be calculated as follows:

$$\text{AF} = \text{TAADT} \cdot P_{\text{HBP}} \cdot 365$$

where

AF = the annual frequency,

TAADT = the heavy-vehicle volume per day, and

P_{HBP} = the probability of the bridge pier to be hit by a heavy vehicle.

Buth et al. further found that striking a pier is a conditional probably, only possible when a vehicle has already run off the road [Buth 2010]. This has been noted in countless prior studies and documented in the RDG for some time [AASHTO 2002a; AASHTO 2006; AASHTO 2011]. Using the Texas data, the estimated frequency of ROR crashes by site can be found as follows:

$$u_i = e^{\ln B_o} L_i F_i^{B_i}$$

where

u_i = the estimated number of ROR crashes per year for site i ,

$\ln B_o$ = constant (-6.354 for undivided and -4.676 for divided),

L_i = the length of segment i in miles,

F_i = vehicles per day (ADT) for segment i , and

B_i = the flow (0.645 for undivided and 0.501 for divided).

The truck volume can be used in place of general traffic volume to determine the estimated frequency of truck ROR crashes per site.

This method is quite simple; however, it does not consider the offset of the pier from the travel lanes, the speed of the encroaching vehicles, the traffic mix, or the possible protection of the pier. It also does not consider the width of the median, the terrain of the median, the number of lanes, the horizontal curvature or vertical grade of the road, and other factors that have been noted to affect the ROR crash rate.

Obviously, a pier located 30 ft from the road will have a much different probability of being struck than one 10 or 15 ft from the road. Likewise, an unshielded pier and a pier shielded by a TL-5 concrete barrier will have much different probabilities of being struck. This regression equation, therefore, implicitly includes the typical offsets and shielding policies in place in the states where the data were collected—in this case, Texas and Minnesota. The prediction equation would have little value in a state where piers have different offsets or shielding policies. A method that includes the offset of the pier from the travel lanes, the speed of the encroaching vehicles, the traffic mix, the possible protection of the pier, the width of the median, the terrain of the median, the number of lanes, the horizontal curvature or vertical grade of the road, and other factors that have been noted to affect runoffs should be used to develop national pier protection guidelines. In the survey of bridge design professionals shown in

Appendix C: Survey of Practice, respondents indicated that “engineering judgement” was the method most often used for accounting for site and traffic conditions. The respondents indicated that the most important characteristics were (in priority order) the traffic volume, the percentage of trucks, speed limit, highway type, and the number of lanes.

Another difficulty with this regression equation is that it was based only on heavy-vehicle volumes without respect to the traffic mix at the site. A particular truck volume might represent a vehicle mix with 10%, 30%, or 50% trucks, but the prediction would be the same. While truck volume is a good measure of exposure, the overall ADT is also a measure of the potential for conflicts on the road. A road with 1,000 heavy vehicles/day and an overall ADT of 2,000 vehicles/day (i.e., 50% trucks) would experience traffic conflicts at a much different rate than a road with 1,000 heavy vehicles/day and overall traffic of 10,000 vehicles/day (i.e., 10% trucks). Since it is these conflicts that often precipitate crashes, the total annual average daily traffic (AADT) and percent trucks should be included.

2.6.2 Roadside Safety Analysis Program Method

Encroachment-based conditional probability models have been used in roadside safety analysis methods since the 1977 AASHTO Barrier Guide [AASHTO 1977, Appendix E]. The computer program Roadside was an encroachment-probability-based software tool used for roadside design in the first RDG [AASHTO 1989a]. The program BCAP was a further development of the method that was used in the 1989 AASHTO Guide Specifications for Bridge Railings [AASHTO 1989b]. BCAP was further improved and modified into the computer program RSAP (Roadside Safety Analysis Program), which was included in the 2002 and subsequent RDGs [AASHTO 2002a]. RSAP was extensively updated and revised in 2012, resulting in a new version of the software (i.e., RSAPv3) [Ray 2012]. Additional updates have been made to RSAPv3 under NCHRP Project 22-12(03) to allow RSAPv3 to include consideration of heavy vehicles’ properties and variations of heavy-vehicle encroachments as well as risk assessment [Ray 2014b]. Updates have been made under NCHRP Project 17-54 to allow for consideration of heavy-vehicle trajectories during encroachments [Carrigan 2017]. These updates have combined to make RSAPv3 the state-of-the-art software tool for roadside encroachment modeling.

RSAPv3 and its predecessors are used to assess the probability of a roadside feature being struck, the severity of the crash if one has occurred, and the resulting crash costs. These programs were designed to assess the risk of a roadside feature being struck and the subsequent benefit–cost of varying the roadside design. The following conditional

probability model is used for each alternative on each segment [Ray 2012]:

$$E(CC)_{N,M} = ADT \cdot L_N \cdot P(\text{Encr}) \cdot P(\text{Cr}|\text{Encr}) \\ \cdot P(\text{Sev}|\text{Cr}) \cdot E(CC_s|\text{Sev}_s)$$

where

$E(CC)_{N,M}$ = expected annual crash cost on segment N for alternative M for a particular vehicle encroachment,

ADT = ADT in vehicles/day,

L_N = length of segment N in miles,

$P(\text{Encr})$ = the probability a vehicle will encroach on the segment,

$P(\text{Cr}|\text{Encr})$ = the probability a crash will occur on the segment given that an encroachment has occurred,

$P(\text{Sev}_s|\text{Cr})$ = the probability that a crash of severity s occurs given that a crash has occurred, and

$E(CC_s|\text{Sev}_s)$ = the expected crash cost of a crash of severity s in dollars.

This equation represents the expected annual crash cost for a particular encroachment on segment N for alternative M . An RSAPv3 analysis is composed of four major steps for assessing each alternative:

- Encroachment probability,
- Crash prediction,
- Severity prediction, and
- Benefit–cost analysis.

Using a series of conditional probabilities, RSAPv3 first predicts the number of encroachments expected on a segment. Given that an encroachment has occurred, the likelihood of a crash is assessed by examining the location of roadside features and comparing those locations to a wide variety of possible vehicle paths across the roadside. If a crash is predicted (i.e., one of the possible trajectories intersects with the location of a roadside hazard), the severity is estimated and converted to units of dollars.

RSAPv3 proceeds by simulating tens of thousands of encroachment trajectories and examining which trajectories strike objects, the probability of penetration or rolling over the object, and the likely severity of those collisions. The passenger vehicle trajectories used in RSAPv3 were gathered from reconstructed ROR crashes performed in NCHRP Project 17-22 [Mak 2010]. NCHRP Project 22-12(03) incorporated a method to account for the differences in passenger vehicle and heavy-vehicle encroachment rates and developed capacity values for concrete median barriers and

bridge railings to be used to estimate the probability of barrier penetration. NCHRP Project 22-12(03) also added output features to support benefit–cost and risk-based analysis methods. These features and data have been incorporated into RSAPv3 and can be used in evaluating the effectiveness of barriers protecting bridge piers [Ray 2014b].

The probabilistic benefit–cost approach long used in roadside design is capable of modeling variations in roadside and median terrain, traffic mix, highway geometry, pier location, pier capacity, and pier protection. Furthermore, RSAPv3 is capable of modeling minor variations in pier size, number, and location. This robust state-of-the-art program has experienced multiple recent updates, making it the best approach for examining the problem of bridge pier protection and shielding.

For example, for a tangent section of divided highway with a two-way AADT of 20,000 vehicles/day, the method from the sixth edition of the *AASHTO LRFD Bridge Design Specifications* estimates an annual bridge-pier heavy-vehicle collision frequency of 0.0009 collisions/year. RSAPv3's encroachment model, which is based on the so-called Cooper data [Cooper 1980], estimates that there will be 1.3091 encroachments/mi/year on a divided highway with a two-way AADT of 20,000. Most encroachments in the Cooper data are less than 300 ft long, or $300/5,280 = 0.0568$ miles, and using an assumption of 10% truck traffic would indicate that RSAPv3 would expect $1.3091 \cdot 0.0568 \cdot 0.1 = 0.0074$ encroachments near a bridge pier/year, and of these only 10% (i.e., 0.0007 heavy-vehicle pier collisions/year) would have a lateral extent greater than 30 ft, so the rough estimates are consistent. The sixth edition procedure, however, has several important assumptions about the location of the pier and the characteristics of the highway built into the procedure that mask the importance of critical design variables like pier offset, grade, curvature, and other site characteristics. On the other hand, RSAPv3 can be used to explicitly examine the effects of length of need, offset from the roadway, and barrier type on the frequency and severity of bridge pier impacts. Each of these variations is critical to protecting existing and proposed structures.

2.7 Benefit/Cost Versus Risk

In roadside safety, the incremental benefit–cost ratio is the present worth over the project life of the reduction in the societal costs of implementing a safety improvement divided by the present worth over the life of the project of increase in construction, maintenance and repair costs of implementing the safety improvement.

$$\text{BCR} = \frac{CC_1 - CC_2}{AC_2 - AC_1}$$

where

BCR = (incremental) benefit–cost ratio,

CC_i = present worth of the annual societal crash costs of alternative i over the project life, and

AC_i = present worth of the owner agency construction cost and the present worth of the annual expected maintenance and repair costs of alternative i over the project life.

Benefit–cost methods were used to develop the guidelines in the RDG, but recent research has shown that using costs presents some difficulties, as shown in the following sections. It should be recognized that the numerator of the BCR equation is really an estimate of the average annual crashes over the life of the project multiplied by the average crash cost of that type of crash. A benefit–cost analysis, therefore, has imbedded within it a risk assessment that has been transformed into units of dollars.

In a study to develop selection guidelines for bridge rails, Ray et al. outlined some of the difficulties in using benefit/cost to develop national guidelines [Ray 2014b]. Ray et al. found that, while construction costs had gone up and down considerably in the previous decade due to economic conditions, the societal cost of highway crashes had only increased. In addition to temporal variations in construction costs, costs also vary geographically. For example, Ray et al. showed that construction costs in the state of New York were more than 3.5 times higher than the national average, while construction costs in some states, such as Arizona, Mississippi, and Montana, were about half the national average [Ray 2014b].

While benefit–cost methods have been widely used in roadside safety for decades, the disparities in how costs change by region and in time and how construction costs vary differently from crash costs are a cause for concern. What is cost beneficial today may not be tomorrow, and what is cost beneficial in one region may not be in another. For these reasons, benefit–cost methods are handicapped in terms of use for national guideline development. Benefit–cost methods are actually a risk assessment method that is used to estimate reductions in anticipated crash costs (i.e., the benefits), which are then used to perform an incremental benefit–cost analysis that includes agency costs like construction, maintenance, and repair over the life of the project.

Another approach common in many other types of engineering fields and becoming more common in roadside safety is risk analysis. In risk analysis, the risk of experiencing a particular type of event is quantified using probabilistic models. An acceptable level of risk is established, and then the system is engineered to ensure that the predicted in-service risk is below the targeted acceptable risk.

There are advantages and disadvantages to each approach. The benefit–cost method has the advantage that it includes

both societal benefits and agency costs such that the benefits are maximized while making the best possible use of agency funds. The disadvantage is that, since costs are explicitly included, regional and temporal variations in the cost elements can make the same solution cost beneficial in one region and not cost beneficial in another. Another disadvantage is that the risk is not necessarily uniform, so one cost-beneficial solution can have a different inherent risk than another with the same benefit–cost ratio.

On the other hand, risk analysis sets a specific risk objective that is uniform across regions and through time such that the risk of an unacceptable event is always kept the same. The disadvantage is that the best risk-based solution may not always be cost beneficial, especially with respect to the agency costs.

The important point is that construction costs vary by region and in time, so any guidelines developed based on a cost–benefit model will likewise vary by region and in time. This is not desirable from the point of view of developing national guidelines that are meant to be used in all regions of the country and are expected to have a reasonably long life. Risk-based approaches avoid this problem by setting the safety-performance goal in terms of the risk of a collision of a particular severity occurring sometime during the design life of the structure. Ray et al. have used this risk-based approach in developing guidelines for the selection of bridge railings [Ray 2014b]. Both the TCRS and SCOBS T7 committees endorsed the risk-based approach over the more traditional cost–benefit approach in reviewing the results of NCHRP Project 22-12(03). A risk-based approach was used in this research for the reasons outlined.

2.8 Summary

The preceding review of the literature has shown that bridge piers are prone to creating two distinct safety problems: (1) the difficulty of protecting vehicle occupants from impacts with piers because bridge piers are one of the most hazardous features of the roadside, and (2) the problem of protecting bridge piers from impacts with vehicles, in

particular heavy vehicles, because high-energy impacts have the potential to significantly damage piers and thereby compromise the structural integrity of bridges.

Research into the crash capacity of bridge piers has indicated that the AASHTO LRFD's suggested equivalent static force of 600 kips may not be adequate to ensure that bridge piers do not fail in some high-energy, heavy-vehicle impacts [AASHTO 2012].

Prior research has demonstrated that there is a strong probabilistic nature to the problem of bridge pier protection. The risk associated with any particular bridge pier is a function of:

- Its location (e.g., offset from the road),
- The importance of the bridge and/or under-crossing route,
- The traffic characteristics (e.g., overall AADT, percent trucks, and speed),
- Highway characteristics (e.g., horizontal curvature, grade, lane width),
- Structural characteristics of the bridge pier and bridge superstructure (e.g., pier capacity, pier arrangement, bridge redundancy), and
- Any shielding by barriers (e.g., type of barrier, barrier height, barrier offset).

Probabilistic design methods have a long history in roadside safety, going back to the 1977 AASHTO Barrier Guide. Additions to the *AASHTO LRFD Bridge Design Specifications* have likewise adopted probabilistic methods to quantify the risk of a catastrophic bridge-pier crash occurring. RSAPv3 is the current encroachment-probability-based roadside design tool recommended by the RDG. This research used the risk tools available within RSAPv3. This approach allows for the incorporation of traffic and highway characteristics along with the precise location of bridge piers on the roadside.

The following chapters document the research, which developed (1) guidelines for designing bridge pier components for heavy-vehicle impacts or determining if they require shielding for structural protection, and (2) guidelines for determining if bridge piers should be shielded to provide passenger-vehicle occupant protection.

CHAPTER 3

Discussion of Proposed LRFD Bridge Design Pier Protection Guidelines

Appendix A: Proposed LRFD Bridge Design Pier Protection Specifications provides preliminary proposed guidelines for bridge pier protection for consideration in a future edition of the *AASHTO LRFD Bridge Design Specifications*. The text has been based on the eighth edition of the *AASHTO LRFD Bridge Design Specifications* [AASHTO 2017], where strikeouts indicate proposed deletions from the eighth edition text, and underlines indicate proposed additions based on the results of this research. Article 3.6.5 in the eighth edition is identical to the language in the sixth edition. This section presents the development and illustrates the application of the guidelines for risk-based assessment of bridge pier protection shown in Appendix A. The bridge pier protection guidelines for the *AASHTO LRFD Bridge Design Specifications* are presented here, and the passenger-vehicle occupant protection guidelines for the RDG are presented in the next chapter. Examples and validation with RSAPv3 are provided in a later chapter.

Article 3.6.5 of the *AASHTO LRFD Bridge Design Specifications* provides two design choices to the user:

1. Provide for structural resistance to heavy-vehicle impacts, or
2. Shield the pier system with a barrier.

Providing structural resistance to heavy-vehicle impacts is discussed in Section 3.2, and shielding the pier system with a barrier for pier protection is discussed in Section 3.3.

3.1 Defining Bridge Collapse

Before exploring the two design choices offered by the *AASHTO LRFD Bridge Design Specifications*, a definition of “bridge collapse” must be established. As a point of comparison, Article 3.14 in the eighth edition dealing with vessel collisions does not define exactly what is meant by a “bridge collapse,”

but it is noteworthy that the first sentence of Section 3.14.5 refers to “bridge component collapse.” This suggests that failure of a pier component constitutes failure of the bridge itself regardless of whether the superstructure collapses. In essence, Article 3.14 ignores any potential redundancy in the pier system or any possible continuity of the superstructure over the piers being considered.

Similarly, Article 3.6.5 of the eighth edition of the *AASHTO LRFD Bridge Design Specifications* dealing with impacts from vehicles takes essentially the same approach as Article 3.14 for vessels, meaning that the failure of any of the major bridge components constitutes failure or potential collapse of the entire bridge. From this point of view, failure of any of the major components will take the bridge out of service until the component is repaired. For example, if a column in a redundant multicolumn bridge-pier system is struck such that it completely fails, the bridge superstructure will not collapse because the pier system is redundant, but the bridge probably will be taken out of service while the pier column is repaired. This repair will likely take months to accomplish even if undertaken on an emergency basis, with the commensurate repair, delay, and rerouting costs. On the other hand, using the same example, if the bridge superstructure itself collapses, the time and cost of repair, delay, and rerouting will be much higher since replacing the bridge is an even more costly and time-consuming activity. The potential for loss of life in the former is obviously smaller. There is no expectation that the structure will experience that type of load and experience no damage. The approaches used in both Articles 3.6.5 and 3.14 in the eighth edition are, therefore, quite conservative since failure of any component is equal to failure of the whole bridge under this definition. This definition is considered to be too conservative at least for use in highway bridges exposed to vehicle traffic.

It is preferable to take advantage of any redundancy of the pier system or continuity over the pier of the superstructure

rather than ignore both. In this research, failure is defined as the inability of the superstructure to support its design dead load and permanent-lane live load. In other words, complete failure or collapse of a pier component is allowable as long as either the pier system is redundant, assuming the loss of that component, or the superstructure is continuous over the pier under consideration such that the loss of the pier component will not prevent the bridge superstructure from supporting its design dead load and permanent-lane live load. In essence, complete failure and loss of a pier component like a column is allowable as long as the superstructure does not collapse.

Given this definition, bridge collapse will be highly unlikely to occur if:

- The critical pier components can be shown by calculation to have sufficient lateral impact resistance to the expected impact loads,
- The pier system can be shown by calculation to be redundant given the loss of a pier component, or
- The bridge superstructure can be shown by calculation to be continuous over the pier system such that the superstructure will not collapse.

These three conditions will be discussed in the following sections. Each of these conditions requires the user to demonstrate by calculation that the criterion is satisfied. If any one of these conditions is true, the bridge pier system does not need to be protected by shielding barriers because it will be able to support its design dead load and permanent-lane live load.

3.1.1 Lateral Resistance to Impact

In assessing the nominal resistance to lateral impact loads on bridge pier components, it is important to recognize that there are several possible failure modes. While a shear failure of a pier column is certainly one important mode, a column may also fail in flexure, the connection between the column and pier cap may fail, or the connection between the column and foundation may fail. In determining the lateral resistance to impact loading, the engineer must consider all possible failure modes and choose the model with the smallest lateral resistance as the controlling design element. Some of these failure modes are illustrated in Figure 9 using the cases collected by Buth et al. [Buth 2010].

The general LRFD design philosophy proceeds by assessing the nominal resistance or strength of each structural component and connection and is expressed by the following equation [AASHTO 2012]:

$$\sum \eta_i \gamma_i Q_i \leq \phi_i R_n$$

where

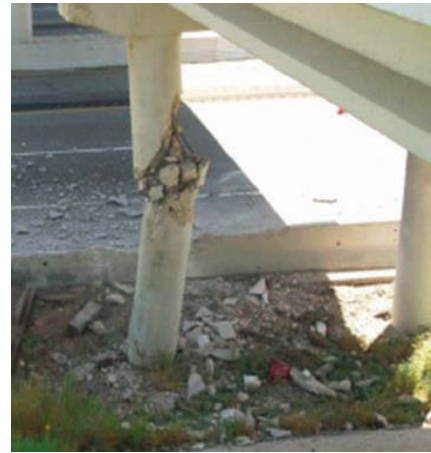
- η_i = load modification factor,
- γ_i = load factor,
- Q_i = force effect,
- ϕ_i = resistance factor, and
- R_n = nominal resistance.

This basic equation is used to evaluate each member and connection in a structure. The nominal resistance (R_n) is the calculated shear, moment, or axial strength of the member based on typical calculations or analysis. The resistance factor (ϕ_i) is used to account for variability in materials and workmanship that may reduce the nominal calculated resistance. On the left side of the equation, the applied loads are represented by the force effect (Q_i), which may be modified for uncertainty in the estimation of loads using the load factor (γ_i) and factors relating to ductility, redundancy, and operational classification (η_i). The load modification factor, load factor, and resistance factors are all intended to be statistical variables that account for the statistical variation of materials, loads, workmanship, and in-service use.

Loads are characterized in the *AASHTO LRFD Bridge Design Specifications* in a variety of limit states. A heavy-vehicle impact is classified by the *AASHTO LRFD Bridge Design Specifications* as a Type II Extreme Event and is addressed in Articles 1.3.2.5 and 3.4.1 [AASHTO 2012]. Table 3.4.1-1 of the *AASHTO LRFD Bridge Design Specifications* defines the overload factor for Extreme Event II vehicle collision forces (CT) to be 1.0 (i.e., $\gamma = 1.0$). These events are rare and seldom experienced in combination with other extreme events, so a value of unity is recommended.

Load modification factors are characterized in the *AASHTO LRFD Bridge Design Specifications* in Article 1.3.2.5 and are classified by redundancy, ductility, and operational importance [AASHTO 2012]. For the extreme event limit state, the load modification factors for ductility, redundancy, and operational importance are also all set to 1.00 in recognition that such events are rare.

Section 5 (reinforced concrete) does not specify resistance factors to be used for extreme events, although Article 6.5.5 (steel construction) states that a value of 1.0 should be used. The seismic design section dealing with inelastic hinging forces on single columns and piers (AASHTO 2012, Article 3.10.9.4.3b) specifies that a resistance factor of 1.3 be used for reinforced concrete columns and 1.25 be used for structural steel columns. Generally, resistance factors are taken to be less than 1.00, but in this case (i.e., inelastic hinges), the nominal calculated resistance is a service load value, so these values greater than 1.00 account for the additional strength of the members in the inelastic range that represents reserve capacity that can be counted on in an extreme event. The



Column-cap connection failure



Column-foundation failure



Column shear failures

Figure 9. Examples of pier system failure models [Buth 2010].

simple-hinge method described in Appendix E: Nominal Resistance to Lateral Impact Loads on Pier Columns is an inelastic analysis method, so using a value of 1.00 or slightly greater would be appropriate and consistent with the seismic provisions if that method were used to calculate the pier column hinge capacity.

Given this general background, the basic LRFD design equation can be rewritten explicitly for piers subjected to Extreme Event II lateral vehicle collision forces as:

$$\eta_D \eta_R \eta_I \gamma_{CT} Q_{CT} \leq \phi_{CPC} R_{CPC}$$

where

$\eta_D = 1.00$ = ductility load modification factor for Extreme Event II vehicle collision forces (AASHTO 2012, Article 1.3.3);

$\eta_R = 1.00$ = redundancy load modification factor for Extreme Event II vehicle collision forces (AASHTO 2012, Article 1.3.4);

$\eta_I = 1.00$ = operational importance load modification factor for Extreme Event II vehicle collision forces (AASHTO 2012, Article 1.3.5);

$\gamma_{CT} = 1.00$ = overload factor for vehicle collision forces (AASHTO 2012, Table 3.4.1-1);

Q_{CT} = expected lateral heavy-vehicle collision force on the critical pier component;

$\phi_{CPC} = 1.30$ = resistance factor for inelastic hinge forces in reinforced concrete columns and piers (AASHTO 2012, Article 3.10.9.4.3b),

1.25 = resistance factor for inelastic hinge forces in structural steel columns and piers (AASHTO 2012, Article 3.10.9.4.3b),

1.00 = resistance factor for inelastic hinge forces in reinforced concrete columns if the simple-hinge method in Appendix E is used to find R_{CPC} ; and

R_{CPC} = nominal lateral load resistance of the critical pier component.

Generally speaking, the gravity loads in a pier system are supported either by columns or walls. Columns may be circular or rectangular and may either have a bent or cap spanning several columns or directly supporting a girder. Columns as small as 18 in. have been observed. Walls may span the entire width of the overpassing bridge, or they may be the base of a hammerhead-type cap. In either case, walls are much longer than they are wide. Typical thicknesses are around 4 ft, and lengths are generally 15 ft or more. For example, a 15.5-ft-long by 5-ft-deep hammerhead pier has a nominal shear capacity based on just the concrete shear strength of over 900 kips—well above the current impact design load of 600 kips [FHWA 2014a].

3.1.1.1 Pier Walls

Article 5.8.3.3 of the eighth edition of the *LRFD Bridge Design Specifications* provides the procedure for calculating the nominal shear strength of compression members. For a wall-type structure with no prestressing, Article 5.8.3.3 assumes that the concrete alone is sufficient for developing adequate shear strength. For walls, the following equation generally controls:

$$V_c = 0.0316\beta\sqrt{f'_c}L_p0.72W_p$$

where

V_c = the shear strength of concrete in ksi,

$\beta = 2$,

L_p = length of the pier wall in ft, and

W_p = thickness of the pier wall in ft.

Assuming a minimum wall thickness of 48 in., concrete strength of 4 ksi, and β of 2, and recognizing that there are two shear planes in a vehicle impact, the minimum length of a wall that will generate 600 kips of capacity using just the concrete can be found as:

$$V_c = 0.0316\beta\sqrt{f'_c}L_p0.72W_p$$

$$600 = (2)0.0316(2)\sqrt{4}L_p0.72(48) \rightarrow b_v = 68 \text{ in.} = 5.7 \text{ ft}$$

Generalizing, this results in $600/(2 \cdot 0.0316 \cdot 2 \cdot 2 \cdot 0.72) = 3,296 = L_p W_p$

Figure 10 shows the relationship between the pier wall thickness and length needed for a shear capacity of 600 kips based only on the contribution of the concrete. Points that plot above and to the right of the line can be considered pier walls with more than 600 kips of available shear capacity, whereas points that plot below and to the left of the line should be considered columns. A typical two-lane bridge would be on the order of 30 ft wide, so if a pier wall the entire width of the structure were used, Figure 10 suggests that a wall at least 1 ft thick would be sufficient. Figure 10 illustrates that pier walls will seldom be at risk in heavy-vehicle collisions.

Figure 11 shows the possible impact orientations for pier walls. The wall may be struck end-on, in which case the full shear capacity of the massive wall will resist the vehicle. This impact orientation would not be particularly vulnerable to failure if the dimensions of the wall plot above and to the right of the line in Figure 10. On the other hand, the wall may also be struck in the middle and may be susceptible to the vehicle punching through it even though the component of the force perpendicular to the wall would be considerably less than in the end-on case. Even this scenario, however, seems unlikely to experience failure since from rigid concrete

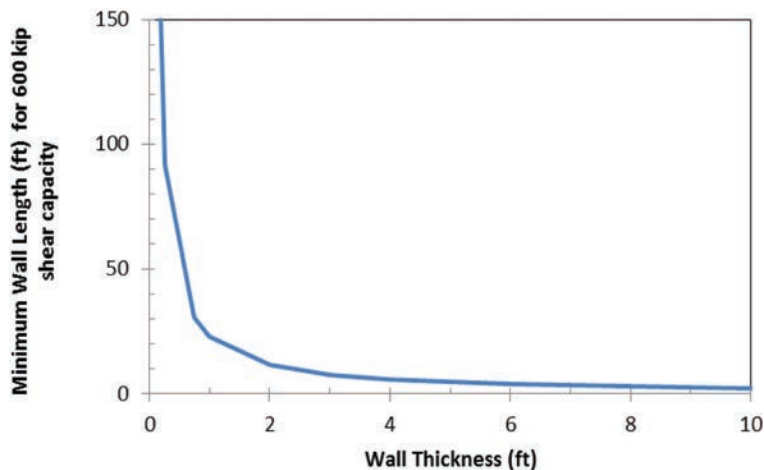


Figure 10. Minimum wall thickness and length needed for at least 600 kips of shear capacity from only the concrete.

barrier design experience it is known that a 10-in. thick TL-5 vertical concrete wall properly reinforced and with proper foundation will contain and redirect an 80,000-lb tractor-trailer truck [AASHTO 1994a]. Anecdotally, it is perhaps significant that none of the bridge pier collisions investigated by Buth involved bridge piers that were in a wall configuration. Pier walls will generally not be at high risk of failure when struck even by large trucks [Buth 2010].

3.1.1.2 Pier Columns

Bridge piers composed of columns either directly supporting girders or supporting a pier cap appear to be the most common type of pier in the National Highway System. Such columns may have cross-sections that are circular, square, or rectangular. The typical bridge pier system in the National Highway System in Ohio, for example, consists of three 36-in.-diameter cap-and-column piers [ODOT 2007]. Generally, the column is about 15 ft tall as measured from the top of the footing or ground line to the bottom of the pier cap. Typical longitudinal reinforcement is proportioned as 1% of the gross area of the column, and typical shear reinforcement

uses #4 spiral bars with a 4.5-in. pitch and 30-in. outside diameter (i.e., 3 in. of cover). Like many states, ODOT's existing bridge piers largely date from the Interstate construction era of the 1960s and 1970s. Bridge piers from this era tend to be dominated by this type of cap-and-column design.

Minnesota DOT has similar design guidelines [MNDOT 2016]. The minimum column diameter for a cap-and-column pier design is 28 in. For columns less than 42 in. in diameter, spiral reinforcement is required with a pitch of no less than 3 in. and at least #4 bars. For circular columns greater than 42 in. in diameter or all square and rectangular columns, ties no smaller than #3 can be used, with various sized ties specified based on the longitudinal steel selected for the gravity loads. TXDOT allows the use of circular columns as small as 18 in., and for all circular columns between 18 and 48 in., #3 spirals with a 6-in. pitch are specified [TXDOT 2013]. Wisconsin requires at least three columns in a cap-and-column pier, and the smallest allowable column size is 30 in. [WIDOT 2013a]. Columns use ties rather than spirals. Wisconsin treats the design of hammerhead piers as a wall.

Figure 12 illustrates the typical impact scenarios for piers with columns. Due to the symmetry of the columns, the

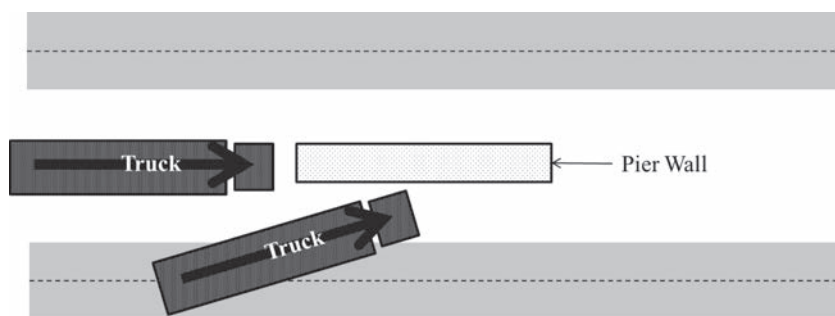


Figure 11. Possible impact orientations for pier walls.

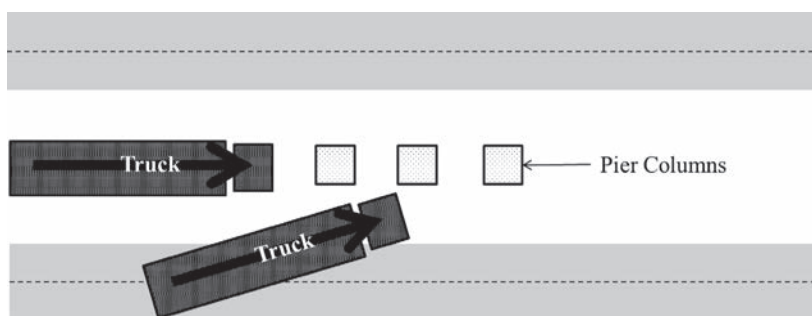


Figure 12. Possible impact orientations for pier columns.

critical impact is the end-on impact scenario since, for circular or square columns, the cross-section is the same at every orientation. The leading column is also the most at-risk column since it can be struck from a variety of orientations, whereas the interior columns are shielded by the leading columns, and the impact angle is limited. As this discussion shows, the dimensions of pier columns can be relatively small, which makes these columns particularly at risk in heavy-vehicle impacts. Considerations and methods for evaluating the nominal lateral capacity of rectangular and circular pier columns are discussed further in Appendix E.

3.1.2 Pier Redundancy and Superstructure Continuity

Pier system redundancy and superstructure continuity are structural features that the current *LRFD Bridge Design Specifications* do not take advantage of when assessing the probability of bridge collapse, as will be discussed in Section 3.1.3. Figure 13 shows two heavy-vehicle impacts with pier systems.

On the right, the bridge superstructure collapsed because the superstructure was not continuous and the pier system was not redundant. On the left, bridge collapse was avoided either because the pier system was redundant or the superstructure was continuous (or both). In a survey of state DOTs shown in Appendix C, several respondents were of the opinion that the current procedures of Article 3.6.5 were too conservative because they do not take advantage of any pier redundancy or superstructure continuity available in a particular design. This section discusses how these structural features were incorporated into the pier protection guidelines.

The design equation for Extreme Event II lateral vehicle collision forces shown at the beginning of Section 3.1.1 is, like most LRFD procedures, based on the design of components and connections rather than the whole bridge system. Ghosn et al. and Liu et al. have examined the use of load and resistance factors to account for bridge system redundancy for both super- and substructures [Ghosn 2014, Liu 2001]. While the details are complicated, the redundancy of substructure components like piers varies from 0.85 for



(a) Pier system was redundant or superstructure was continuous (or both).



(b) Superstructure was not continuous, and the pier system was not redundant.

Figure 13. Examples of the effect of pier system redundancy and superstructure continuity [Buth 2010].

nonredundant piers up to about 1.05 for redundant pier systems [Ghosn 2014, Appendix A, Article 1.3.6.2]. In the context of piers, Ghosn et al. define redundancy as a pier system with two or more columns supporting the bent and detailing sufficient to allow plastic moment capacity of the columns to develop. Similarly, the system factors for the superstructure under vertical loads (i.e., traffic live loads and dead loads) are between 0.80 and 1.20, depending on the structural form of the cross-section [Ghosn 2014, Appendix A, Article 1.3.6.1]. The Ghosn recommendations have not, as yet, been incorporated into the *LRFD Bridge Design Specifications*, but they do provide some insight into accounting for pier redundancy and superstructure continuity in the case of pier components subjected to vehicle impacts.

The system factors as developed by Ghosn et al. are resistance factors that are used to reduce the nominal strength of the bridge component, in this case the critical pier component. A low value of the system factor would cause the engineer to increase (i.e., overdesign) the strength of the member to provide additional capacity to guard against system failure. The purpose of these guidelines, however, is somewhat different in that the guidelines are meant to estimate the probability of failure rather than provide a criterion for design. Table 5 and Table 6 show the types of structural characteristics that determine the redundancy of the pier system and continuity of the superstructure.

An alternative, simpler approach for addressing redundancy is illustrated by the Minnesota DOT Bridge Office Substructure Protection Policy from 2007 and their updated guidance in 2016 [MNDOT 2007b, MNDOT 2016]. The policy is categorized by a variety of design cases and preferred solution strategies. Pier systems with two or fewer columns supporting a bent are categorized as nonredundant. When there are three or more columns in the pier system, the designer must “validate that the structure will not collapse by analyzing the structure considering removal of any single column. Consider all dead load with a 1.1 load factor. Use live load only on the permanent travel lanes, not the shoulders, with a

1.0 load factor” [MNDOT 2007b]. The purpose of this load case is to provide sufficient time for any traffic on the bridge to clear after a bridge pier collision without the superstructure collapsing. The same rationale can be used for evaluating superstructure continuity. For the proposed guidelines, it is suggested that a pier system be considered redundant or a superstructure continuous if it is demonstrated by calculation that the bridge can support all its dead load with a load factor of 1.1 and the design live load on the permanent lanes (i.e., not the shoulders) with a load factor or 1.0. This is the approach that was taken in developing the proposed LRFD Bridge Design Specifications guidelines shown in Appendix A.

3.1.3 Acceptance Criteria

Now that a definition of bridge collapse has been chosen, the values for the acceptance criterion need to be established. The acceptance criterion is the maximum probability of bridge collapse that is acceptable to the owner agency. One aspect of Article 3.14 dealing with vessel collisions of interest here is the acceptance limit for the expected annual frequency of bridge component collapse. Article 3.14.5 dealing with vessel collisions states that:

[F]or critical or essential bridges, the maximum annual frequency of collapse, AF, for the whole bridge, shall be taken as 0.0001. For typical bridges, the maximum frequency of collapse, AF, for the whole bridge, shall be taken as 0.001 [AASHTO 2012].

In essence, critical or essential bridges have an “importance factor” of 10 with respect to more typical bridges. The commentary for Section C3.6.5.1 dealing with vehicle collisions in the eighth edition of the *LRFD Bridge Design Specifications* uses this same acceptance criterion in stating:

Design for collision force is not required if AF_{HBP} is less than 0.0001 for critical or essential bridges or 0.001 for typical bridges [AASHTO 2017].

Table 5. System factors for pier redundancy (ϕ_{PR}) [adapted from Ghosn 2014].

Nonredundant Pier Systems			
$\phi_{PR} =$	Value	If any of the following are true, the pier system is not redundant:	
	0.85	<ul style="list-style-type: none"> • One column supports a bent. • System failure is controlled by shear. • Column connections with the bent or foundation have insufficient detailing to allow the full plastic moment capacity of the column to develop. 	
Redundant Pier Systems			
$\phi_{PR} =$	Value	Columns	If all of the following are true, the pier system is redundant:
	0.95	2	<ul style="list-style-type: none"> • Two or more columns support the bent. • There are integral connections between the superstructure and substructure. • Detailing is sufficient to allow the full plastic moment capacity of the columns to develop.
	1.00	3	
	1.05	4+	

Table 6. System factors for superstructure continuity ($\phi_{SU\ SC}$) [adapted from Ghosn 2014].

	Value	Superstructure Cross-Section Type
$\phi_{SU\ SC} =$	0.80-0.96	Continuous steel I-girder with non-compact negative bending sections [see Ghosn 2014, Appendix A, Table 1.3.6.1-1].
	0.80-1.20	All other simple span and continuous I-girder bridges [see Ghosn 2014, Appendix A, Table 1.3.6.1-1].
	0.83-0.97	Simple span box-girder bridges ≤ 24 ft wide [see Ghosn 2014, Appendix A, Table 1.3.6.1-2].
	0.80-1.20	Simple span box-girder bridges > 24 ft wide [see Ghosn 2014, Appendix A, Table 1.3.6.1-2].
	0.80-1.20	Continuous box-girder bridges ≤ 24 ft wide [see Ghosn 2014, Appendix A, Table 1.3.6.1-2].
	0.80-1.20	Continuous steel box-girders w/non-compact negative bending sections [see Ghosn 2014, Appendix A, Table 1.3.6.1-2].
	0.80-1.20	Continuous box-girder bridges with compact negative bending sections [see Ghosn 2014, Appendix A, Table 1.3.6.1-2].
	0.80	Single-cell box-girder bridge [see Ghosn 2014, Appendix A, Table 1.3.6.1-3].
	1.00	Multicell box-girder bridge [see Ghosn 2014, Appendix A, Table 1.3.6.1-3].

Since the eighth edition of the *LRFD Bridge Design Specifications* uses a value of 0.0001 for essential bridges and 0.001 for typical bridges in both the vessel collision provisions in Article 3.14 as well as the heavy-vehicle collisions in Article 3.6.5, there appears to be some history of using these values for the critical acceptance annual risk for bridge collapse. These values are retained in this research, although they can be modified by AASHTO should it want to make the acceptance criteria either more or less conservative.

3.2 Design Choice Is Structural Resistance

3.2.1 Practical Worst-Case Collision Force: Q_{CT}

The objective of developing pier protection guidelines is to minimize the chance of bridge collapse due to heavy-vehicle collisions with pier components. The most vulnerable type of pier components are generally pier columns. It is necessary to estimate the probable range and distribution of extreme event impact forces in heavy-vehicle impacts with pier components. Appendix D: Lateral Impact Loads on Pier Columns provides a discussion of the finite element modeling of tractor-trailer truck impacts with bridge columns as well as a comparison to the tractor-trailer rigid-pole tests conducted by Buth et al. [Buth 2011].

The force–time history in Figure 14 shows the origin of the 600-kip design load used in the eighth edition of the *LRFD Bridge Design Specifications*. The engine impact with the rigid pole created a peak force of just over 600 kips. The particular magnitude of this peak force is dependent on the filter strategy used in analyzing the data; the 10-ms average first peak was over 900 kips, and the 25-ms average was just over 600 kips. Buth et al. chose the 25-ms average acceleration as being

essentially equivalent to the quasi-static design load, and this was adopted in the eighth edition.

The results of the analyses described in Appendix D and summarized in Figure 14 show that the peak impact force is not a function of the total mass and speed of the vehicle but, rather, the impact is actually a series of loosely coupled impact events. The first major event is the collision of the essentially rigid engine block with the pier, followed by the crushing of the tractor cabin and eventually the impact with the front of the trailer. While the trailer load could potentially subject the pier to a large loading if it were massive and rigid, the first practical worst-case impact force (Q_{CT}) was found to be directly related to the impact between the truck engine and the pier column. The engine is the first large essentially rigid mass that is encountered in a head-on impact, and it dominates the impact force–time history. In other words, the total kinetic energy of the vehicle is not predictive of the practical worst-case impact force (Q_{CT}).

The structural design of bridges and bridge piers is accomplished primarily in the force domain, whereas collisions occur in the energy and momentum domains. It is necessary, therefore, to transform the dynamic impact force–time response into an equivalent quasi-static load that can be used as a design criterion. An approach to estimating the peak impact load was developed by assuming that the early phases of the impact can be represented by two square wave impulses: one caused by the frame and body structures between the column and the front of the engine, and the second caused by the engine–column impact. The following simple equation provided good and slightly conservative predictions of the finite element analysis (FEA) impact force at impact velocities between 35 and 50 mph.

$$Q_{CT} = \left[\frac{W_e \cdot V}{32.2 \cdot 1000 \cdot T_e} \right] + \left[\frac{W_f \cdot V}{32.2 \cdot 1000 \cdot \left[T_e + \frac{d_1}{V} \right]} \right]$$

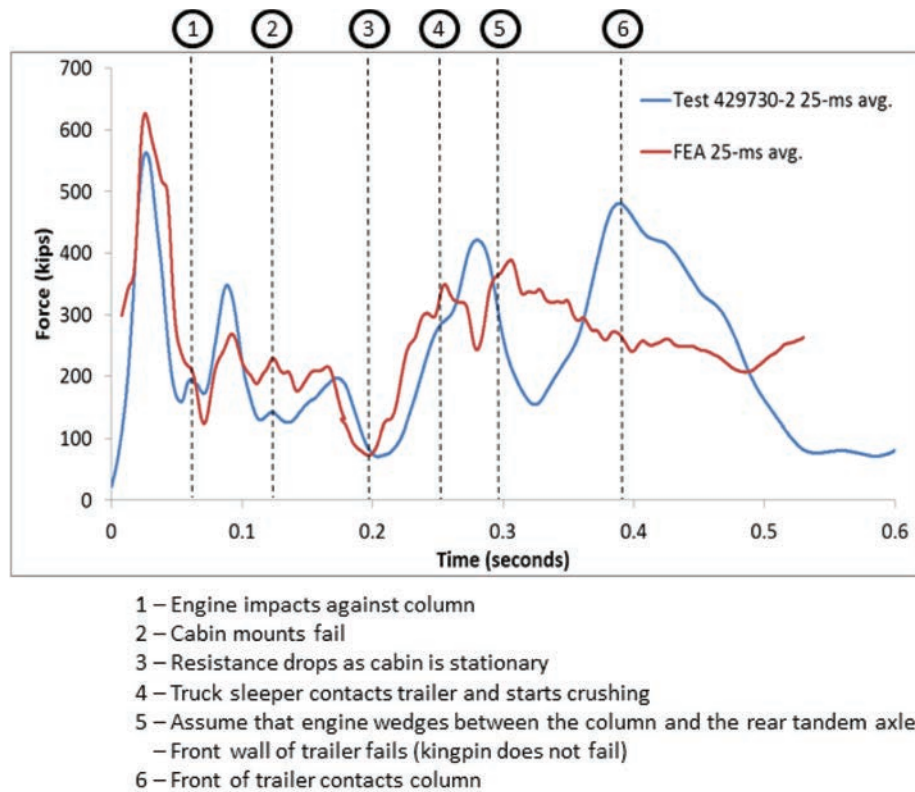


Figure 14. Force–time history for Test 429730-2 and finite element analysis (FEA) results indicating key impact events.

where

	Tractor Trailer	Single-Unit Truck
W_e = effective weight of engine (lb),	4,500	1,965
W_f = effective weight of structure in front of the engine (lb),	3,000	1,310
T_e = period of the engine pulse (s),	0.0241	0.0241
d_1 = distance from front bumper to front of engine (ft),	1.146	2.210
V = impact velocity (ft/s), and		
Q_{CT} = practical worst-case impact force (kips).		

All of the variables in this equation for Q_{CT} are normal random variables. Typical values based on the dimensions and masses of commonly used crash-test vehicles are shown to the right of the equation's where list. The impact velocity in particular is expected to have an important effect on the distribution of impact forces.

To determine the cumulative distribution of impact forces that are likely given that a heavy-vehicle impact occurs with a pier system component, this equation was used in a Monte Carlo simulation to generate data for a cumulative distribution. In a Monte Carlo simulation, a random number is generated and used to choose a particular value for each random variable according to the known statistical parameters of that distribution; for a normal distribution, the mean and the

standard deviation are sufficient. Monte Carlo simulations using 25,000 cases per category were performed for speeds of between 35 and 75 mph in 5 mph increments for each of the four functional classes to be used in the guidelines (i.e., rural Interstate, rural collector, urban Interstate, and urban collector). The cumulative distributions created using these Monte Carlo simulations are shown in Figure 15 through Figure 18, which plot the nominal lateral resistance (R_{CPC}) on the x -axis and the probability of the impact force (Q_{CT}) exceeding the nominal lateral resistance (R_{CPC}) on the y -axis. For example, the probability of exceeding a nominal lateral resistance (R_{CPC}) of 600-kip on a 55-mph rural Interstate is shown by Figure 15 to be 0.50, whereas the probability of exceeding a nominal lateral resistance (R_{CPC}) of 600-kip on a 45-mph urban collector is 0.0140, as shown in Figure 18.

Figure 15 through Figure 18 show several interesting features. First, as expected, for a nominal lateral resistance (R_{CPC}), the probability of exceeding that force increases as the posted speed limit (PSL) increases. Second, all four figures have a unique “S” shape where the smaller nominal lateral resistances (R_{CPC}) are primarily associated with the lighter single-unit trucks, and the higher nominal lateral resistances (R_{CPC}) are associated with heavier tractor-trailer trucks. The nature of the “S” is controlled by the proportion of each type of truck on each functional class of roadway.

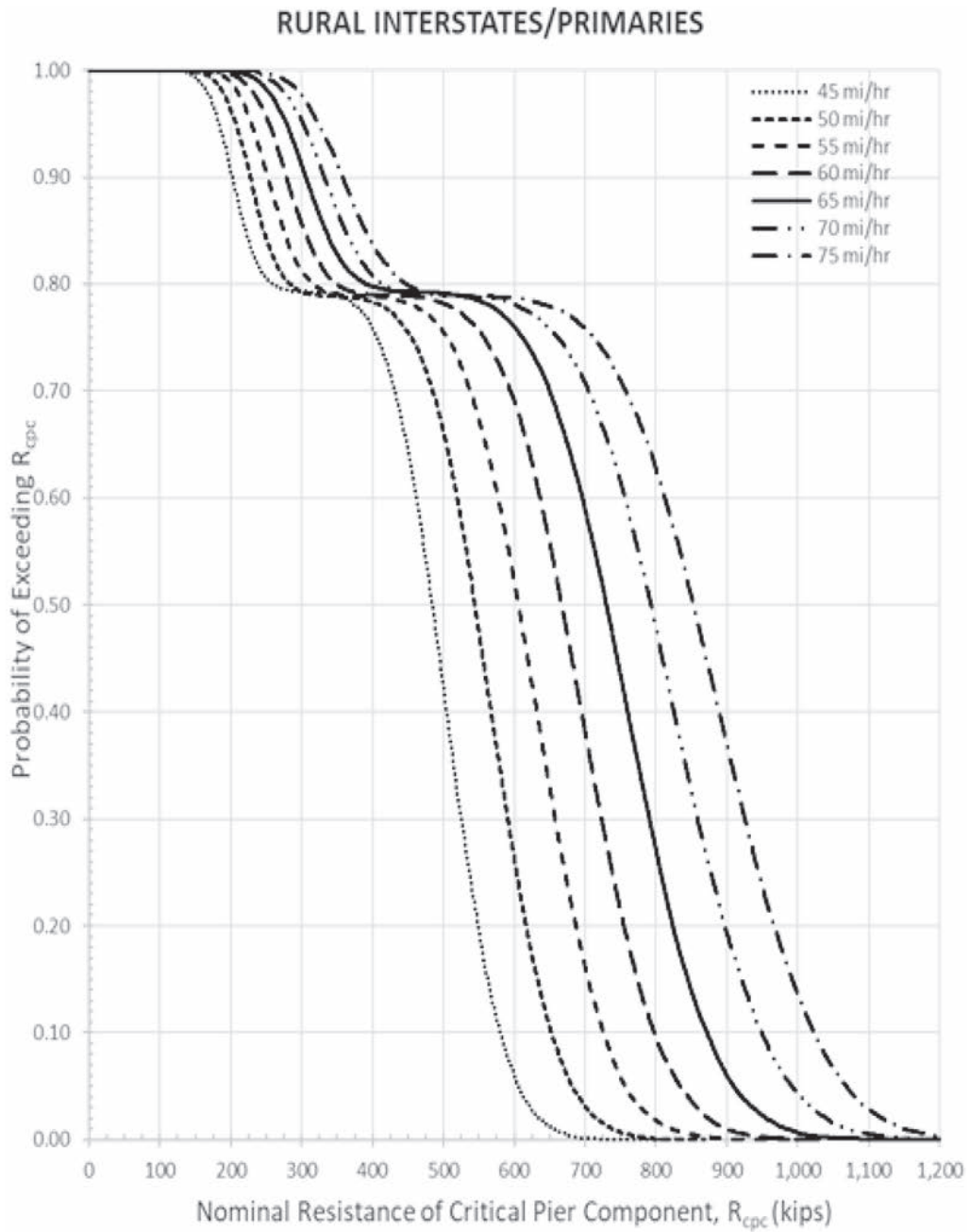


Figure 15. Cumulative distribution of expected impact force – rural Interstates/primaries.

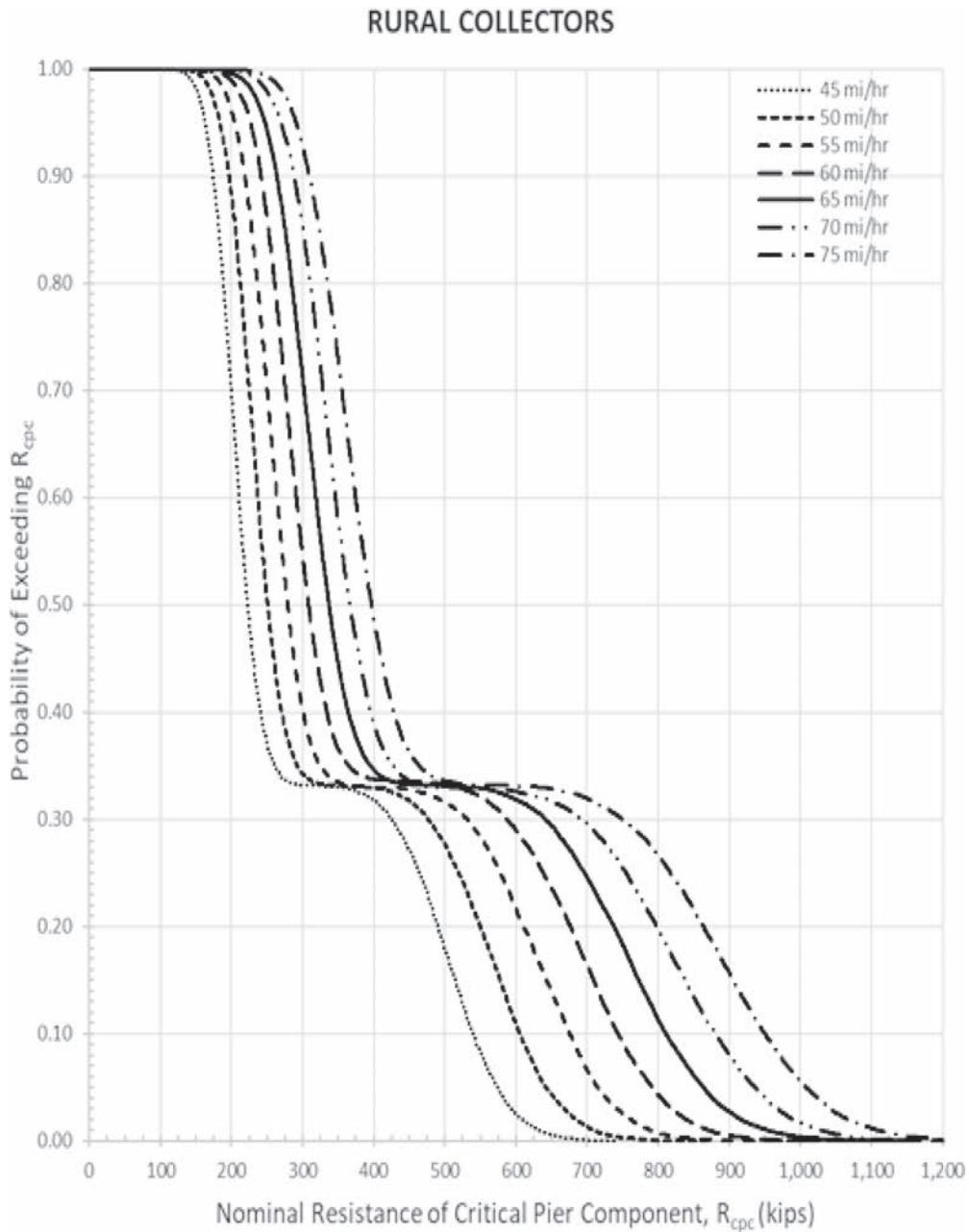


Figure 16. Cumulative distribution of expected impact force – rural collectors.

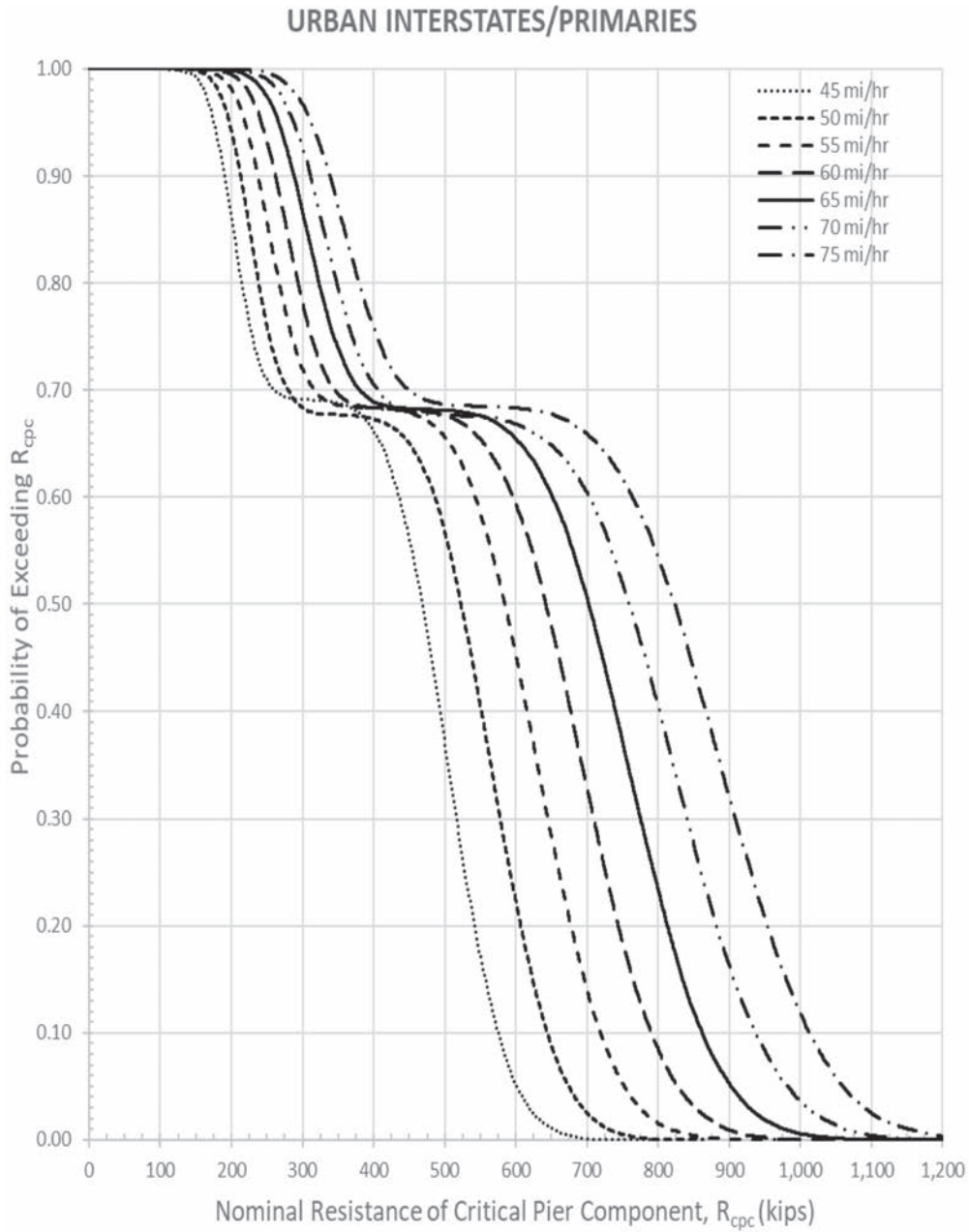


Figure 17. Cumulative distribution of expected impact force – urban Interstates/primaries.

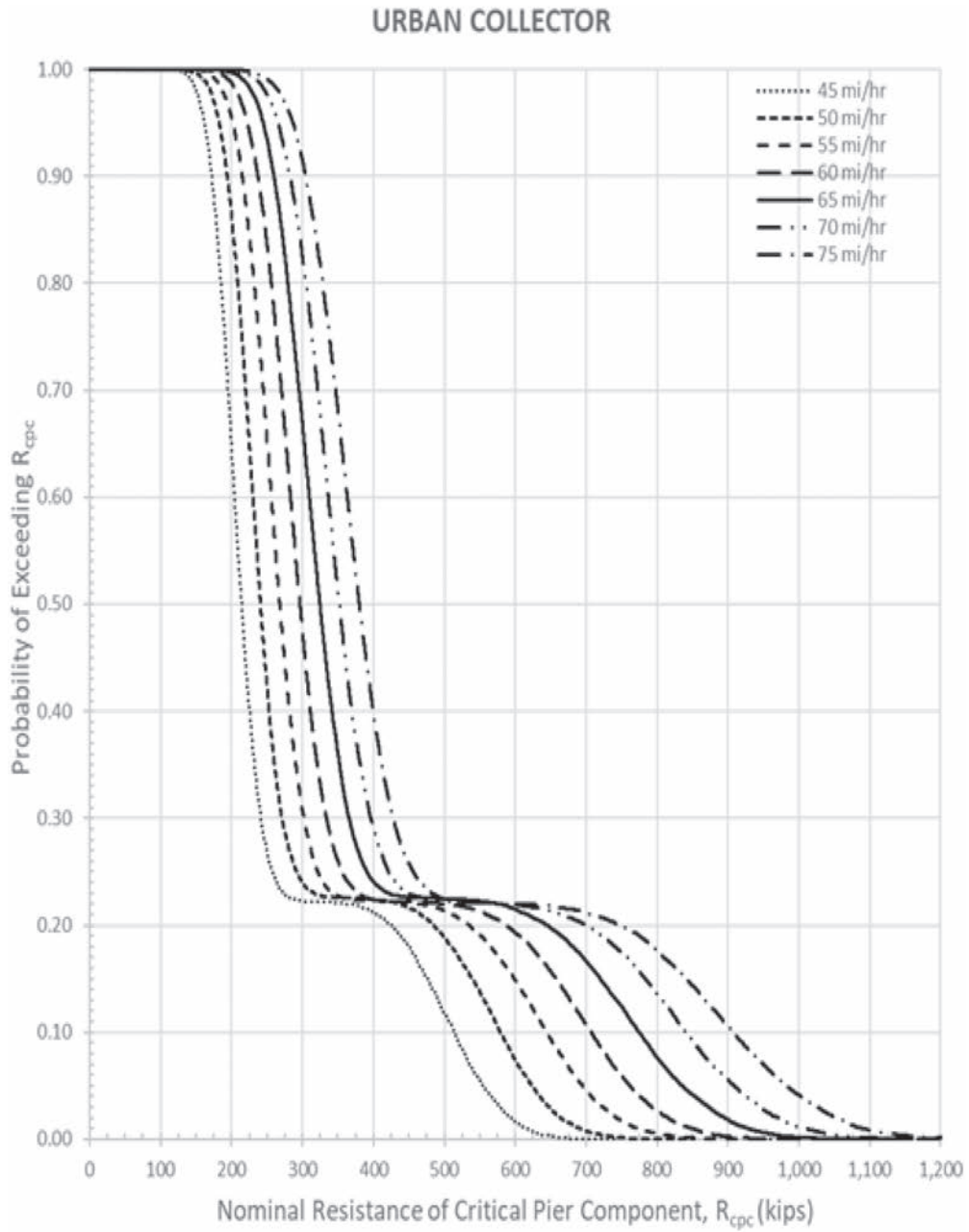


Figure 18. Cumulative distribution of expected impact force – urban collectors.

These figures indicate that large impact forces are primarily associated with tractor trailers, as expected. This is also confirmed by Table 3 and Table 4, where all but two of the 24 real-world crashes found in the literature involved tractor trailers. Of the two non-tractor-trailer trucks, one was an intercity bus that did not cause the pier column to fail, and the other was a single-unit truck that caused the column to fail but did not cause the bridge to collapse. There were 16 cases where a truck caused the pier column to fail, and all but one was a tractor-trailer truck. Table 3 also lends support to the idea that the total weight of the truck is not determinative of pier column failure. While some cases did involve very heavy vehicles hauling heavy, rigid loads, at least one (e.g., Buth #19 [Buth 2010]) was an unloaded tractor-trailer that was still able to cause a pier column to fail.

Figure 15 through Figure 18 are shown in guideline form in Table 7. The user enters the table for the appropriate functional classification of the roadway of interest with nominal lateral load capacity of the column (R_{CPC}) and reads over to the column corresponding to the PSL of interest. The value tabulated is the probability that the impact force (Q_{CT}) will exceed the nominal lateral load capacity of the column (R_{CPC}).

In Table 7, the probability of exceeding the nominal lateral resistance increases in each row as the PSL increases, as expected. Similarly, the probability of exceeding the nominal lateral resistance decreases in each column as the nominal lateral resistance increases, which is also as expected. If the probability of exceeding a nominal lateral resistance of 600 kips on a 65-mph roadway is examined in Table 7, the highest probability of exceed the lateral resistance is 0.76 (rounded) on a rural primary route. Rural primary roadways have the highest percentage of tractor trailers of the four functional class categories, and the long-distance movement of goods is one of the primary functions of rural primary routes. The probability of exceeding 600 kips on a 65-mph rural collector is much less (i.e., 0.32 rounded) because there are fewer tractor-trailer trucks, and the weight distribution on those roads is not as heavy. Similarly, a pier located on a 65-mph urban primary highway would have a probability of 0.65 (rounded) of exceeding 600 kips, a little lower than the rural primary roads because the percentage of trucks is somewhat lower. Like the rural collectors, a bridge pier on a 65-mph urban collector would have a probability of exceeding 600 kips of only 0.22 (rounded) because the heavy-vehicle mix is dominated by smaller, lighter, single-unit trucks. In other words, the data summarized in Figure 15 through Figure 18 and Table 7 make intuitive sense. The most at-risk piers are those on high-speed rural Interstates, whereas those on low-speed urban collectors are at relatively low risk, all other characteristics being equal.

3.2.2 Design Load

Appendix D describes scaled model impact tests, finite element impact analyses of the representative pier column designs, a full-scale tractor-trailer truck crash test, and finite element analyses of 80,000-lb tractor-trailer truck impacts with the representative pier designs. The research team suggests that the current *LRFD Bridge Design Specifications* recommendation of a 600-kip lateral load capacity be retained. This value was based on the peak 25-ms impact force observed in a full-scale 50-mph head-on crash test of an 80,000-lb tractor-trailer truck and a rigid column. The analyses described in Appendix D showed that circular columns 30 in. in diameter and smaller are likely to fail in an impact with an 80,000-lb tractor-trailer truck striking the column head-on at 50 mph. Such columns generally have a simple-hinge lateral impact load capacity of under 600 kips, so they are at high risk of catastrophic failure in the field.

The 600-kip design load, however, should not be limited to the shear capacity of the column. The limiting loading may arise from any of the following:

- Shear strength of the column,
- Flexural strength of the column,
- Connection strength between the column and pier cap or bent, or
- Connection strength between the column base and foundation.

In accessing the nominal lateral capacity, the user should determine which of these components is the limiting loading on the pier component.

3.2.3 Point of Load Application

The eighth edition of the *LRFD Bridge Design Specifications* recommends that the 600-kip impact load be applied to the column 5 ft above the grade [AASHTO 2017], but the FEA described in Appendix D shows clearly that the peak load is associated with the impact of the engine of the tractor, which is located much lower, typically at the bumper level of 2 ft. The impact load should be applied at a distance between 2 and 5 ft, whichever results in the worst-case loading. The guidelines user should check not only the impact load capacity at the level of impact but also the resulting moments at the pier cap and foundation to ensure that the connections have sufficient strength to resist the impact. For example, 2 ft might be used when assessing the column–cap connection because this would maximize the moment on the connection, whereas 5 ft might be appropriate for assessing the column–foundation connection.

Table 7. Probability of impact force (Q_{CT}) exceeding critical pier component nominal lateral resistance (R_{CPC}).

R_{CPC}	Rural Interstates and Primaries							Rural Collectors						
	Posted Speed Limit (mi/hr)							Posted Speed Limit (mi/hr)						
	≤45	50	55	60	65	70	≥75	≤45	50	55	60	65	70	≥75
100	0.9999	1.0000	1.0000	1.0000	1.0000	1.0000	1.0000	1.0000	1.0000	1.0000	1.0000	1.0000	1.0000	1.0000
150	0.9939	0.9989	0.9999	1.0000	1.0000	1.0000	1.0000	0.9817	0.9969	0.9993	1.0000	1.0000	1.0000	1.0000
200	0.9063	0.9629	0.9890	0.9966	0.9992	0.9996	0.9999	0.6980	0.8826	0.9609	0.9892	0.9960	0.9994	0.9998
250	0.8058	0.8422	0.9049	0.9565	0.9824	0.9935	0.9974	0.3710	0.5055	0.7018	0.8602	0.9431	0.9792	0.9930
300	0.7931	0.7928	0.8125	0.8566	0.9116	0.9533	0.9771	0.3322	0.3429	0.4023	0.5462	0.7134	0.8523	0.9283
350	0.7892	0.7884	0.7907	0.7996	0.8279	0.8684	0.9142	0.3302	0.3315	0.3350	0.3657	0.4455	0.5800	0.7291
400	0.7584	0.7832	0.7886	0.7902	0.7978	0.8079	0.8370	0.3179	0.3294	0.3300	0.3374	0.3464	0.3897	0.4873
450	0.6440	0.7550	0.7820	0.7887	0.7931	0.7914	0.7990	0.2720	0.3177	0.3280	0.3358	0.3327	0.3357	0.3622
500	0.4232	0.6620	0.7552	0.7817	0.7912	0.7894	0.7901	0.1797	0.2770	0.3163	0.3328	0.3313	0.3296	0.3360
550	0.1964	0.4754	0.6731	0.7570	0.7843	0.7879	0.7888	0.0817	0.1993	0.2837	0.3213	0.3290	0.3285	0.3323
600	0.0597	0.2628	0.5216	0.6903	0.7602	0.7810	0.7870	0.0254	0.1086	0.2163	0.2895	0.3183	0.3261	0.3313
650	0.0125	0.1054	0.3292	0.5582	0.6999	0.7584	0.7790	0.0056	0.0432	0.1397	0.2356	0.2942	0.3174	0.3287
700	0.0016	0.0312	0.1614	0.3816	0.5883	0.7076	0.7586	0.0008	0.0130	0.0657	0.1645	0.2463	0.2956	0.3193
750	0.0002	0.0067	0.0584	0.2132	0.4338	0.6144	0.7095	0.0000	0.0028	0.0253	0.0916	0.1833	0.2550	0.2998
800	0.0000	0.0008	0.0177	0.0958	0.2706	0.4781	0.6263	0.0000	0.0005	0.0070	0.0429	0.1129	0.1975	0.2666
850	0.0000	0.0001	0.0048	0.0361	0.1390	0.3246	0.5072	0.0000	0.0001	0.0016	0.0158	0.0610	0.1343	0.2167
900	0.0000	0.0000	0.0007	0.0098	0.0594	0.1934	0.3692	0.0000	0.0000	0.0003	0.0048	0.0269	0.0796	0.1571
950	0.0000	0.0000	0.0001	0.0024	0.0224	0.0988	0.2362	0.0000	0.0000	0.0001	0.0012	0.0107	0.0400	0.0998
1,000	0.0000	0.0000	0.0000	0.0006	0.0065	0.0431	0.1363	0.0000	0.0000	0.0001	0.0002	0.0033	0.0165	0.0559
1,050	0.0000	0.0000	0.0000	0.0000	0.0018	0.0155	0.0670	0.0000	0.0000	0.0000	0.0000	0.0010	0.0063	0.0260
1,100	0.0000	0.0000	0.0000	0.0000	0.0006	0.0054	0.0285	0.0000	0.0000	0.0000	0.0000	0.0002	0.0018	0.0117
1,150	0.0000	0.0000	0.0000	0.0000	0.0001	0.0015	0.0102	0.0000	0.0000	0.0000	0.0000	0.0000	0.0005	0.0042
1,200	0.0000	0.0000	0.0000	0.0000	0.0000	0.0001	0.0034	0.0000	0.0000	0.0000	0.0000	0.0000	0.0002	0.0014
1,250	0.0000	0.0000	0.0000	0.0000	0.0000	0.0000	0.0011	0.0000	0.0000	0.0000	0.0000	0.0000	0.0001	0.0004
1,300	0.0000	0.0000	0.0000	0.0000	0.0000	0.0000	0.0002	0.0000	0.0000	0.0000	0.0000	0.0000	0.0000	0.0001

R_{CPC}	Urban Interstates and Primaries							Urban Collectors						
	Posted Speed Limit (mi/hr)							Posted Speed Limit (mi/hr)						
	≤45	50	55	60	65	70	≥75	≤45	50	55	60	65	70	≥75
100	1.0000	1.0000	1.0000	1.0000	1.0000	1.0000	1.0000	1.0000	1.0000	1.0000	1.0000	1.0000	1.0000	1.0000
150	0.9924	0.9986	0.9996	0.9999	1.0000	1.0000	1.0000	0.9798	0.9961	0.9996	0.9997	0.9999	1.0000	1.0000
200	0.8599	0.9419	0.9813	0.9947	0.9987	0.9995	0.9998	0.6462	0.8638	0.9551	0.9870	0.9969	0.9990	0.9996
250	0.7093	0.7597	0.8573	0.9322	0.9743	0.9903	0.9966	0.2676	0.4239	0.6550	0.8368	0.9350	0.9763	0.9908
300	0.6915	0.6837	0.7196	0.7815	0.8663	0.9264	0.9673	0.2228	0.2396	0.3082	0.4745	0.6701	0.8248	0.9155
350	0.6876	0.6769	0.6858	0.6962	0.7394	0.7954	0.8723	0.2211	0.2260	0.2274	0.2599	0.3610	0.5123	0.6816
400	0.6622	0.6728	0.6832	0.6832	0.6890	0.7054	0.7587	0.2129	0.2245	0.2228	0.2237	0.2410	0.2901	0.3987
450	0.5611	0.6504	0.6791	0.6816	0.6826	0.6795	0.6997	0.1798	0.2166	0.2210	0.2216	0.2258	0.2295	0.2579
500	0.3724	0.5678	0.6562	0.6764	0.6812	0.6764	0.6869	0.1187	0.1887	0.2139	0.2199	0.2248	0.2223	0.2245
550	0.1718	0.4055	0.5845	0.6542	0.6758	0.6751	0.6850	0.0552	0.1377	0.1914	0.2128	0.2227	0.2211	0.2208
600	0.0513	0.2231	0.4522	0.5932	0.6544	0.6681	0.6833	0.0161	0.0742	0.1486	0.1932	0.2151	0.2191	0.2200
650	0.0110	0.0886	0.2836	0.4795	0.6024	0.6485	0.6775	0.0029	0.0284	0.0937	0.1574	0.1975	0.2134	0.2180
700	0.0010	0.0252	0.1410	0.3302	0.5068	0.6042	0.6589	0.0003	0.0079	0.0461	0.1071	0.1666	0.1998	0.2118
750	0.0002	0.0051	0.0529	0.1847	0.3724	0.5194	0.6170	0.0000	0.0019	0.0172	0.0592	0.1246	0.1741	0.1992
800	0.0000	0.0005	0.0155	0.0851	0.2344	0.4050	0.5437	0.0000	0.0003	0.0054	0.0266	0.0758	0.1356	0.1761
850	0.0000	0.0001	0.0038	0.0315	0.1200	0.2770	0.4387	0.0000	0.0000	0.0012	0.0100	0.0417	0.0924	0.1435
900	0.0000	0.0000	0.0008	0.0092	0.0529	0.1636	0.3200	0.0000	0.0000	0.0003	0.0026	0.0182	0.0554	0.1055
950	0.0000	0.0000	0.0001	0.0022	0.0184	0.0836	0.2076	0.0000	0.0000	0.0000	0.0005	0.0067	0.0279	0.0698
1,000	0.0000	0.0000	0.0000	0.0003	0.0055	0.0356	0.1186	0.0000	0.0000	0.0000	0.0001	0.0018	0.0116	0.0411
1,050	0.0000	0.0000	0.0000	0.0000	0.0016	0.0138	0.0584	0.0000	0.0000	0.0000	0.0000	0.0006	0.0041	0.0210
1,100	0.0000	0.0000	0.0000	0.0000	0.0004	0.0042	0.0252	0.0000	0.0000	0.0000	0.0000	0.0001	0.0015	0.0088
1,150	0.0000	0.0000	0.0000	0.0000	0.0000	0.0010	0.0104	0.0000	0.0000	0.0000	0.0000	0.0000	0.0004	0.0038
1,200	0.0000	0.0000	0.0000	0.0000	0.0000	0.0001	0.0031	0.0000	0.0000	0.0000	0.0000	0.0000	0.0002	0.0013
1,250	0.0000	0.0000	0.0000	0.0000	0.0000	0.0000	0.0008	0.0000	0.0000	0.0000	0.0000	0.0000	0.0000	0.0004
1,300	0.0000	0.0000	0.0000	0.0000	0.0000	0.0000	0.0002	0.0000	0.0000	0.0000	0.0000	0.0000	0.0000	0.0001

3.3 Design Choice Is Shielding with a Barrier

If the design choice is to shield the bridge pier system, the bridge engineer should evaluate whether a shielding barrier is necessary given the traffic, site, and structural characteristics of the pier system. The procedure suggested for evaluating bridge piers for protection is outlined in Table 8 and involves finding the following four values:

- HVE_{*i*} = The expected annual number of heavy-vehicle encroachments in direction *i* is found using Table 13 using the highway type, traffic volume, and percentage of trucks.
- N_{*i*} = The site-specific adjustment factor is found using Table 15 and the characteristics of the study site.
- P(C|HVE_{*i*}) = The probability of a crash given a heavy-vehicle encroachment in direction *i* is found by using Table 19 using the pier component offset and size in each direction *i*.

$P(Q_{CT} > R_{CPC} | C)$ = The probability of the worst-case collision force (Q_{CT}) exceeding the critical pier component capacity (R_{CPC}) from Table 7.

The product of these four values is the estimated annual frequency of bridge collapse for the unshielded pier. If this value is less than 0.0001 for a critical bridge or 0.0010 for a typical bridge, the pier system need not be shielded for pier protection. If this value is greater than or equal to 0.0001 for a critical bridge or 0.0010 for a typical bridge, the pier system should be shielded with a rigid concrete MASH TL-5 barrier that is at least 42 in. tall. The research to determine these four values and apply them to assessing the need for pier protection is presented in the following sections.

3.3.1 Heavy-Vehicle Encroachment: HVE_{*i*}

The first value needed to assess the need for pier protection in Table 8 is the estimated number of heavy vehicles that will leave the travel lanes in a year under “base conditions” (HVE_{*i*}). Base conditions assume that the highway is straight and flat with 12-ft travel lanes, zero major access points/mi, and a PSL

Table 8. LRFD Bridge Design Specifications pier protection procedure.

Find:	The annual frequency of bridge collapse for an unshielded pier system (i.e., AF _{BC CUSP}).
Given:	<p>The following traffic and site characteristics for each approach direction where a pier component is exposed to approaching traffic:</p> <ul style="list-style-type: none"> • The highway type (i.e., divided, undivided, or one-way); • The lateral structural resistance to impact (R_{CPC}); • Site-specific characteristics like the number of lanes, lane width, major access points, PSL, radius of horizontal curvature, and grade of the highway; • Total two-way AADT in vehicles/day; • Percentage of trucks (PT_{<i>i</i>}) in each approach direction; • Perpendicular distance in ft from the edge of the travel for each direction of travel to the face of the nearest pier component (P_i); and • Diameter in ft for circular pier columns, the smallest cross-sectional dimension for rectangular pier columns, or the thickness for pier walls of the pier component (D_i) nearest to relative direction of travel where the offset (P_i) is measured perpendicular to nearest edge of the lane for the travel direction under consideration to the face of the pier.
Procedure:	<p>Calculate the annual frequency of bridge collapse with an unshielded pier (AF_{BC}) as:</p> $AF_{BC} = \sum_{i=1}^m HVE_i \cdot N_i \cdot P(C HVE_i) \cdot P(Q_{CT} > R_{CPC} C)$ <p>where</p> <ul style="list-style-type: none"> HVE_{<i>i</i>} from Table 13, N_{<i>i</i>} from Table 15, P(C HVE_{<i>i</i>}) from Table 19, and $P(Q_{CT} > R_{CPC} C)$ from Table 7. <p>If AF_{BC} > 0.0010 for a typical bridge, Or AF_{BC} > 0.0001 for a critical bridge, Then Shield with a MASH TL-5 rigid concrete barrier, Else Does not require shielding for pier protection, but consider shielding for occupant protection as outlined in the RDG.</p>

Table 9. Procedure to find the heavy-vehicle encroachments: HVE_i.

Find:	The annual frequency of heavy-vehicle encroachments for the pier system under consideration for base conditions.
Given:	The following traffic and site characteristics for each approach direction where a pier component is exposed to approaching traffic: <ul style="list-style-type: none"> • The highway type (i.e., divided, undivided, or one-way), • Site-specific encroachment adjustment factor (N_i) for each approach direction from the last step, • Total two-way AADT in vehicles/day, and • Percentage of trucks (PT_i).
Procedure:	Calculate the base annual frequency of heavy-vehicle collisions with an unshielded pier component from each direction of travel as follows: $HVE_i = \left[\frac{ENCR_i \cdot PT_i \cdot f_{HV} \cdot ENCR_i}{7,040} \right] \text{ (Table 13)}$ where ENCR = base vehicle encroachment. Repeat this step for each direction of travel where a pier component is exposed to approaching traffic.

of 65 mph. In addition, if the highway is a divided highway, it is assumed that there are two lanes in each direction, whereas if it is an undivided highway, it is assumed there is one lane in each direction. Accounting for departures from the base conditions (e.g., lanes 11 ft wide or a 6-lane divided highway) will take place in the next step. The number of heavy vehicles that are expected to leave the roadway in a typical year are estimated for each direction of interest, as outlined in Table 9.

The so-called Cooper encroachment data are used in RSAPv3 to predict the number of vehicle encroachments based on the highway type and AADT. Details of the development of the models used in the prediction model are found in the RSAPv3 Engineer's Manual [Ray 2012]. Encroachment modeling is based on the assumption that traffic is in a free-flow condition, which implies service levels better than D. For the base conditions, service level D [HCM 2016] occurs for two-lane undivided highways at an AADT of 46,000 vehicles/day, and for a four-lane divided highway at an AADT of 90,000 vehicles/day; therefore, the values in Table 10 are limited to these values [Ray 2014b]. For traffic volumes above these values, the encroachment frequency at 90,000 for divided highways and 46,000 for undivided highways should be used. This approach ensures that the assumptions used in developing the underlying models are not violated in the application of the models.

One of the interesting features of the Cooper data is that there is a pronounced “hump” for both the undivided and divided models. This means, for example, that the encroachments reach a peak of 2.5811 encroachments/mi/year for undivided highways at an AADT of 6,000 vehicles/day, and then the encroachments decrease to a value of 0.9819 encroachments/mi/year at an AADT of 15,000 vehicles/day. After this point, the encroachments increase linearly with AADT. The divided highway encroachment model exhibits a similar peak feature, as shown in Figure 19.

For the purpose of developing guidelines, it would be conservative to ignore the valley that follows the peak and adopt a constant value, as shown by the dotted lines Figure 19. Otherwise, a small change in AADT due to either imprecise measurement or traffic growth might change the prediction. The dotted lines in Figure 19 and the values in Table 11 smooth out the Cooper encroachment data for use in these guidelines.

The encroachment models given in Table 11 are used to estimate the number of heavy-vehicle encroachments given the percentage of trucks (PT) in each direction of interest. Also, the encroachment models are based on a 1-mile segment length, but the maximum trajectory length in RSAPv3 based on the collected field trajectories from NCHRP Project 17-22

Table 10. Base encroachment frequencies in encroachments/mile/year.

<u>Undivided Highways</u>	
$0 \leq \text{AADT} < 15,000$:	$ENCR_{\text{UNDIV_BASE}} = 915.712 \text{ AADT} 10^{-6} e^{(0.4997 - 0.2092 \text{ AADT}/1000)}$
$15,000 \leq \text{AADT} \leq 46,000$:	$ENCR_{\text{UNDIV_BASE}} = 65.473 \text{ AADT} 10^{-6}$
$\text{AADT} > 46,000$:	$ENCR_{\text{UNDIV_BASE}} = 3.0119$
<u>Divided Highways</u>	
$0 \leq \text{AADT} < 41,000$:	$ENCR_{\text{DIV_BASE}} = 1089.744 \text{ AADT} 10^{-6} e^{(-0.2104 - 0.04128 \text{ AADT}/1000)}$
$41,000 \leq \text{AADT} \leq 90,000$:	$ENCR_{\text{DIV_BASE}} = 169.346 \text{ AADT} 10^{-6}$
$\text{AADT} > 90,000$:	$ENCR_{\text{DIV_BASE}} = 15.2412$

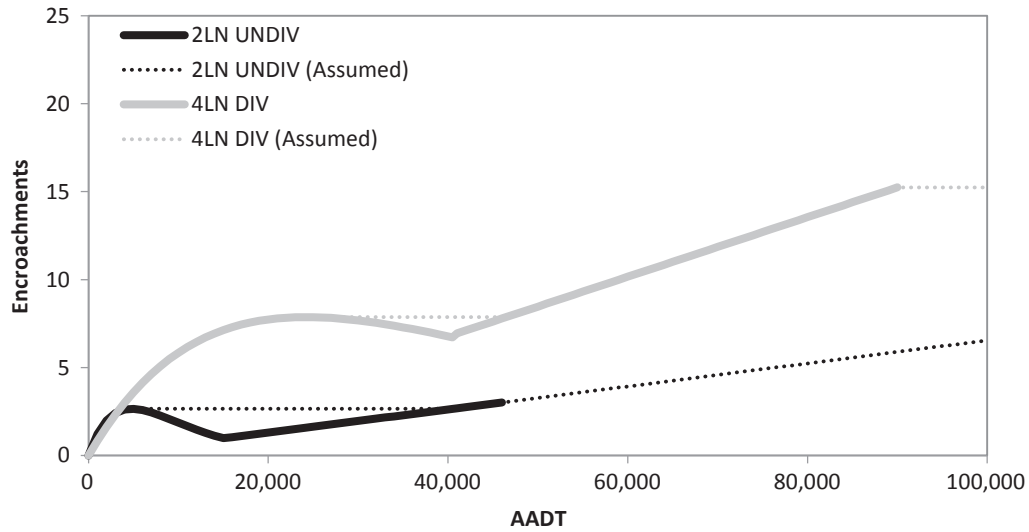


Figure 19. Cooper encroachment frequency (solid lines) and approximation use for guidelines (dotted lines).

is 300 ft. For fixed-point hazards like bridge piers, only trajectories that depart within 300 ft upstream of the pier are likely to strike the leading component of the pier, so the segment length is 300 ft; the encroachment frequency should therefore be multiplied by $300/5,280 = 0.0568$.

Research has also found that heavy vehicles do not encroach at the same rate as passenger vehicles [Carrigan 2014]. Carrigan et al. developed a heavy-vehicle encroachment adjustment factor to account for the difference in encroachment frequency for heavy vehicles as a function of PT, as shown in Table 12 [Carrigan 2014].

Now that all the pieces needed to develop an equation to estimate heavy-vehicle encroachments under base conditions are available, an equation can be assembled. The encroachment frequencies given previously are for all possible encroachment directions, but each encroachment direction must be evaluated separately in this procedure, so the

total number of encroachments should be divided by four to get the expected frequency in a single encroachment direction. For both divided and undivided highways, there are four possible encroachment directions: primary right, primary left, opposing right, and opposing left. Therefore, the heavy-vehicle base encroachment frequency in direction i for a highway segment 300 ft upstream of a bridge pier can be written as:

$$HVE_i = \left[\frac{ENCR_i}{4} \right] \cdot \left[\frac{PT_i}{100} \right] \cdot f_{HV\ ENCR_i} \cdot \left[\frac{300}{5,280} \right]$$

$$= \frac{ENCR_i \cdot PT_i \cdot f_{HV\ ENCR_i}}{7,040}$$

Where $ENCR_i$ is the value or equation from Table 11 for the appropriate highway type and traffic volume and $f_{HV\ ENCR}$ is the appropriate value from Table 12. This equation was used to

Table 11. Suggested base vehicle encroachment frequencies for guidelines.

<u>Undivided Highways</u>	
$0 \leq AADT < 5,000$	$= 915.712 AADT 10^{-6} e^{(0.4997 - 0.2092 AADT/1000)}$
$5,000 \leq AADT < 41,000$	$= 2.6514$
$41,000 \leq AADT < 46,000$	$= 65.473 AADT 10^{-6}$
$AADT > 46,000$	$= 3.0109$
<u>Divided Highways[†]</u>	
$0 \leq AADT < 24,000$	$= 1089.744 AADT 10^{-6} e^{(-0.2104 - 0.04128 AADT/1000)}$
$24,000 \leq AADT < 47,000$	$= 7.8686$
$47,000 \leq AADT \leq 90,000$	$= 169.346 AADT 10^{-6}$
$AADT > 90,000$	$= 15.2412$

Note: Encroachment data are not available for one-way roadways. Traditionally, one-way roadways have been evaluated using the encroachment model for divided highways. The one-way AADT value should be multiplied by 2 and used to determine $ENCR_{DIV\ BASE}$ to be used in the remaining calculations.

Table 12. Heavy-vehicle encroachment adjustment factor ($f_{HV\ ENCR}$).

Undivided Highways		Divided and One-Way Highways			
PT < 10 $f_{UNDIV} = 1.00$		PT ≤ 5 $f_{DIV} = 1.00$			
PT ≥ 10 $f_{UNDIV} = 6.951 PT^{-0.828}$		PT > 5 $f_{DIV} = 4.6588 PT^{-0.953}$			
PT	$f_{UNDIV\ HV\ ENCR}$	PT	$f_{DIV\ HV\ ENCR}$	PT	$f_{DIV\ HV\ ENCR}$
10	1.00	1	1.00	10	0.52
15	0.74	5	1.00	15	0.35
20	0.58	6	0.84	20	0.27
25	0.48	7	0.73	25	0.22
30	0.42	8	0.64	30	0.18
40	0.33	9	0.57	40	0.14

develop the values of HVE_i for various traffic volumes, percentage of trucks, and highway types, as shown in Table 13.

3.3.2 Site-Specific Adjustment Factor: N_i

The second value needed to assess the need for pier protection in Table 14 is the site-specific adjustment factor, N_i . The

previous section described estimating the number of heavy-vehicle encroachments under ideal base conditions. This step modifies that ideal base condition value to account for the particular features of the site. The likelihood of a vehicle leaving the travel lanes has been shown to be related to traffic and roadway characteristics such as lane width, vertical grade, and horizontal curvature. There is a large body of literature documenting the change in crash or encroachment frequency based on the geometric characteristics of the roadway and the operational characteristics of traffic. Since these characteristics are important predictors of the probability of leaving the road, it is important to include them in a risk-based pier protection procedure.

Fortunately, the important adjustment factors have already been determined in other research projects. The currently available site-specific adjustment factors used in this research are shown in Table 15. Details about the development of the site-specific encroachment adjustment factors used to develop Table 15 can be found in the RSAPv3 Engineer’s Manual [Ray

Table 13. Base annual heavy-vehicle encroachments in direction i (HVE_i).

Two-Way AADT	Undivided Highways							
	PT							
	5	10	15	20	25	30	35	≥40
veh/day								
0	0	0	0	0	0	0	0	0
1,000	0.0009	0.0017	0.0019	0.0020	0.0021	0.0022	0.0022	0.0023
2,000	0.0014	0.0028	0.0031	0.0033	0.0034	0.0035	0.0036	0.0037
3,000	0.0017	0.0034	0.0038	0.0040	0.0042	0.0043	0.0044	0.0045
4,000	0.0019	0.0037	0.0041	0.0043	0.0045	0.0046	0.0048	0.0049
5,000–41,000	0.0019	0.0038	0.0042	0.0044	0.0046	0.0047	0.0048	0.0049
42,000	0.0020	0.0039	0.0043	0.0045	0.0047	0.0049	0.0050	0.0051
43,000	0.0020	0.0040	0.0044	0.0047	0.0048	0.0050	0.0051	0.0052
44,000	0.0020	0.0041	0.0045	0.0048	0.0049	0.0051	0.0052	0.0054
45,000	0.0021	0.0042	0.0046	0.0049	0.0051	0.0052	0.0054	0.0055
≥46,000	0.0021	0.0043	0.0047	0.0050	0.0052	0.0053	0.0055	0.0056
Two-Way AADT	Divided Highways							
veh/day	PT							
	5	10	15	20	25	30	35	≥40
1,000	0.0006	0.0006	0.0006	0.0006	0.0007	0.0007	0.0007	0.0007
5,000	0.0026	0.0026	0.0027	0.0027	0.0028	0.0028	0.0028	0.0028
10,000	0.0042	0.0043	0.0044	0.0045	0.0045	0.0045	0.0046	0.0046
15,000	0.0051	0.0053	0.0054	0.0054	0.0055	0.0055	0.0056	0.0056
20,000	0.0055	0.0057	0.0058	0.0059	0.0060	0.0060	0.0060	0.0061
24,000–47,000	0.0056	0.0058	0.0059	0.0060	0.0061	0.0061	0.0062	0.0062
50,000	0.0060	0.0062	0.0064	0.0065	0.0065	0.0066	0.0066	0.0067
55,000	0.0066	0.0069	0.0070	0.0071	0.0072	0.0072	0.0073	0.0073
60,000	0.0072	0.0075	0.0076	0.0077	0.0078	0.0079	0.0079	0.0080
65,000	0.0078	0.0081	0.0083	0.0084	0.0085	0.0085	0.0086	0.0087
70,000	0.0084	0.0087	0.0089	0.0090	0.0091	0.0092	0.0093	0.0093
75,000	0.0090	0.0094	0.0095	0.0097	0.0098	0.0099	0.0099	0.0100
80,000	0.0096	0.0100	0.0102	0.0103	0.0104	0.0105	0.0106	0.0107
85,000	0.0102	0.0106	0.0108	0.0110	0.0111	0.0112	0.0113	0.0113
≥ 90,000	0.0108	0.0112	0.0115	0.0116	0.0117	0.0118	0.0119	0.0120

Note: Encroachment data are not available for one-way roadways. One-way roadways should be evaluated using the encroachment model for divided highways where the one-way AADT value should be multiplied by 2 and used to determine HVE_i for use in the calculations.

Table 14. Procedure to find the site-specific adjustment factor (N_i).

Find:	The site-specific encroachment adjustment factor (N_i) for the pier system under consideration with respect to direction.
Given:	The following characteristics of the pier system under consideration by direction: <ul style="list-style-type: none"> • Number of major access points within 300 ft in advance of the pier system, • Radius of horizontal curvature in ft, • Number of lanes approaching the pier system, • PSL (in mph) approaching the pier system, • Lane width in ft, and • Grade (as a percentage) approaching the pier system.
Procedure:	Use Table 15 to find each encroachment adjustment factor with respect to approach direction. Multiply the adjustments together to obtain the site-specific encroachment adjustment factor for each approach direction (N_i).

2012] and the forthcoming final reports for NCHRP Project 22-12(03) and NCHRP Project 17-54 [Ray 2014b, Carrigan 2017]. Each site-specific adjustment factor (N_i) should be calculated for each direction of possible encroachment (i). The direction number (e.g., $i = 1, 2, 3$) is arbitrary, but the site-specific adjustment must always be matched to the offset

(P_i) and traffic characteristics (HVE_{*i*}, etc.) associated with that direction of travel in later steps. The procedure for calculating the site-specific adjustment factor (N_i) is outlined in Table 14. The quantity HVE_{*i*} · N_i is the estimated annual frequency of heavy-vehicle encroachments with the particular site and traffic characteristics of interest.

Table 15. Site-specific adjustment factor (N_i).

Major Accesses [‡]			Lane Width			Horizontal Curve Radius [†]	
Number of access points within 300ft upstream of the pier system	Undivided	Divided and one-way	Avg. lane width in ft	Undivided	Divided and one-way	Horizontal curve radius at centerline in ft	All highway types
	0	1.0		1.0	≤9		
1	1.5	2.0	10	1.30	1.15	10,000 ≥ AR > 432	Exp(474.4/AR)
2 ≤	2.2	4.0	11	1.05	1.03	432 ≥ AR > 0	3.00
			≥12	1.00	1.00	TR > 10,000	1.00
						10,000 ≥ TR > 432	Exp(173.6/TR)
						432 ≥ TR > 0	1.50
$f_{ACC} =$			$f_{LW} =$			$f_{HC} =$	
Lanes in One Direction			Posted Speed Limit [¶]			Grade Approaching the Pier System ^{††}	
No. of through lanes in one direction	Undivided	Divided and one-way	Posted speed limit	Undivided	Divided and one-way	Percent grade	All highway types
	1	1.00		1.00	<65		
2	0.76	1.00	≥65	1.00	1.00	-6 < G < -2	0.5 - G/4
≥3	0.76	0.91				-2 ≤ G	1.00
$f_{LN} =$			$f_{PSL} =$			$f_G =$	
$N_i = f_{ACC} \cdot f_{LN} \cdot f_{LW} \cdot f_G \cdot f_{HC} \cdot f_{PSL} =$							

Notes: ACC = major accesses, LW = lane width, HC = horizontal curve radius, LN = lanes in one direction, and G = grade approaching the pier system.
[‡]Major accesses include ramps and intersections. Commercial and residential driveways should not be included as access points unless they are signalized or stop-sign controlled.
[†]The horizontal curve radius may either curve away (AR) from the pier system under consideration or toward it (TR). When the driver is turning the wheel of the vehicle away from the pier, the AR adjustments should be used. When the driver is turning the wheel of the vehicle toward the pier, the TR adjustments should be used. This adjustment must be considered for each direction of travel (i) where an encroaching vehicle could approach the pier system.
^{††}The grade (G) approaching the pier system must be considered for each direction of travel (i). Positive values indicate an uphill grade, and negative values indicate a downhill grade.
[¶]For roads with unposted speed limits, use the adjustment for <65 mph.

3.3.3 Probability of a Collision Given a Heavy-Vehicle Encroachment: $P(C|HVE_i)$

The third value needed to assess the need for pier protection in Table 8 is the probability of a collision given a heavy-vehicle encroachment has occurred [$P(C|HVE_i)$]. Not all heavy vehicles that leave the roadway will strike the pier system. Some will stop prior to contacting the pier system, and some will pass in front of or behind the pier system. The closer the pier components are to the road, the more likely they are to be struck. Similarly, the larger the pier system, the more likely it is to be struck. The procedure for finding the probability of a collision given a heavy-vehicle encroachment [$P(C|HVE_i)$] is outlined in Table 16.

Now that the annual frequency of heavy-vehicle encroachments at the study location is known (i.e., $HVE_i \cdot N_i$), the probability of any particular heavy-vehicle encroachment striking a pier component must be determined based on the pier component size and offset from the direction of travel. RSAPv3 simulations were performed with the leading pier column offset distance between the edge of the nearest lane and the face of the nearest pier component varied in 2-ft increments. The objective was to determine the conditional probability of a crash with a pier component given that an encroachment has occurred [$P(C|HVE_i)$] when the size of the pier component and the offset to the pier component are known. It was assumed that the probability of observing a crash given that an encroachment has occurred is the same on both the median and roadside. A study design that distinguished between vehicles that crash and vehicles that do not

crash given an encroachment for various pier offsets and sizes was, therefore, pursued.

A database of simulated heavy-vehicle trajectories that encroached onto the roadside within 300 ft of the pier component was generated using RSAPv3 [Ray 2016] for a variety of pier component offsets and diameters. The predicted probability of a heavy-vehicle crash by pier component offset and diameter was then determined.

Ray et al. conducted a study to develop heavy-vehicle trajectories from the limited trajectory data currently available [Ray 2017a]. These heavy-vehicle trajectories were added to RSAPv3 and used to simulate 165,120 heavy-vehicle encroachments within 300 ft of a critical pier component where the component of interest was a single pier column with a variable diameter

The pier component was studied at a variety of offsets measured from the edge of the travel lane to the pier face. These discrete offsets (4, 6, 8, 10, 15, 20, 25, and 30 ft) were considered for four different pier column diameters (1, 2, 3, and 4 ft). The 165,120 heavy-vehicle encroachment trajectory study population is tabulated for each offset and diameter in Table 17.

The trajectory data include two variables of interest for crashes with piers: offset and size (e.g., diameter). The probability of a crash given an encroachment [$P(C|HVE_i)$] with any pier component is simply the portion or percentage of the vehicle type of interest that strikes the pier component divided by the total number of the vehicle type of interest that encroaches onto the roadside. Proportional data is strictly bounded between 0% and 100%; no less than 0% of the

Table 16. Procedure to find the probability of a collision given a heavy-vehicle encroachment: $P(C|HVE_i)$.

Find:	The probability of a collision given a heavy-vehicle encroachment with an unshielded pier [$P(C HVE_i)$] for the pier system under consideration.
Given:	The following traffic and site characteristics for each approach direction where a pier component is exposed to approaching traffic: <ul style="list-style-type: none"> • The highway type and layout (i.e., divided, undivided, or one-way), • Perpendicular distance in ft from the edge of the travel lane for each direction of travel to the face of the nearest pier component (P_i), and • Diameter in ft for circular pier columns, the smallest cross-sectional dimension for rectangular pier columns, or the thickness for pier walls of the pier component (D_i) nearest to the direction of travel where the offset (P_i) is measured perpendicular to nearest edge of the lane for the travel direction under consideration to the face of the pier.
Procedure:	Calculate the probability of a collision given a heavy-vehicle encroachment with an unshielded pier [$P(C HVE_i)$] for the pier system under consideration as follows: $P(C HVE_i) = \left[\frac{e^{-0.0396 P_i + 0.0706 D_i - 1.5725}}{1 + e^{-0.0396 P_i + 0.0706 D_i - 1.5725}} \right] \text{ (Table 19)}$ Repeat this step for each direction of travel where a pier component is exposed to approaching traffic.

Table 17. Simulated heavy-vehicle encroachment trajectory study population.

Offset (ft)	Outcome	Diameter (ft)			
		1	2	3	4
4	Crash	973	1,048	1,109	1,175
	Non-crash	4,187	4,112	4,051	3,985
6	Crash	835	899	957	922
	Non-crash	4,325	4,261	4,203	4,238
8	Crash	682	679	741	831
	Non-crash	4,478	4,481	4,419	4,329
10	Crash	576	644	724	753
	Non-crash	4,584	4,516	4,436	4,407
15	Crash	549	588	573	620
	Non-crash	4,611	4,572	4,587	4,540
20	Crash	474	503	544	590
	Non-crash	4,686	4,657	4,616	4,570
25	Crash	436	434	476	517
	Non-crash	4,724	4,726	4,684	4,643
30	Crash	377	411	442	467
	Non-crash	4,783	4,749	4,718	4,693

vehicles encroaching will avoid the crash and no more than 100% of the encroachment vehicles will have a crash. A logistic curve reaches asymptotes of 0 and unity; therefore, it prevents the model from fitting negative proportions and proportions greater than unity. Log odds provide an appropriate solution for regression, modeling a line fit using the maximum-likelihood method, as shown here:

$$\ln\left(\frac{C}{N}\right) = a + bX$$

where

- C = number of encroachments that resulted in a crash,
- N = number of encroachments where no crash occurred,
- $\frac{C}{N}$ = odds of a crash to no crash for all encroaching trajectories, and
- a, b = regression coefficients.

All of the encroachment trajectories in these datasets were considered either crash events (C) or non-crash events (N). The logit as a function of offset and diameter is transformed back to the probability of crash using the original relationship:

$$P(C|HVE_i) = \frac{e^{\beta_P P_i + \beta_D D_i + \epsilon}}{1 + e^{\beta_P P_i + \beta_D D_i + \epsilon}}$$

The statistical analysis and visual inspection of the data were completed using the software program R [R Core Team 2016].

The probabilities of a crash for each offset and diameter were determined from the RSAPv3 simulations and are shown in Figure 20. The dependent variable [P(C)] is shown on the

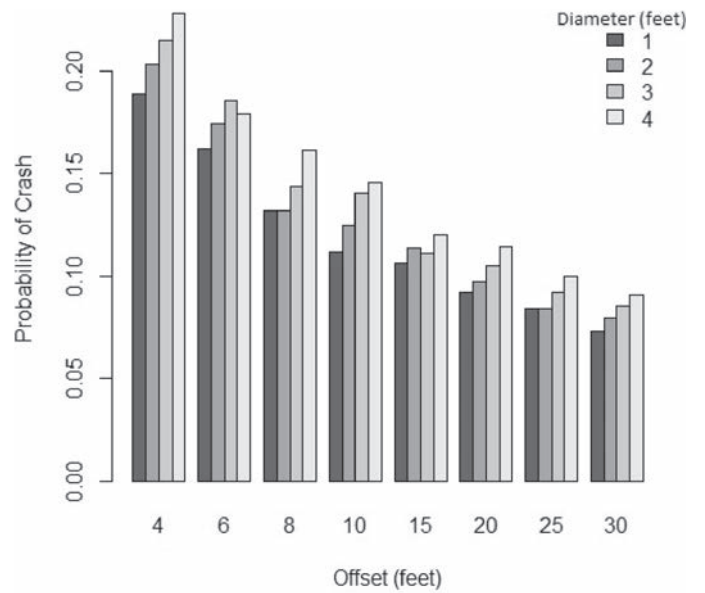


Figure 20. Observed probability of crash by offset and diameter.

y-axis. The main effects of the independent variables, diameter and offset, are shown on the x-axis. Figure 20 shows that the probability of a collision decreases as offset increases and size decreases. This is what would be expected since smaller pier components located farther from the road are expected to be less likely to be struck. A two-way interaction between variables is said to be present when the effect of one variable depends on the value of another variable. Figure 20 shows that there is little if any interaction between the variables' offset and diameter.

A regression function from the MASS package in the statistical analysis software R was used to fit the logit model discussed previously [Venables 2002, R Core Team 2016]. Based on the visual analysis of the data shown in Figure 20, modeling interaction between the variables was not considered necessary. On fitting a binomial logit distribution on the proportion of crash and non-crash data, both offset and diameter were found to be statistically significant predictors of a crash. The coefficients for the heavy-vehicle model are shown in Table 18. These coefficients are in logits. The process for changing from logit *x* to probabilities was shown in the previous equation. The predicted probability is shown graphically in Figure 21.

The probability of a crash given a heavy-vehicle encroachment [P(C|HVE_{*i*})] can now be written by inserting the coefficients found in Table 18 into the equation shown earlier as follows:

$$P(C|HVE_i) = \frac{e^{\beta_P P_i + \beta_D D_i + \epsilon}}{1 + e^{\beta_P P_i + \beta_D D_i + \epsilon}} = \frac{e^{-0.0398 P_i + 0.0709 D_i - 1.5331}}{1 + e^{-0.0398 P_i + 0.0709 D_i - 1.5331}}$$

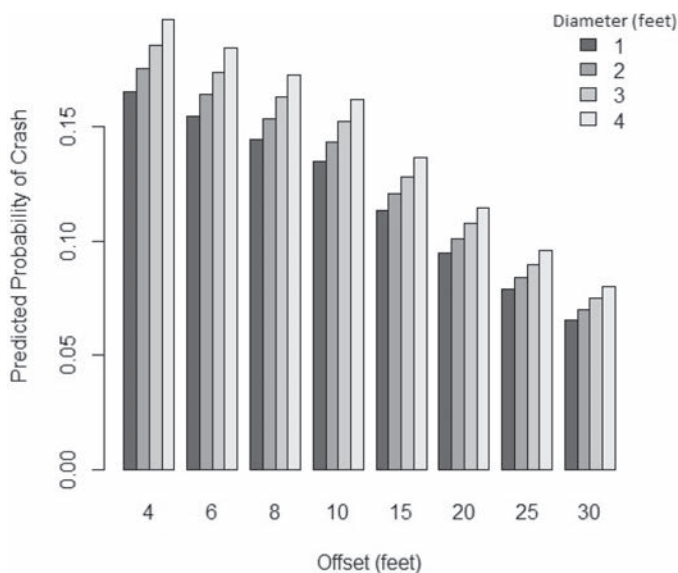
Table 18. Heavy-vehicle model coefficients on crash proportion.

	Estimate	Std. Error	z value	Pr(> t)	2.50%	97.50%
(Intercept)	-1.5331	0.02	-70.97	<2E-16	-1.5755	-1.4908
offset	-0.0398	0.00	-43.96	<2E-16	-0.0416	-0.0381
diameter	0.0709	0.01	10.77	<2E-16	0.0580	0.0839

Figure 22 is a plot of the observed probability of a crash for each simulated diameter and offset with an overlay of the predicted probability of a crash. The predicted probabilities closely track the observed probabilities; therefore, this model is a reasonable representation of the observed data. Pier component size in this context is either (1) the diameter of a circular pier column or (2) the largest dimension of a rectangular pier column. Values for a range of pier column offsets and sizes were calculated using the previous equation and are the basis of Table 19.

3.3.4 Probability of Worst-Case Collision Force Exceeding the Critical Pier Component Capacity Given a Collision: $P(Q_{CT} > R_{CPC} | C)$

The fourth value needed to assess the need for pier protection in Table 8 is the probability of a worst-case collision force exceeding the critical pier component's capacity [$P(Q_{CT} > R_{CPC} | C)$]. Even if a heavy vehicle encroaches onto the roadside and collides with a pier component, the pier component will only fail if its lateral impact resistance is less than the impact load. It is necessary in this step to (1) estimate the probability

**Figure 21. Predicted probability of crash by offset and diameter.**

distribution of the likely impact loads and (2) calculate the lateral resistance of the critical pier component. The procedure for finding the probability of the worst-case collision force exceeding the critical pier component capacity given a collision [$P(Q_{CT} > R_{CPC} | C)$] is outlined in Table 20.

3.3.4.1 Nominal Lateral Resistance of the Critical Pier Component: R_{CPC}

The guideline user must first establish, by calculation, the nominal lateral resistance of the critical pier component, as discussed in Appendix D.

3.3.4.2 Annual Frequency of Bridge Collapse: AF_{BC}

Now that the number of heavy vehicles expected to encroach onto the roadside (HVE_i) has been estimated, the site-specific adjustment factor (N_i) has been calculated, and the probability of a crash with a pier given a heavy-vehicle encroachment [$P(C | HVE_i)$] and the probability of an impact force greater than the capacity of the critical pier component [$P(Q_{CT} > R_{CPC})$] have been estimated, the annual frequency of bridge collapse (AF_{BC}) can be calculated, as outlined in Table 21. The acceptance criteria for the annual frequency of bridge collapse were presented in Section 3.1.3. If the estimated annual frequency of bridge collapse AF_{BC} is less than 0.0001 for a critical bridge or 0.0010 for a typical bridge, then the bridge pier need not be shielded for pier protection, although shielding for occupant protection may still be necessary according to the

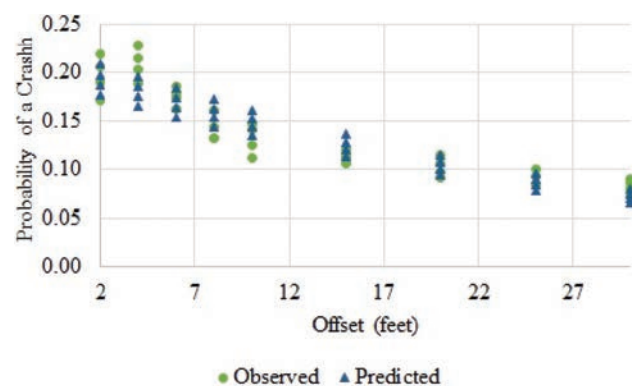
**Figure 22. Observed and predicted probability of a crash by offset and diameter.**

Table 19. Probability of a heavy-vehicle collision given a heavy-vehicle encroachment as a function of pier column diameter or wall thickness and offset from the direction of travel [$P(C|HVE)_i$].

Offset [‡] (ft)	Pier Column Size (ft) [†]				
	1	2	3	4	6
2	0.1763	0.1868	0.1978	0.2093	0.2337
4	0.1650	0.1750	0.1855	0.1964	0.2198
6	0.1543	0.1638	0.1738	0.1842	0.2064
8	0.1442	0.1532	0.1626	0.1725	0.1937
10	0.1347	0.1432	0.1521	0.1614	0.1816
15	0.1131	0.1204	0.1282	0.1363	0.1539
20	0.0946	0.1009	0.1075	0.1145	0.1297
25	0.0789	0.0842	0.0899	0.0958	0.1088
30	0.0656	0.0701	0.0749	0.0799	0.0910
35	0.0544	0.0582	0.0622	0.0665	0.0758
40	0.0450	0.0482	0.0515	0.0551	0.0630

$$P(C|HVE)_i = \frac{e^{-0.0398 P_i + 0.0709 D_i - 1.5331}}{1 + e^{-0.0398 P_i + 0.0709 D_i - 1.5331}}$$

[‡] P_i = Offset to critical pier component in direction (i) in ft, where the distance is from the face of the critical pier component to the closest edge of travel lane (i).

[†] D_i = Size of the critical component of the pier in direction (i), where size is either the diameter of the critical circular column or the smallest cross-sectional dimension of a rectangular column.

procedures to be discussed in Chapter 4. If AF_{BC} exceeds these critical values, then the pier system should be shielded as discussed in the next section or redesigned such that shielding is not needed [e.g., increase the nominal lateral resistance of the critical pier component (R_{CPC})].

3.3.5 Shielding Barrier Layout for Pier Protection

Suggestions for barrier placement and layout are provided in Chapter 5 and, particularly, in Section 5.6.4 of the AASHTO RDG. In addition, the RDG includes an example problem in Chapter 5, summarized in RDG Figure 5-46, that illustrates barrier layout for bridge pier shielding. The following

suggestions for placement and layout of barriers used for pier protection generally conform to the RDG guidance.

3.3.5.1 Shielding Barrier Type

The barrier options for shielding bridge piers to minimize the chance of bridge collapse will only include barriers that meet the MASH crash-testing guidelines [AASHTO 2016]. The *LRFD Bridge Design Specifications* have referred to 42- and 54-in. TL-5 barriers since the fourth edition [AASHTO 2007], but the only crash-tested options for rigid TL-5 roadside and median barriers are the closed-section concrete family of barriers: the New Jersey shape, the F shape, the single-slope, and the vertical wall. The New Jersey, F, and single-slope barriers all have similar capacities and passenger-vehicle crash severities, so any of these could be used to represent the entire class of closed-profile concrete safety shapes. While TL-6 barriers are designed for the heaviest vehicles anticipated by MASH, there is only one 90-in.-tall *NCHRP Report 350* crash-tested design, and this design is a bridge railing and not a roadside or median barrier. Since there is no independent foundation design available for the 90-in.-tall wall, it is unlikely this design could be used without further design and crash-testing research. It would be unreasonable to suggest a barrier for use that does not exist in practice; therefore, TL-6 barriers are not considered.

While these guidelines address both roadside and median placement, the types of barriers used for pier protection are the same for both. Barriers used in the median for pier protection generally have only one traffic face since the pier is on the back side of the barrier.

The AASHTO MASH crash-testing guidelines were adopted in 2009 and revised in 2016, but as yet few crash tests have been performed on TL-5 closed-profile concrete roadside or median barriers [AASHTO 2009, AASHTO 2016]. It is highly likely that *NCHRP Report 350* TL-5 barriers would also satisfy MASH since the TL-5 conditions are similar to

Table 20. Procedure to find the probability of the worst-case collision force exceeding the critical pier component capacity given a collision: $P(Q_{CT} > R_{CPC}|C)$.

Find:	The probability of a worst-case collision force (Q_{CT}) exceeding the critical pier component capacity (R_{CPC}) given that a heavy-vehicle collision occurs for each pier system under consideration.
Given:	The following pier system characteristics: <ul style="list-style-type: none"> • Design capacity or nominal resistance of the critical pier component [e.g., first column, leading corner of wall (R_{CPC})], • Practical worst-case impact force (Q_{CT}), and • Highway functional classification.
Procedure:	Using the calculated design capacity (R_{CPC}), look up the probability of an impact load (Q_{CT}) exceeding the nominal capacity of the critical pier component for the highway functional class of concern using Table 7.

Table 21. Procedure to find the annual frequency of bridge collapse (AF_{BC}).

Find:	The annual frequency of bridge collapse for an unshielded pier (AF_{BC}) for the pier system under consideration.
Given:	<ul style="list-style-type: none"> • The site-specific adjustment factor (N_i) from Table 15. • The heavy-vehicle base encroachment frequency (HVE_i) from Table 13. • The probability of a collision given a heavy-vehicle encroachment [$P(C HVE_i)$] from Table 19. • The probability of the impact load (Q_{CT}) exceeding the nominal resistance of the critical pier component (R_{CPC}) given that a collision occurs [$P(Q_{CT} > R_{CPC} C)$] from Table 7.
Procedure:	<p>Calculate the annual frequency of bridge collapse as follows:</p> $AF_{BC} = \sum_{i=1}^m HVE_i \cdot N_i \cdot P(C HVE_i) \cdot P(Q_{CT} > R_{CPC} C)$ <p>If $AF_{BC} < 0.0010$ for a typical bridge.</p> <p>Or $AF_{BC} < 0.0001$ for a critical bridge.</p> <p>Then The pier system need not be shielded. Proceed to the RDG procedure to check for vehicle occupant protection.</p> <p>Else A 42-in. tall or higher, crash-tested, rigid MASH TL-5 barrier for shielding the pier system should be used. Proceed to barrier layout options.</p>

NCHRP Report 350 TL-5 conditions, but an official equivalence has not yet been established by either AASHTO or the FHWA. *NCHRP Project 20-07/Task 395* investigated *NCHRP Report 350* bridge railings to determine MASH equivalency [Dobrovolny 2017].

While a 54-in.-tall TL-5 barrier is referred to in the LRFD Bridge Specifications, there are actually no crash-tested 54-in.-tall barriers even under *NCHRP Report 350*. Presumably these were included based on engineering judgement that the taller barrier would inhibit the tractor-trailer truck rolling. While this is highly likely, there are no crash-test results to demonstrate this or indicate how effective 54-in.-tall barriers are at reducing the roll angle. The tallest rigid concrete barrier tested according to MASH at present is the 49.25-in. TL-5 single-slope Manitoba Tall Wall [Rosenbaugh 2016]. The proposed guidelines shown in Appendix A state that 42-in. or taller MASH crash-tested rigid concrete barriers be used for pier protection. The available TL-5 rigid barriers are predominantly 42 in. tall if *NCHRP Report 350* equivalence is assumed. If rigid barriers taller than 42 in. are tested according to MASH in the future, they could also be used with the wording of these proposed guidelines.

In addition, it was assumed in developing these guidelines that the terrain between the edge of the road and the pier is relatively flat (i.e., 10:1 or flatter) since these types of rigid concrete barriers can only be used with approach terrains that are 10:1 or flatter [AASHTO 2011]. Since the approach terrain and barrier options are the same for both the roadside and the median, the guidelines apply to both.

3.3.5.2 Zone of Intrusion

The zone of intrusion (ZOI) is “the region measured above and behind the face of a barrier system where an impacting vehicle or any major part of the system may extend during an impact” [AASHTO 2011]. The zone of intrusion is typically a concern for truck impacts because the vehicle can lean over the barrier during an impact and interact with pier components. The RDG discusses ZOI in Section 5.5.2, but it provides no guidance for TL-5 barriers aside from referring to the eighth edition of the *LRFD Bridge Design Specifications* Article 3.6.5 [AASHTO 2017].

The eighth edition of the *LRFD Bridge Design Specifications* requires a 54-in.-tall shielding barrier if a pier is located within 10 ft of the barrier, and a 42-in.-tall shielding barrier if the pier is more than 10 ft from the barrier. The purpose of this provision is to reduce the likelihood of a truck that strikes the barrier subsequently contacting the pier, but the foundation of these values and the risk reduction are unclear. Figure 23 shows an example where a single-unit truck rolled on to the top of a 32-in. barrier during a crash test. While the truck did not penetrate the barrier, the top of the cargo box extended about 8 ft beyond the back of the barrier. Had a pier or pier column been located within 8 ft of the back side of the barrier, the box of the truck would have struck the pier. In this example, however, the engine block and truck itself would not have struck the pier, so the risk of bridge collapse remains small. As discussed earlier, the majority of the impact force and subsequent damage when a pier is struck comes from



Figure 23. Example of a single-unit truck rolling over onto a 32-in.-tall concrete safety shaped barrier [Sheikh 2011].

the impact with the front of the truck. The box of the truck contacting the pier is only a concern if the box of the truck is carrying a rigid load and traveling at a high speed.

Similar rolling-over-the-barrier results occurred in several *NCHRP Report 350* and 1989 AASHTO Guide Specifications for Bridge Railings [AASHTO 1989b] crash tests involving 80,000-lb tractor-trailer trucks. In one such test, the 80,000-lb tractor redirected after striking the barrier, but the trailer rolled over the barrier such that the trailer came to rest on its side on the non-traffic side of the barrier. The maximum distance behind the barrier for the top rear corner of the trailer was 16 ft. Clearly, had a bridge pier been within 16 ft of the back of the barrier, the trailer would have contacted the pier. In this situation, the tractor interacting with the pier is again not a concern, but the possibility that the trailer might contain a rigid load that could interact with the pier could be.

Even when the barrier contains and redirects the tractor, the trailer can lean a considerable distance over the back side of the barrier, as shown in Figure 24. In this crash test, the trailer rolled 22.5 degrees, which would mean that anything within about 4 ft of the back side of the barrier would have been struck by the trailer. This leaning of the trailer or box of a single-unit truck or tractor-trailer truck is an acceptable *NCHRP Report 350* or MASH test result even though a fixed object like a pier may be behind the barrier because *NCHRP Report 350* and MASH are predominantly concerned with occupant protection. Keeping this area free of a pier may prove to be difficult in many situations. The objective of this activity was to determine how far from the back side of the barrier the bridge pier must be located to minimize the chance of striking and subsequently damaging the pier. This is a two-part question: (1) how far does the heavy vehicle roll



Figure 24. Tractor-trailer truck leaning over a 42-in.-tall concrete barrier [Rosenbaugh 2007].

over the barrier and (2) is bridge collapse likely if a heavy vehicle extends over the barrier?

The offset distance between the back of the shielding barrier and the face of the pier was examined by reviewing all available single-unit and tractor-trailer truck crash tests involving closed-profile concrete barriers (e.g., F shape, New Jersey shape, constant slope). An extensive literature review to obtain all the crash-test reports available involving SUTs and TTs with these closed-profile roadside and median barriers was conducted. A total of 24 crash tests were obtained; 10 involved nominal 80,000-lb TTs, two involved 50,000-lb TTs, and the remaining 12 involved SUTs between 18,000 and 22,000 lb. Most of the tests were performed at nominal 50-mph impact speeds with an impact angle of around 15 degrees. A summary of the crash-test data is presented in Table 22.

Sheikh et al. performed an investigation of the minimum height and lateral design loads for SUTs in MASH TL-4 impacts [Sheikh 2011]. Based on a combination of full-scale crash testing and finite element simulations, Sheikh et al. found that the minimum height for a rigid constant-slope concrete barrier in the MASH TL-4 impact conditions that would prevent intruding behind the barrier was 36 in., as shown in Figure 25. Sheikh et al. reported that the maximum height of the vehicle was 133 in., the barrier deflection during the event was 0 in., and the maximum vehicle roll angle was 27 degrees, so the maximum distance the vehicle intruded behind the barrier was 44 in.

Figure 25 shows diamonds representing the results of finite element simulations of SUT TL-4 impacts performed by Sheikh et al. A linear regression line using these data suggests that a 50-in.-tall constant-slope concrete barrier would result in a roll angle of 0 for a 22,000-lb SUT striking the barrier at 15 degrees and 50 mph. Unfortunately, Sheikh et al. only examined MASH TL-4 impacts (i.e., SUTs) and did not perform a similar study for MASH TL-5 impacts (i.e., TTs),

Table 22. Summary of SUT and TT crash tests.†

General Test Information									Impact Information												Barrier Condition - Post test		X dist (in)	
Test Number	Reference File	Vehicle Information			Test Information		Barrier Information			Impact Conditions					SUT/Tractor Tandem/Entire Vehicle if Trailer Tandem Is Unknown			Trailer Tandem			Barrier deflection			
		Type	Weight (lbs)	Height TT=W,SUT=D	Procedure	Criteria	Type	Name	Height	Test inertial weight	Speed	Angle	Subsequent roll beyond barrier length	Max roll angle - entire unit considered	SUT (entire) or TT (front axle) Weight (kips)	IS (k-ft)	Max roll (+ or -) within barrier length	Center axle Weight (kips)	IS (k-ft)	Max roll (+ or -) within barrier length	Cross barrier roll (feet)	Max	Permanent	X = (veh. height-Barrier height) ² /sin(max angle)+max deflection
401761-SBG1	Buth 2011	TT	28,500 lbs.	155.00 in.	MASH	TL-5	Schock ComBAR parapet		42 in.	79,220 lbs.	50.5 mph.	15.6 deg.	upright	12.0 deg.	9.52	59	12.0 deg.	31.98	197	12.0 deg.	NA	0.0 in.	0.0 in.	-60.63
7069-10	Buth 1993b	TT	29,900 lbs.	156.00 in.	1989 GSBRR	PL-3	F-Shape	safety shape	42 in.	50,000 lbs.	52.2 mph.	14.0 deg.	upright	12.5 deg.	9.4	50	12.5 deg.	21.76	116	12.5 deg.	NA	0.0 in.	0.0 in.	-7.56
405511-2	Alberson 1996	TT	30,628 lbs.	157.40 in.	Report 350	TL-5	Vertical wall	vertical-face barrier	42 in.	79,366 lbs.	49.7 mph.	14.5 deg.	upright	14.0 deg.	5.08	26	14.0 deg.	34.25	177	14.0 deg.	NA	0.0 in.	0.0 in.	114.32
4348-2	Buth 1982	TT	30,800 lbs.	158.00 in.	Report 230		high performance	safety shape	42 in.	80,420 lbs.	52.8 mph.	16.0 deg.	90.0 deg.	90.0 deg.	12.38	88	28.0 deg.	34.03	241	90.0 deg.	16	0.0 in.	0.0 in.	103.70
7069-13	Buth 1993a	TT	27,690 lbs.	162.00 in.	1989 GSBRR	PL-3	concrete parapet	vertical-face barrier	42 in.	50,050 lbs.	51.4 mph.	16.2 deg.	90.0 deg.	7.5 deg.	7.9	54	7.5 deg.	22.25	153	7.5 deg.	NA	0.0 in.	0.0 in.	112.56
TLSCMB-2	Rosenbaugh 2007	TT	28,820 lbs.	160.00 in.	Report 350	TL5	42-inch TL-5 Concrete Median Barrier	vertical-face median barrier	42 in.	79,705 lbs.	52.7 mph.	15.4 deg.	upright	22.5 deg.	9.79	64	11.5 deg.	37.51	245	22.5 deg.	NA	1.5 in.	0.0 in.	-55.99
4798-13	Campise 1985	TT	29,600 lbs.	144.00 in.	Report 350	TL5	New Jersey	safety shape median barrier	42 in.	80,180 lbs.	52.1 mph.	16.5 deg.	upright	52.0 deg.	12.15	89	52.0 deg.	34.01	249	52.0 deg.	NA	0.0 in.	0.0 in.	100.64
7162-1	Mak 1990	TT	29,710 lbs.	154.30 in.	1989 GSBRR	PL-3	Ontario tall wall	un-reinforced safety shape	42 in.	80,000 lbs.	49.6 mph.	15.1 deg.	NA	90.0 deg.	11.58	65	17.0 deg.	34.35	192	90.0 deg.	23	0.0 in.	0.0 in.	100.40
2416-1	Hirsch 1984	TT	32,080 lbs.	156.00 in.	Report 230	S20	Texas T5 w/ C4 top rail	safety shape w/ steel top rail	50 in.	80,080 lbs.	48.4 mph.	14.5 deg.	90.0 deg.	90.0 deg.	12.02	59	23.0 deg.	34.17	168	90.0 deg.	NA	11.0 in.	6.0 in.	105.76
230-6	Hirsch 1984	TT	32,670 lbs.	158.00 in.	Report 230	S20	Texas C202 concrete parapet w/ Texas C4 Steel Rail	Post and beam w/ top rail	54 in.	79,770 lbs.	49.1 mph.	15.0 deg.	upright	unk	11.49	62	10.0 deg.	33.76	182	unk	NA	unk	unk	
2911-1	Hirsch 1985	TT	28,320 lbs.	122.00 in.	Report 230	S21	90-inch Modified T5 Bridge Rail	safety shape w/ conc. top rail	90 in.	80,120 lbs.	51.4 mph.	15.0 deg.	upright	17.0 deg.	10.59	63	17.0 deg.	34.05	201	15.0 deg.	NA	4.0 in.	0.6 in.	-26.76
RF 476460-1b	Bullard 2010	SUT	12,200 lbs.	145.00 in.	MASH	TL-4	NJ-Shape	safety shape	32 in.	22,090 lbs.	57.4 mph.	14.4 deg.	upright	101.0 deg.	22.09	150	101.0 deg.	NA	NA	NA	NA	0.0 in.	0.0 in.	51.08
7069-08	Buth 1993a	SUT	13,850 lbs.	147.50 in.	1989 GSBRR	PL-2	F-Shape	safety shape	32 in.	18,050 lbs.	46.7 mph.	15.0 deg.	upright	34.0 deg.	18.05	88	34.0 deg.	NA	NA	NA	NA	0.0 in.	0.0 in.	61.11
7069-09	Buth 1993a	SUT	13,850 lbs.	147.50 in.	1989 GSBRR	PL-2	F-Shape	safety shape	32 in.	18,050 lbs.	47.3 mph.	15.3 deg.	upright	25.0 deg.	18.05	94	25.0 deg.	NA	NA	NA	NA	0.0 in.	0.0 in.	-15.29
7069-11	Buth 1993a	SUT	13,530 lbs.	148.50 in.	1989 GSBRR	PL-2	F-Shape	safety shape	32 in.	18,000 lbs.	52.1 mph.	14.8 deg.	upright	31.0 deg.	18	106	31.0 deg.	NA	NA	NA	NA	0.0 in.	0.0 in.	-47.07
7069-12	Buth 1993a	SUT	10,900 lbs.	134.25 in.	1989 GSBRR	PL-2	New Jersey Safety Shape	safety shape	32 in.	18,000 lbs.	51.6 mph.	15.5 deg.	90.0 deg.	44.0 deg.	18	114	44.0 deg.	NA	NA	NA	NA	0.0 in.	0.0 in.	1.81
7069-15	Buth 1993a	SUT	12,320 lbs.	149.25 in.	1989 GSBRR	PL-2	Illinois 2399-1	steel post and beam	32 in.	18,000 lbs.	50.8 mph.	15.1 deg.	upright	24.0 deg.	18	105	24.0 deg.	NA	NA	NA	NA	0.0 in.	0.0 in.	-106.18
7069-16	Buth 1993a	SUT	13,820 lbs.	142.25 in.	1989 GSBRR	PL-2	concrete parapet	vertical parapet	32 in.	18,000 lbs.	50.0 mph.	14.0 deg.	90.0 deg.	17.6 deg.	18	88	17.6 deg.	NA	NA	NA	NA	0.0 in.	0.0 in.	-104.61
7069-37	Buth 1993a	SUT	10,810 lbs.	133.50 in.	1989 GSBRR	PL-2	Illinois Side-Mounted Railing	steel side mounted	32 in.	18,000 lbs.	51.4 mph.	14.7 deg.	upright	53.0 deg.	18	102	53.0 deg.	NA	NA	NA	NA	2.5 in.	2.5 in.	42.69
7118-1	Buth 1989	SUT	13,590 lbs.	136.00 in.	1988 AASHTO	PL-2	L.B. Foster Precast Bolt-Down Barrier	safety shape	34 in.	18,000 lbs.	51.7 mph.	14.6 deg.	90.0 deg.	57.0 deg.	18	102	57.0 deg.	NA	NA	NA	NA	0.0 in.	0.0 in.	44.49
420020-9B	Sheikh 2011	SUT	12,400 lbs.	133.00 in.	MASH	TL-4	Single Slope	safety shape	36 in.	22,150 lbs.	57.2 mph.	16.1 deg.	upright	13.0 deg.	22.15	186	13.0 deg.	NA	NA	NA	NA	0.0 in.	0.0 in.	40.76
7069-26	Buth 1989	SUT	10,550 lbs.	139.50 in.	1989 GSBRR	PL-2	BR27C on Sidewalk	vertical parapet w/ steel top rail	42 in.	18,000 lbs.	51.0 mph.	13.7 deg.	upright	17.5 deg.	18	88	17.5 deg.	NA	NA	NA	NA	0.0 in.	0.0 in.	-95.12
7069-34	Buth 1989	SUT	10,490 lbs.	145.75 in.	1989 GSBRR	PL-2	BR27C on Deck	vertical parapet w/ steel top rail	42 in.	18,000 lbs.	52.5 mph.	12.8 deg.	upright	10.5 deg.	18	81	10.5 deg.	NA	NA	NA	NA	1.5 in.	1.5 in.	-89.77

† Several successful full-scale crash tests of bridge railings have been performed using the MASH guidelines, including the use of 53-ft-long trailers. There have been three successful MASH Test 5-12 crash tests performed on nominal 42-in.-tall fiberglass New Jersey shapes. Test reports for these railings were not available, so they were not included in this table.

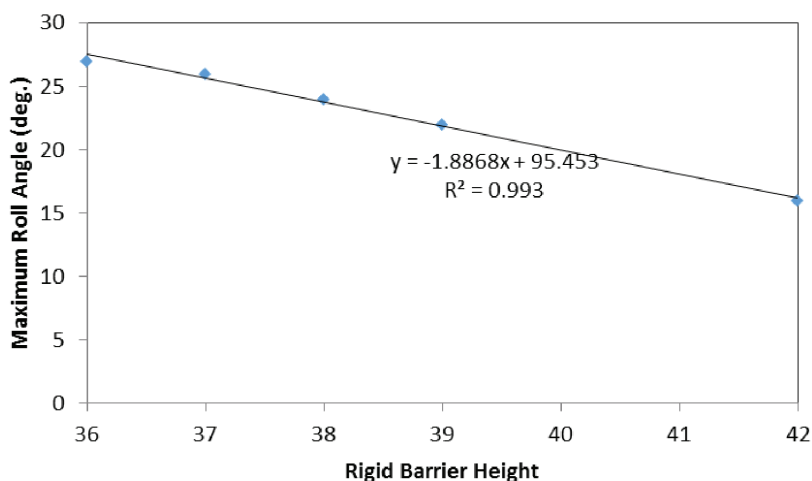


Figure 25. Minimum barrier height to prevent intrusion behind barrier based on finite element simulations [after Sheikh 2011].

so the results in Figure 25 are not directly transferable to the development of these guidelines.

Table 22 shows a summary of the 24 single-unit and tractor-trailer crash tests that were found in the crash-testing literature. In two of the nine tractor trailer crash tests with 42-in.-tall barriers, the TT rolled completely onto its side. Even when the TT redirected without the trailer rolling completely over the barrier, the top of the rear corner of the trailer extended almost 9.5 ft behind the barrier line. As shown in Table 22, the distance could be as much as 16 ft if the trailer landed on the non-traffic side of the barrier. There is relatively little crash-test experience with barriers taller than 42 in., but as shown in Table 22, a test of a 50-in.-tall rigid concrete barrier also resulted in the trailer rolling onto its side, although both the tractor and trailer remained on the traffic side of the barrier.

Finite element analysis was used to simulate MASH TL-5 impacts into rigid barriers to assess the amount of roll of the trailer during the impact and the resulting maximum ZOI of the trailer behind the barrier. The barrier type selected for this study was a single-slope barrier shape based on the Manitoba Tall-Wall, the only known MASH TL-5 crash-tested rigid barrier. This barrier type was selected to allow for the

model to be validated against the crash test. Figure 26 shows a photograph of the 49.25-in.-tall Manitoba Tall Wall that was used as the baseline barrier in this study. Six barrier heights were evaluated: 42, 44, 46, 48, 50, and 54 in. Development of a detailed model of the test article was beyond the scope of the project, so the barrier was modeled as a rigid material rigidly attached to the ground. The friction coefficient between the vehicle body and the barrier was set to 0.2, and the friction coefficient between the tires and the barrier was set to 0.45. The coefficient of friction between the tires and ground was set to 0.7.

The impact conditions were set to the nominal conditions for MASH Test 5-12 (i.e., 50 mph and 15 degrees). The suspension systems on the tractor and trailer models were initialized based on the weight of the model; however, the model was not at a steady state at the beginning of the analysis. The trailer's response was somewhat affected by the additional vertical dynamics associated with the sudden loading of the ballast mass under gravity [Miele 2010].

The analysis was performed using LS-DYNA version smp_s_R8.0.0, revision number 95309, with a time-step of 1.0 microsecond for a time period of 1.5 s. The results of the analyses are summarized in Figure 27.



Figure 26. Test installation for Test MAN-1 [Rosenbaugh 2016].

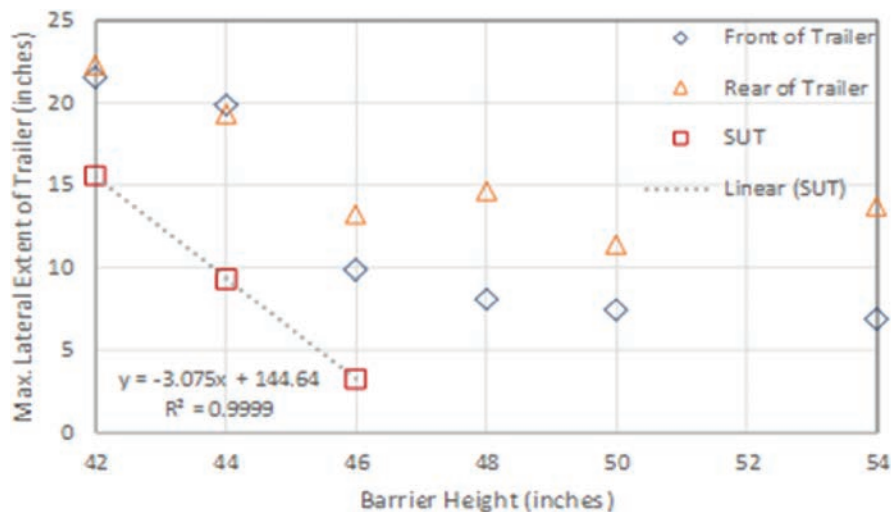


Figure 27. Maximum lateral distance that the top of the trailer or truck cargo-box intrudes behind the barrier during MASH TL-4 and TL-5 impacts.

The resulting ZOI of the trailer behind the barrier during impact is shown Figure 27. The intrusion is measured from the top traffic-face of the barrier to the point on the trailer with the greatest lateral extent behind the barrier. There were two peak ZOI events. The first occurred soon after the front of the trailer contacted the barrier and corresponded to the lateral intrusion of the front top of the trailer (i.e., diamond markers in Figure 27). A second peak intrusion occurred soon after the rear of the trailer contacted the barrier and corresponded to the rear top of the trailer extending behind the barrier (i.e., triangle markers in Figure 27). Also included in Figure 27 are the results from Sheikh's investigation of barrier roll versus barrier height for SUT collisions under MASH TL-4 conditions discussed previously. The square markers and dotted line represent Sheikh's analysis results as compared to those for the TTs performed in this project.

These FEA simulations and Sheikh's simulations, summarized in Figure 25, indicate that there is relatively little risk of either the trailer of a TT or the box of a SUT interacting with a bridge pier component as long as there is at least 22 in. of clear space behind a 42-in.-tall barrier. A review of the simulation data also showed that, in all cases except the 42-in.-tall barrier, the maximum roll occurred at the rear impact-side top corner of the trailer. In the 42-in.-tall barrier, the maximum roll occurred on the front top impact-side corner.

Comparing to the results of the older tractor-trailer crash tests performed under *NCHRP Report 350* Test 5-12 conditions (see Table 22), there is significantly less roll in these FEA simulations under MASH Test 5-12 conditions. The reason is that older *NCHRP Report 350* tests generally used 43- to 48-ft-long trailers with leaf-spring suspensions, and these have largely disappeared from the trailer fleets. Newer trailers

tend to be 53-ft long and use air-ride suspensions. These two differences (trailer length and suspension type) have made the trailers more stable and resulted in much less roll than the earlier generation of shorter, leaf-spring trailers.

A full-scale MASH crash test, Test MAN-1, performed at the Midwest Roadside Safety Facility on April 13, 2016, involved an 80,076-lb tractor trailer striking a 49.25-in.-tall single-slope concrete bridge rail at 51.72 mph and an impact angle of 15.2 degrees [Rosenbaugh 2016]. The maximum roll angle reported for Test MAN-1 was 13.3 degrees with a corresponding lateral intrusion of 37.4 in. The FEA simulation of Test MAN-1 resulted in a maximum roll angle of 8 degrees for the trailer and a corresponding lateral intrusion of 23 in. The crash-test results related to Figure 29 were somewhat higher than the results related to Figure 28. The impact severity for Test MAN-1 was 491,842 ft-lb, which was approximately 10% higher than the impact severity for the FEA analysis cases from Figure 28.

TTI performed two tests using MASH Test 5-12 conditions: Test 603911-3 and Test 490025-2-1. Test 603911-3 involved a 76,620-lb tractor trailer striking a 42-in.-tall steel post and beam bridge rail at 49.9 mph and 15.1 degrees. The maximum roll angle of the trailer in the test was 11 degrees, which is comparable to the values in Figure 30. However, the trailer ruptured at the kingpin box early in the test, causing the front side-wall of the trailer to break apart, as shown in Figure 30. The resulting maximum intrusion of the trailer side-wall behind the barrier was 62 in. The ballast remained inside the trailer during impact and redirection, and the test was considered successful. This test may be somewhat of an outlier in that no other full-scale test has resulted in this type of kingpin behavior [Sheikh 2017].

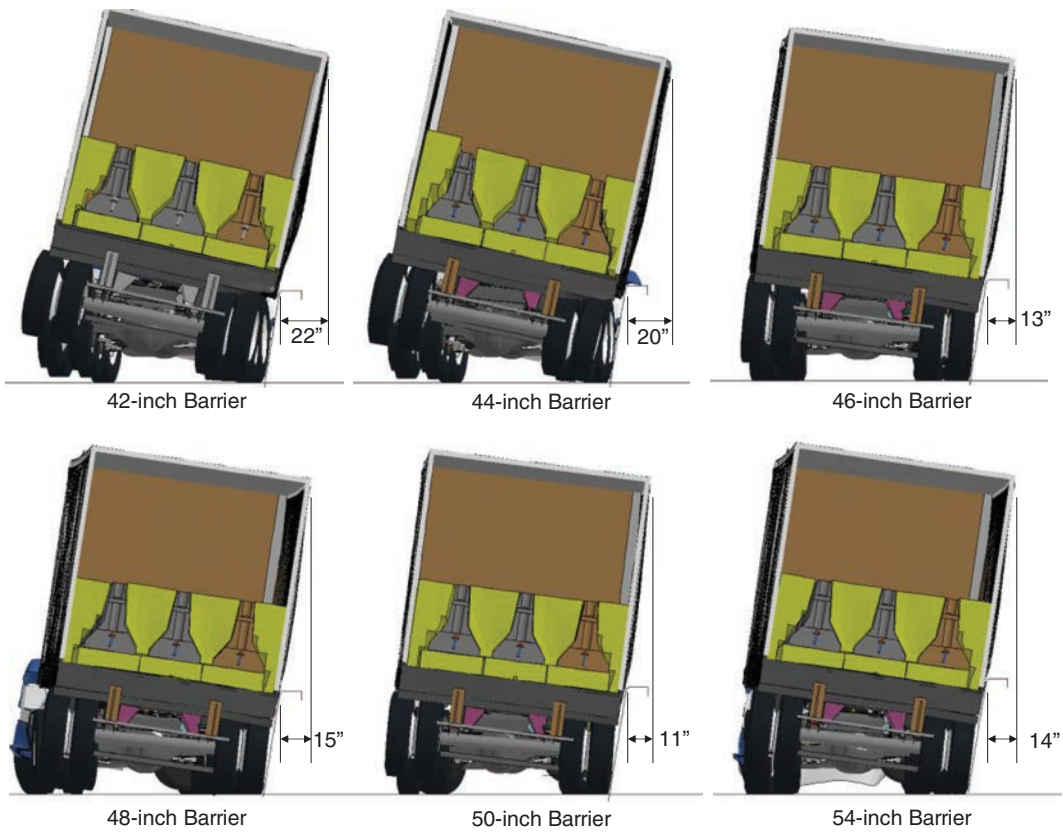


Figure 28. Images from analyses at time of maximum lateral intrusion of trailer behind barrier for each barrier-height case.

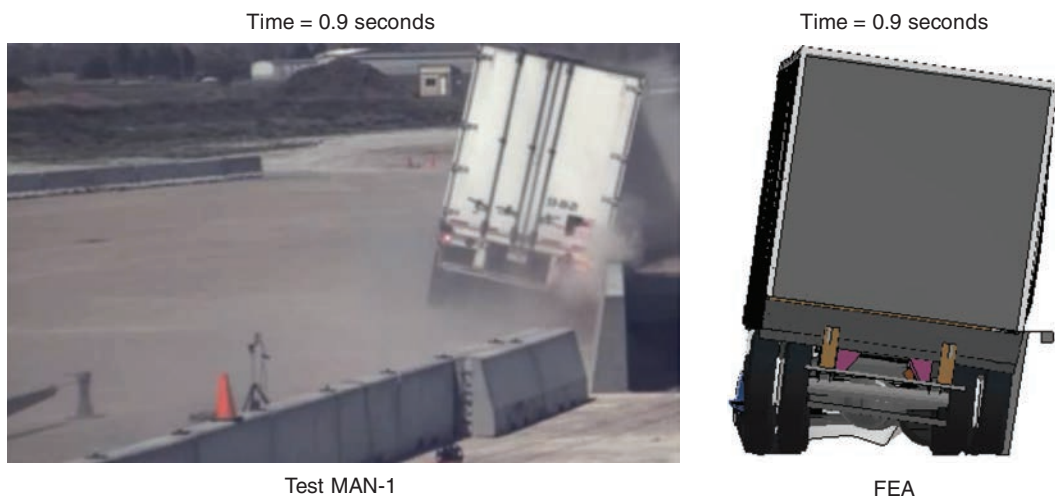


Figure 29. Test MAN-1 on 49.25-in. barrier and FEA model at time of maximum lateral intrusion [Rosenbaugh 2016].



(a) Trailer rupture



(b) Max. lateral intrusion

Figure 30. Test 603911-3 on 42-in. steel rail barrier showing (a) time of trailer rupture at the kingpin box and (b) time of maximum lateral intrusion of the trailer [Sheikh 2017].

Test 490025-2-1 involved a 79,945-lb tractor trailer striking a 42-in.-tall concrete post and beam bridge rail at 50.5 mph and 14.1 degrees [Williams 2017]. The test article and test vehicle are shown in Figure 31. The maximum roll angle of the trailer was 18 degrees. The maximum intrusion of the trailer behind the face of the barrier was 38.5 in.

Based on the FEA simulations performed in this study, the work by Sheikh et al., and MASH TL-5 full-scale crash tests, it was determined that there is relatively little risk of either a trailer or the cargo box of an SUT striking a bridge pier as long as there is at least 22 in. of clear space behind a 42-in.-tall barrier. The tests performed at TTI, while not using rigid closed-face concrete barriers, indicate that some higher intrusion may be possible, so for the sake of conservatism, it is suggested for these pier protection guidelines that the face of the nearest pier component be at least 39 in. (3.25 ft) from

the top traffic-face edge of the shielding barrier since TTI Test 603911-3 extended almost 39 in. behind the barrier. This value should be reevaluated as additional MASH TL-5 crash tests are conducted.

3.3.5.3 Shielding Barrier Layout

The placement of a shielding barrier for pier protection should follow the recommendations of Section 5.6.4 of the RDG. The layout requires determination or selection of the following six dimensions shown in RDG Figure 5-39:

1. The run-out length (L_R) (RDG Table 5-10);
2. The shy-line offset distance (L_S) (RDG Table 5-7);
3. The flare rate, if desired and terrain is relatively flat (a/b) (RDG Table 5-8);



Figure 31. MASH Test 5-12 setup for the Texas T224 bridge rail [Williams 2017].

4. The tangent length (L_1), if desired;
5. The barrier offset from the edge of lane (L_2); and
6. The lateral extent of the area of concern (L_A).

Once these values are found or selected, RDG Equation 5-1 (flared) or Equation 5-2 (tangent) can be used to find the length of need (x), as shown in RDG Figure 5-39.

RDG Section 5.5.2 recommends that the full height of a rigid barrier used for pier protection should start at least 10 ft upstream of the leading edge of the pier system [AASHTO 2011]. This recommendation, however, was based on engineer judgement rather than any analysis or review of crash tests. Crash tests performed under *NCHRP Report 350* TL-5 conditions showed large variations in the distance that the tractor-trailer truck was in contact with the barrier; some were as small as 41 ft and others as large 200 ft, although the largest was a case where the trailer rolled on to the top of the barrier and remained there.

The full-height length of need should be long enough that the tractor-trailer truck can reach its maximum roll angle, indicating that it is starting to stabilize and redirect. As discussed earlier, newer trailers appear to be more stable than trailers crash tested in the past. In MASH TL-5 Test MAN-1, the trailer reached its maximum roll angle 56.8 ft downstream of the impact point. The finite element simulation of the crash test resulted in a value of 56.4 ft. While additional

testing would be preferable, this particular test indicates that 10 ft may not be a long enough distance for the vehicle to start redirecting before it reaches the leading pier component. The results of Test MAN-1 indicate that a value of 60 ft may be more appropriate.

When the design choice is shielding the pier from heavy-vehicle impacts, it is suggested that the barrier length of need (x) be established through reference to Section 5.6.4 of the RDG. It is further suggested that the minimum length of a MASH TL-5 shield barrier should be 60 ft upstream of the leading pier component plus the entire length of the pier system. If, for example, a designer determines that the length of need (x) is 200 ft, then 200 ft of MASH TL-5 barrier should be installed, and the length in front of the pier system should also have a TL-5 barrier. If, however, it is determined through application of the length-of-need procedure within the RDG that the length of need (x) could be 50 ft, then the minimum of 60 ft upstream of the leading pier component would be necessary for shielding the pier from heavy-vehicle impacts.

At the current time, the RDG procedure has a minimum length of need of 70 ft; therefore, the 60-ft minimum for redirection of a tractor-trailer truck is not necessary. This provision is suggested for application in the LRFD since the length-of-need procedure in the RDG is under review and may change.

CHAPTER 4

Discussion of Proposed RDG Occupant Protection Guidelines

Appendix B: Proposed RDG Occupant Protection Guidelines provides a proposal regarding occupant protection for inclusion in a future edition of the RDG. Unlike the *AASHTO LRFD Bridge Design Specifications*, the RDG does not contain a single section that is applicable only to impacts with bridge piers. The RDG contains guidance applicable to all impacts with roadside objects where the objective is to minimize the risk to a vehicle occupant. In the RDG, a bridge pier is treated like any other fixed object in the clear zone (e.g., utility pole, high-mast light).

An objective of NCHRP Project 15-65 (in process) is to “develop safety performance-based guidance to address high-priority needs that support quantitative design decisions, and that promote consistency in interpretation and implementation” in anticipation of rewriting a future edition of the RDG [Ray 2017b]. The proposed procedures presented in Appendix B are consistent with the objective of NCHRP Project 15-65 in that they use the risk of a severe or fatal injury crash to quantify the roadside design goal. Further, a workbook approach is anticipated in NCHRP Project 15-65; therefore, the occupant protection guidelines developed under this research are presented using a workbook approach.

4.1 Proposed RDG Guidelines

This section presents the development of the procedure for shielding bridge piers for vehicle occupant protection anticipated for inclusion in a future edition of the RDG. Examples and validation with RSAPv3 are provided in Chapter 5.

These guidelines are applicable to all bridge pier components except those that require shielding with a MASH TL-5 rigid barrier in order to protect the pier system according to the *AASHTO LRFD Bridge Design Specifications* as discussed in the previous chapter. Users are referred to the proposed *AASHTO LRFD Bridge Design Specifications*, Article 3.6.5,

for determining if the bridge pier system requires shielding to protect the bridge from collapse due to heavy-vehicle collisions.

The general procedure suggested for evaluating bridge piers, as outlined in Table 23, involves finding four values:

PVE_i = The expected annual number of passenger vehicle encroachments in direction (i) is found using Table 24 knowing the highway type, traffic volume, and percentage of trucks.

N_i = The site-specific adjustment factor is found using Table 15 and the characteristics of the study site.

$P(C|PVE_i)$ = The probability of a crash given an encroachment in direction (i) is found by using Table 25 knowing the pier component offset and size for each direction (i).

$P(KA_{CUSP}|C)$ = The probability of a severe injury or fatal crash with a bridge pier component given that a crash occurs is found from Table 26 based on the PSL of the roadway.

The product of these four values is the estimated annual frequency of severe and fatal injury crashes involving the unshielded pier system. If this value is less than 0.0001 annual fatal and severity injury crashes, the pier system need not be shielded for occupant protection. If this value is greater than or equal to 0.0001 annual fatal and severity injury crashes, the pier system should be shielded with a MASH TL-3 w-beam guardrail.

4.2 Proposed Preliminary RDG Guideline Development

As shown in Table 23, estimating the annual number of severe injury and fatal passenger vehicle crashes ($AF_{KA\ CUSP}$) involves calculating the following four quantities:

Table 23. RDG occupant protection procedure.

Find:	The annual frequency of severe and fatal passenger vehicle collisions with an unshielded pier system (i.e., $AF_{KA_{CUSP}}$). This step is not necessary if the LRFD risk-based pier protection procedure determined that a MASH TL-5 rigid barrier is needed.
Given:	The following traffic and site characteristics for each approach direction where a pier component is exposed to approaching traffic: <ul style="list-style-type: none"> • The highway type (i.e., divided, undivided, or one-way); • The number of columns in the pier system (n); • Site-specific characteristics like the number of lanes, lane width, major access points, posted speed limit, radius of horizontal curvature, and the grade of the highway; • Total two-way AADT in vehicles/day; • Percentage of trucks (PT_i) in each approach direction; • Perpendicular distance in ft from the edge of the travel for each direction of travel to the face of the nearest pier component (P_i); and • Diameter in ft for circular pier columns, the largest cross-sectional dimension for rectangular pier columns or the thickness for pier walls of the pier component (D_i) nearest to relative direction of travel, where the offset (P_i) is measured perpendicular to nearest edge of the lane for the travel direction under consideration to the face of the pier.
Procedure:	<p>Calculate the annual frequency of severe and fatal passenger vehicle collisions with an unshielded pier ($AF_{KA_{CUSP}}$) as:</p> $AF_{KA_{CUSP}} = \sum_{i=1}^m \left[\frac{(n+2)}{3} \right] \cdot N_i \cdot PVE_i \cdot P(C PVE_i) \cdot P(KA_{CUSP} C)$ $PVE_i = \left[\frac{ENCR_{BASE}}{4} \right] \cdot \left[\frac{300}{5,280} \right] \cdot \left[1 - \left[\frac{PT_i}{100} \right] \right]$ $P(C PVE_i) = \frac{e^{-0.0299 P_i + 0.1118 D_i - 2.1544}}{1 + e^{-0.0299 P_i + 0.1118 D_i - 2.1544}}$ $P(KA_{CUSP} C) = 2.3895 \cdot 10^{-7} \cdot PSL_i^3$ <p>If $AF_{KA_{CUSP}} > 0.0001$, Then Shield with a MASH TL-3 guardrail for occupant protection, Else The pier system may remain unshielded.</p>

1. The annual frequency of passenger vehicle encroachments in each direction (PVE_i).
2. The site-specific adjustment factor (N_i).
3. The probability of a crash given a passenger vehicle encroachment [$P(C|PVE_i)$].
4. The probability of a severe or fatal injury given that a crash with an unshielded pier component has occurred [$P(KA_{CUSP}|C)$].

Once these four values are found, the annual frequency of severe and fatal injury passenger vehicle crashes is found as follows:

$$AF_{KA_{CUSP}} = \sum_{i=1}^m \left[\frac{(n+2)}{3} \right] PVE_i \cdot N_i \cdot P(C|PVE_i) \cdot P(KA_{CUSP}|C)$$

The derivation and procedure for calculating each of these quantities is discussed in the following sections.

4.2.1 Annual Frequency of Passenger Vehicle Encroachments: PVE_i

The procedure for estimating the number of passenger vehicle encroachments for each direction of interest is outlined in Table 27.

The first step in estimating the number of passenger vehicle encroachments is to estimate the base encroachment expected on a typical base segment of the highway. The process of estimating the base encroachments ($ENCR_{BASE}$) is identical to the process described for heavy vehicles in Section 3.3.1 and summarized in Table 11.

The encroachment models given in Table 11 can be used to estimate the number of passenger vehicle encroachments by using the AADT and PT. Also, the encroachment models are based on a 1-mile segment length, but the maximum trajectory length in RSAPv3 based on the collected field trajectories in NCHRP Project 17-22 is 300 ft. For fixed-point hazards like bridge piers, only trajectories that depart within 300 ft upstream of the pier are likely to strike the leading component of the pier, so the segment length is 300 ft; the encroachment frequency should therefore be multiplied by $300/5,280 = 0.0568$.

The encroachment frequencies tabulated in Table 11 are for passenger vehicles at base conditions (i.e., flat, straight sections with 12-ft lanes, no major access points, and 65-mph posted speed limits) for all possible encroachment directions. Each encroachment direction must be evaluated separately, so the total number of encroachments should be divided by four to get one encroachment direction. The

Table 24. Base annual passenger vehicle encroachments in direction (i): PVE_i.[†]

Two-Way AADT	Undivided Highways							
	PT							
	5	10	15	20	25	30	35	40
veh/day								
1,000	0.0165	0.0157	0.0148	0.0139	0.0130	0.0122	0.0113	0.0104
2,000	0.0268	0.0254	0.0240	0.0226	0.0212	0.0198	0.0183	0.0169
3,000	0.0326	0.0309	0.0292	0.0275	0.0258	0.0240	0.0223	0.0206
4,000	0.0353	0.0334	0.0316	0.0297	0.0279	0.0260	0.0241	0.0223
5,000–41,000	0.0358	0.0339	0.0320	0.0301	0.0282	0.0264	0.0245	0.0226
42,000	0.0371	0.0351	0.0332	0.0312	0.0293	0.0273	0.0254	0.0234
43,000	0.0380	0.0360	0.0340	0.0320	0.0300	0.0280	0.0260	0.0240
44,000	0.0389	0.0368	0.0348	0.0327	0.0307	0.0286	0.0266	0.0245
45,000	0.0397	0.0377	0.0356	0.0335	0.0314	0.0293	0.0272	0.0251
≥46,000	0.0406	0.0385	0.0364	0.0342	0.0321	0.0299	0.0278	0.0257
Two-Way AADT	Divided Highways							
	PT							
	5	10	15	20	25	30	35	40
veh/day								
1,000	0.0114	0.0108	0.0102	0.0096	0.0090	0.0084	0.0078	0.0072
5,000	0.0485	0.0459	0.0434	0.0408	0.0383	0.0357	0.0332	0.0306
10,000	0.0789	0.0747	0.0706	0.0664	0.0623	0.0581	0.0540	0.0498
15,000	0.0962	0.0912	0.0861	0.0810	0.0760	0.0709	0.0658	0.0608
20,000	0.1044	0.0989	0.0934	0.0879	0.0824	0.0769	0.0714	0.0659
24,000–47,000	0.1062	0.1006	0.0950	0.0894	0.0838	0.0782	0.0727	0.0671
50,000	0.1143	0.1082	0.1022	0.0962	0.0902	0.0842	0.0782	0.0722
55,000	0.1257	0.1191	0.1125	0.1058	0.0992	0.0926	0.0860	0.0794
60,000	0.1371	0.1299	0.1227	0.1155	0.1082	0.1010	0.0938	0.0866
65,000	0.1485	0.1407	0.1329	0.1251	0.1173	0.1094	0.1016	0.0938
70,000	0.1600	0.1515	0.1431	0.1347	0.1263	0.1179	0.1094	0.1010
75,000	0.1714	0.1624	0.1533	0.1443	0.1353	0.1263	0.1173	0.1082
80,000	0.1828	0.1732	0.1636	0.1540	0.1443	0.1347	0.1251	0.1155
85,000	0.1942	0.1840	0.1738	0.1636	0.1533	0.1431	0.1329	0.1227
≥90,000	0.2057	0.1948	0.1840	0.1732	0.1624	0.1515	0.1407	0.1299

[†]Encroachment data are not available for one-way roadways. Traditionally, one-way roadways have been evaluated using the encroachment model for divided highways. The one-way AADT value should be multiplied by 2 and used to determine PV ENCR_{DIV} BASE for use in the remaining calculations.

Table 25. Probability of a collision given a passenger vehicle encroachment: P(C|PVE_i).

Offset (ft) [‡]	Pier Column Size (ft) [†]				
	1	2	3	4	6
2	0.1125	0.1242	0.1369	0.1507	0.1818
4	0.1066	0.1178	0.1300	0.1432	0.1730
6	0.1011	0.1117	0.1233	0.1360	0.1646
8	0.0957	0.1059	0.1170	0.1291	0.1565
10	0.0907	0.1004	0.1109	0.1225	0.1487
15	0.0790	0.0876	0.0970	0.1073	0.1307
20	0.0688	0.0763	0.0846	0.0937	0.1146
25	0.0598	0.0664	0.0737	0.0817	0.1002
30	0.0519	0.0577	0.0641	0.0712	0.0875
35	0.0450	0.0501	0.0557	0.0619	0.0762
40	0.0390	0.0434	0.0483	0.0537	0.0663

$$P(C|PVE_i) = \frac{e^{-0.0300 P_i + 0.1122 D_i - 2.1177}}{1 + e^{-0.0300 P_i + 0.1122 D_i - 2.1177}}$$

[‡]P_i = Offset to critical pier component in direction (i) in ft where the distance is from the face of the critical pier component to the closest edge of travel lane (i).

[†]D_i = Size of the critical component of the pier in direction (i) where size is either the diameter of the critical circular column or the smallest cross-sectional dimension of a rectangular column.

Table 26. Probability of a severe or fatal injury given a crash with an unshielded pier component occurs: P(KA_{CUSP}|C).

Posted Speed Limit (mph)	P(KA _{CUSP} C)	Posted Speed Limit (mph)	P(KA _{CUSP} C)
≥75	0.1008	50	0.0299
70	0.0820	45	0.0218
65	0.0656	40	0.0153
60	0.0516	35	0.0102
55	0.0398	30	0.0065
		≤25	0.0037

Table 27. Procedure to find the passenger vehicle encroachments: PVE_i.

Find:	The base annual frequency of passenger vehicle encroachments for the pier system under consideration.
Given:	The following traffic and site characteristics for each approach direction where a pier component is exposed to approaching traffic: <ul style="list-style-type: none"> • The highway type (i.e., divided, undivided, or one-way), • Total two-way AADT in vehicles/day, and • PT.
Procedure:	Calculate the base annual frequency of passenger vehicle collisions with an unshielded pier component from each direction of travel as follows: $PVE_i = \left[\frac{ENCR_{BASE}}{4} \right] \cdot \left[\frac{300}{5,280} \right] \cdot \left[1 - \left[\frac{PT}{100} \right] \right]$ Repeat this step for each direction of travel where a pier component is exposed to approaching traffic.

smoothed Cooper data used in the heavy-vehicle portion of the guidelines is also used here for the same reasons. Heavy-vehicle encroachments were already considered in the LRFD portion of the guidelines; therefore, only passenger vehicles are considered in this step. The passenger vehicle encroachment frequency in direction *i* for a highway segment 300 ft upstream of a bridge pier can be written as:

$$PVE_i = \left[\frac{ENCR_{BASE}}{4} \right] \cdot \left[\frac{300}{5,280} \right] \cdot \left[1 - \left[\frac{PT}{100} \right] \right]$$

The values for PVE_{*i*} in Table 24 were generated using this equation.

4.2.2 Site-Specific Adjustment Factor: *N_i*

The value of PVE_{*i*} is the expected number of passenger vehicle encroachments under base conditions. Base conditions can be adjusted up or down based on the particular characteristics of the site and traffic using the site-specific adjustment factor (*N_i*). The procedure to calculate *N_i* for the occupant protection guidelines is exactly the same as was discussed for the LRFD procedures in Section 3.3.2 and outlined in Table 14. Details about the development of the site-specific encroachment adjustment factors used in this step can be found in the RSAPv3 Engineer's Manual [Ray 2012], the final report for NCHRP Project 22-12(30) [Ray 2014b], and the final report for NCHRP Project 17-54 [Carrigan 2017].

Each site-specific adjustment factor (*N_i*) should be calculated for each direction of possible encroachment (*i*) using the values in Table 15. Recall that the direction number (*i* = 1, 2, 3, etc.) is arbitrary, but the site-specific adjustment must always be matched to the offset (*P_i*) and traffic characteristics (*PT_i*, PVE_{*i*}, etc.) that are also associated with that direction of travel in later steps.

4.2.3 Probability of a Crash Given a Passenger Vehicle Encroachment: *P(C|PVE_i)*

Now that the annual frequency of passenger vehicle encroachments (i.e., PVE_{*i*}, *N_i*) at the study location is known, the probability of any particular passenger vehicle encroachment striking a pier component [*P(C|PVE_i)*] can be estimated as outlined in Table 28.

A process similar to that described in Section 3.3.2 for estimating the conditional probability of heavy vehicles striking a pier component is followed here for passenger vehicles. RSAPv3 simulations were performed with the leading pier column offset distance between the edge of the nearest lane and the face of the nearest pier component varied in 2-ft increments. The objective of this effort was to determine the conditional probability of a crash with a pier component, given an encroachment [*P(C|PVE_i)*] when the size of the pier component and the offset to the pier component are known. It has been assumed that the probability of observing a crash, given an encroachment has occurred, is the same on both the median and roadside. A study design that distinguishes between vehicles that crash and vehicles that do not crash given an encroachment for various pier offsets and sizes is, therefore, desired.

A database of simulated passenger vehicle trajectories that encroached onto the roadside within 300 ft of the pier component was generated using RSAPv3 [Ray 2016] for a variety of pier component offsets and diameters. This database is what statisticians refer to as cross-sectional dataset. The predicted probability of a passenger vehicle crash by pier component offset and diameter was then determined.

RSAPv3 was used to simulate 549,120 passenger-vehicle encroachment trajectories within 300 ft of a critical pier component where the component of interest was a single pier

Table 28. Procedure to find the probability of a collision given a passenger vehicle encroachment: $P(C|PVE_i)$

Find:	The probability of a collision given a passenger vehicle encroachment with an unshielded pier [$P(C PVE_i)$] for the pier system under consideration.
Given:	The following traffic and site characteristics for each approach direction where a pier component is exposed to approaching traffic: <ul style="list-style-type: none"> • The highway type and layout (i.e., divided, undivided, or one-way); • Perpendicular distance in ft from the edge of the travel lane for each direction of travel to the face of the nearest pier component (P_i); and • Diameter in ft for circular pier columns, the largest cross-sectional dimension for rectangular pier columns, or the thickness for pier walls of the pier component (D_i) nearest to relative direction of travel, where the offset (P_i) is measured perpendicular to nearest edge of the lane for the travel direction under consideration to the face of the pier.
Procedure:	Calculate the probability of a collision given a passenger vehicle encroachment with an unshielded pier [$P(C PVE_i)$] for the pier system under consideration as follows: $P(C PVE_i) = \frac{e^{-0.0300 P_i + 0.1122 D_i - 2.1177}}{1 + e^{-0.0300 P_i + 0.1122 D_i - 2.1177}}$ Repeat this step for each direction of travel where a pier component is exposed to approaching traffic.

column with a variable diameter. The pier component was studied at a variety of offsets measured from the edge of the travel lane to the pier face. These discrete offsets (4, 6, 8, 10, 15, 20, 25, and 30 ft) were considered for four pier column diameters (1, 2, 3, and 4 ft). The 549,120 passenger-vehicle encroachment trajectory study population is tabulated in Table 29.

The trajectory data include two variables of interest for crashes with piers: offset and diameter. The probability

of a crash given an encroachment [$P(C|PVE_i)$] with any pier is simply the portion or percentage of the vehicle type of interest that strikes the pier component divided by the total number of the vehicle type of interest that encroaches onto the roadside and does not crash. Proportional data are strictly bounded between 0% and 100%. No less than 0% of the vehicles encroaching will avoid the crash, and no more than 100% of the encroachment vehicles will have a crash. A logistic curve reaches asymptotes of 0 and unity; therefore, it prevents the model from fitting negative proportions and proportions greater than unity. Log odds provide an appropriate solution for regression, modeling a line fit using the maximum-likelihood method, as shown here:

Table 29. Simulated passenger-vehicle encroachment trajectory study population.

Offset (ft)	Outcome	Diameter (ft)			
		1	2	3	4
4	Crash	1,850	2,091	2,326	2,560
	Non-crash	15,310	15,069	14,834	14,600
6	Crash	1,761	1,981	2,208	2,317
	Non-crash	15,399	15,179	14,952	14,843
8	Crash	1,623	1,769	1,978	2,175
	Non-crash	15,537	15,391	15,182	14,985
10	Crash	1,510	1,674	1,899	2,051
	Non-crash	15,650	15,486	15,261	15,109
15	Crash	1,258	1,429	1,501	1,696
	Non-crash	15,902	15,731	15,659	15,464
20	Crash	1,180	1,333	1,496	1,655
	Non-crash	15,980	15,827	15,664	15,505
25	Crash	1,102	1,168	1,299	1,430
	Non-crash	16,058	15,992	15,861	15,730
30	Crash	879	1,013	1,131	1,227
	Non-crash	16,281	16,147	16,029	15,933

$$\ln\left(\frac{C}{N}\right) = a + bX$$

where

- C = Number of encroachments that resulted in a crash.
- N = Number of encroachments where no crash occurred.
- $\frac{C}{N}$ = Odds of a crash.

All of the encroachment trajectories in this dataset were considered either crash events (C) or non-crash events (N). These definitions were used to conceptualize the relationships used in this analysis. The statistical analysis and visual inspection of the data were completed using the software program R [R Core Team 2016].

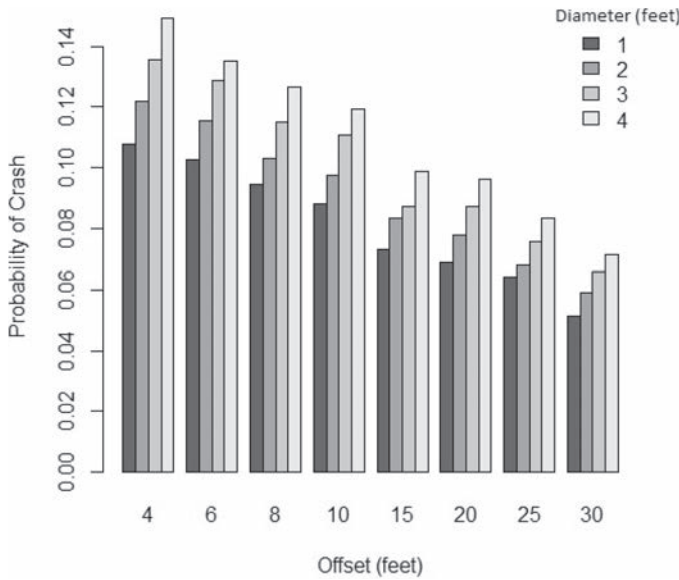


Figure 32. Observed probability of crash by offset and diameter.

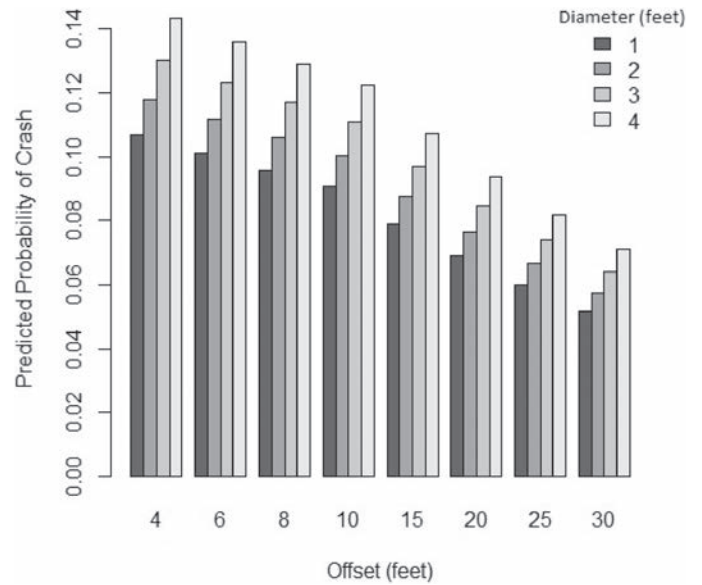


Figure 33. Predicted probability of crash by offset and diameter.

The probability of a crash for each level of offset and diameter was determined as shown in Figure 32. The dependent variable $[P(C|PVE_i)]$ is shown on the y -axis. The main effects of the independent variables are shown on the x -axis. A two-way interaction between variables is said to be present when the effect of one variable differs depending on the level of another variable. There appears to be little if any interaction between the offset and diameter variables.

A regression function from the MASS package available in the R software was used to fit the logit model discussed previously [Venables 2002, R Core Team 2016]. Based on the visual analysis of the data shown in Figure 32, modeling interaction between the variables was not considered necessary. On fitting a binomial logit distribution on the proportion of crash and non-crash data, both offset and diameter were found to be statistically significant predictors of a crash. The coefficients for the passenger vehicle model are shown in Table 30. These coefficients are in logits. The process for changing from logit x to probabilities was discussed previously. The predicted probability is shown graphically in Figure 33 for the model. The predicted probability of a crash

over a range of offsets and diameters is tabulated in Table 25 for the passenger vehicle model.

The probability of a crash given a passenger vehicle encroachment $[P(C|PVE_i)]$ can now be written by inserting the coefficients found in Table 30 into the equation shown earlier, as follows:

$$P(C|PVE_i) = \frac{e^{\beta_P P_i + \beta_D D_i + \epsilon}}{1 + e^{\beta_P P_i + \beta_D D_i + \epsilon}} = \frac{e^{-0.0300 P_i + 0.1122 D_i - 2.1177}}{1 + e^{-0.0300 P_i + 0.1122 D_i - 2.1177}}$$

Probabilities of a passenger vehicle colliding with a bridge pier column as function of column diameter and offset from the edge of lane are shown in Table 25 based on this equation. Figure 34 is a plot of the observed probability of a crash for each simulated diameter and offset, with an overlay of the predicted probability of a crash. These predicted probabilities closely track the observed probabilities; therefore, this model is a good representation of the observed data. This model is suggested to be used to represent the probability of a passenger vehicle crash, given a passenger vehicle encroachment, for a variety of offsets and diameters.

Table 30. Passenger-vehicle model coefficients on crash proportion.

	Estimate	Std. Error	z Value	Pr(> t)	2.50%	97.50%
(Intercept)	-2.1177	0.01	-154.22	<2e - 16	-2.1447	-2.0908
Offset	-0.0300	0.00	-53.98	<2e - 16	-0.0311	-0.0289
diameter	0.1122	0.00	27.16	<2e - 16	0.1041	0.1203

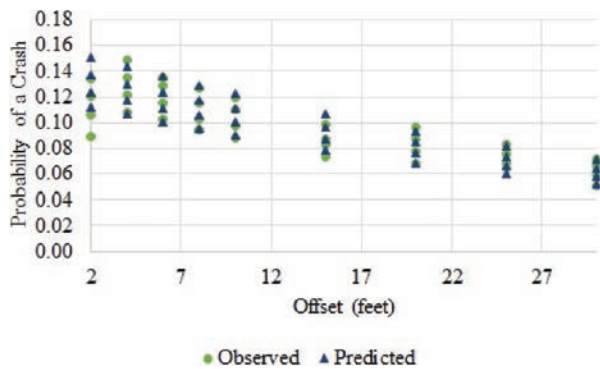


Figure 34. Observed and predicted probability of a crash by offset and diameter.

4.2.4 Probability of a Severe or Fatal Crash Given a Collision with an Unshielded Pier Component: $P(KA_{CUSP}|C)$

Next a model for the conditional probability of a severe or fatal (KA) crash with a pier component given a collision has occurred [$P(KA_{CUSP}|C)$] is needed. Models for the probability of a vehicle encroaching onto the roadside or median and the conditional probability of a collision given an encroachment have been described previously. This section uses the available crash data and extends the equivalent fatal crash cost ratio (EFCCR) procedure used in RSAPv3 to develop the conditional probability [$P(KA_{CUSP}|C)$]. First, the EFCCR procedure and the extension of that procedure are discussed, and then the methodology is applied to the available bridge-pier crash data. Finally, $P(KA_{CUSP}|C)$ is documented for use in the proposed guidelines.

4.2.4.1 Methodology

The severity model developed and used in RSAPv3, the EFCCR, is based on observed police-reported crashes that are adjusted to account for unreported crashes and scaled to account for speed effects. The process for developing an EFCCR for any hazard was documented by Ray et al., who explained that the process for developing an EFCCR included the following five steps:

1. Isolate a census of police-reported crashes with a particular feature over a range of posted speed limits.
2. Determine the crash severity distribution for crashes that do not have harmful events preceding or following the impact with the hazard under evaluation and do not result in a penetration or rollover.
3. Determine or estimate the percentage of unreported crashes, and add these crashes to the reported crash severity distribution.

4. Calculate the average crash cost of the severity distribution for each posted speed limit and determine the EFCCR, and
5. Adjust for speed effects by determining the EFCCR for a baseline posted speed of 65 mph (i.e., $EFCCR_{65}$) [Ray 2014a].

The resulting tabulation of data includes the number of crashes by each discrete severity level (i.e., K, A, B, C, and O) as well as the estimated unreported crashes and total crashes across a range of posted speed limits. Including an estimate of unreported crashes ensures that the higher-severity crashes are not overpredicted [Ray 2012].

While RSAPv3 uses the continuous measure of crash severity (i.e., EFCCR) to facilitate benefit–cost analysis, this risk-based procedure requires an estimate of the probability of a KA crash and is not concerned with estimating costs, so the EFCCR procedure was extended to calculate $P(KA|C)$ while maintaining the calculation of unreported crashes and adjustments for speed using a similar five-step process to that shown previously. In this extension of the procedure, rather than calculating an EFCCR for each posted speed limit within each dataset, the conditional probability $P(KA_{CUSP}|C)$ is determined for the entire sample. EFCCR Step 5 is carried forward to determine the speed-weighted probability of a KA crash given a collision at a base PSL of 65 mph [$P(KA_{CUSP}|C)_{65}$]. The value for $P(KA_{CUSP}|C)_{65}$ is calculated based on observed crash data using the following five-step process adapted from the EFCCR method:

4.2.4.2 Step 1: Census of Police-Reported Crashes

Data from five states were reviewed for bridge pier collisions. The states/agencies and data collection years used were:

- Ohio Highway Safety Information System (HSIS): 2000–2012
- Washington: 1993–1996 and 1999–2011
- New Jersey Transit Authority: 2001–2013
- North Carolina HSIS: 2003–2012
- Wyoming: 2008–2013

The data for each state were screened in order to identify crashes where a bridge pier collision was the first and only collision in the crash sequence. These types of single-event bridge-pier crashes are referred to as “clean” crashes since they only involve a collision with a bridge pier. Each state codes crashes in a slightly different manner. The screening procedure used for each state is listed in the following.

Ohio. Any crash records with code “27 – Bridge Pier or Abutment” in any of the Events 1–4 were coded as being bridge-pier-related crashes. Out of these crashes, only those that had “27” in Event 1 and nothing afterward or had

“8 – Ran off road right,” “9 – Ran off road left,” “10 – Cross median/centerline,” or “11 – Downhill runaway” in Event 1 followed by “27” in Event 2 and a blank in Event 3 were considered clean bridge-pier crashes.

Washington. Any crash records with code “12 – Bridge Column, Pier, or Pillar” in either the Object 1 or Object 2 fields were coded as being bridge-pier-related crashes. (The Events 1–4 fields are used differently in Washington than in most states.) Out of these crashes, only those that had “12” in Object 1 followed by a blank in Object 2 were considered to be clean bridge-pier crashes.

New Jersey. Any crash records with code “43 – Bridge Pier or Support” in any of Events 1–4 were coded as being bridge-pier-related crashes. Out of these crashes, only those that had “43” in Event 1 followed by nothing or had codes “05 – Ran Off Road – Right,” “06 – Ran Off Road – Left,” “07 – Crossed Median/Centerline,” or “08 – Downhill Runaway” followed by “43” and nothing after were considered clean bridge-pier crashes.

North Carolina. Any crash records with code “52 – Pier on Shoulder” or “53 – Pier on Median” in any of Events 1–4 were coded as being bridge-pier-related crashes. Out of these crashes, only those that had “52” or “53” in Event 1 followed by nothing, or had codes “01 – Ran Off Road – Right,” “02 – Ran Off Road – Left,” “03 – Ran Off Road – Straight,” “06 – Crossed Median/Centerline,” or “07 – Downhill Runaway” followed by “43” and nothing after were considered clean bridge-pier crashes.

Wyoming. These crash records were provided by the Wyoming DOT based on the assumption that they represented clean bridge-pier crashes, as defined previously.

Initial examination of the data revealed that there were numerous miscoded crash locations. In order to isolate the crash severity of just the bridge pier, it was necessary to verify (1) that there was a bridge pier at the crash locations and (2) the bridge pier was not shielded by longitudinal barriers of any type. The crash data include the route and milepost of each clean bridge-pier crash. Using this information, the corresponding state’s photologs for the nearest year were viewed to determine if there was, in fact, an unshielded bridge pier at that location.

The top row in Figure 35 shows several typical examples of bridge pier collision locations from the Washington State photologs. Figure 35(A) shows what was intended for bridge pier crash locations to be used in the analysis; the pier is exposed and unprotected. These types of pier locations accounted for only 20% of the cases in Washington State. Figure 35(B) and Figure 35(C) show several other locations where the pier was protected by a barrier: a w-beam guardrail

in the case of Figure 35(B) and a cable median barrier in the case of Figure 35(C). Even though the vehicle would have had to strike and penetrate or vault over the barrier, the reporting police officer coded the cases such that the only object struck was a bridge pier. In other words, the police officer neglected to include the collision with the protecting guardrail. Unfortunately, 39% of the single-event cases in Washington appeared to have an unrecorded collision with a barrier prior to the pier collision and had to be excluded. Another 40% did not appear to involve bridge piers at all but were miscoded bridge railings or bridge abutments.

The situation for the Ohio data was even more discouraging, as shown by the examples in the second row of Figure 35. More than 70% of the collision locations in Ohio were similar to Figure 35(D), where there was no apparent bridge pier at the site. In these cases, it appears that the reporting police officer miscoded bridge railings or abutments as bridge piers. Figure 35(E) and Figure 35(F) show that, like in Washington, the protecting barrier was often not included in the sequence of event’s codes. Another 20% appeared to be bridge piers protected by some type of longitudinal barrier. Only 10% of the cases in Ohio were truly unprotected pier locations with a single crash event involving a bridge pier.

An updated dataset of crash cases where the location was verified to be either an unprotected pier or a pier protected by a barrier was assembled for New Jersey, North Carolina, Ohio, Wyoming, and Washington State. Table 31 shows the results for the calculated EFCCR₆₅ based on the verified crash locations.

Washington State yielded the highest EFCCR₆₅ value (0.3303) for unprotected piers, and New Jersey yielded the lowest (0.0075). Data from all five states were combined and re-analyzed as shown in Table 31. For bridge piers that were unprotected and were the only object struck, the EFCCR₆₅ was found to be 0.0784.

4.2.4.3 Step 2: Severity Distribution

The datasets developed in Step 1 for each state are summarized by crash severity level in Table 32 through Table 36 for first and only harmful events (FOHEs) with unshielded bridge piers. As earlier, crash severity is represented in these datasets using the KABCO scale, where the maximum injury of a crash is reported. K is taken to equal a fatal crash, A is an incapacitating injury crash, B is a non-incapacitating injury crash, C is a possible injury crash, and O is a property-damage-only crash. Not surprisingly, the distributions are different for different speeds, partly due to exposure and partly due to speed. For example, the higher speed limits (e.g., 55 mph and above) would be representative of controlled-access facilities where one might expect more bridges, larger offsets, and wider clear zones.



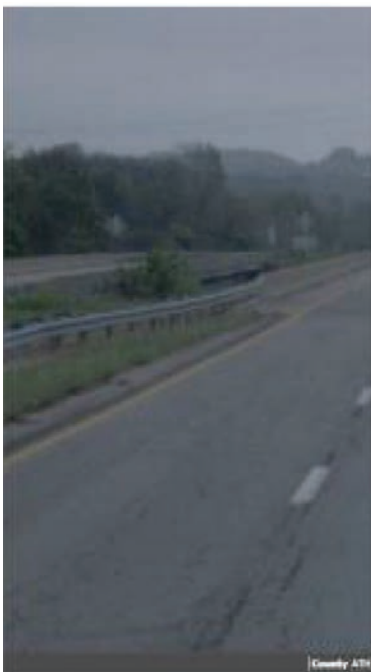
(A) WA Case



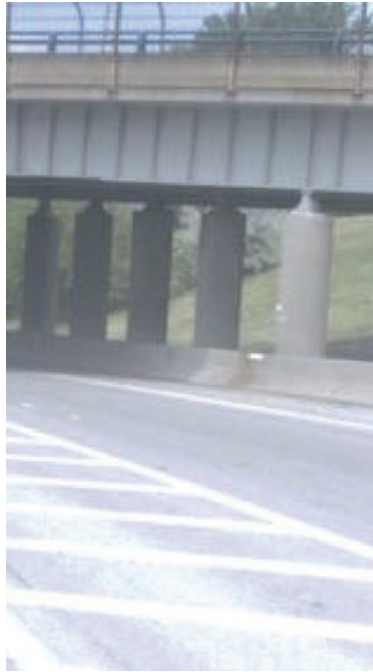
(B) WA Case



(C) WA Case



(D) OH Case



(E) OH Case



(F) OH Case

Figure 35. Typical bridge-pier crash locations in Washington State and Ohio.

Table 31. Summary of bridge pier EFCCRs.

State/Years	Number Reported Cases	Number Estimated Unreported	EFCCR ₆₅
Bridge Pier First and Only Object Struck			
NJ 2001–2013	25	72	0.0075
NC 2003–2012	52	72	0.0889
OH 2000–2012	86	203	0.0623
WA 1993–1996 and 1999–2011	46	60	0.3303
WY 2008–2013	30	113	0.0473
Combined	239	520	0.0784

Table 32. Ohio FOHE bridge pier: 2000–2012.

PSL	K	A	B	C	O	Unknown	Row Totals
65	1	2	3	1	6	0	13
55	0	5	7	2	11	0	25
50	0	0	1	1	0	0	2
45	0	0	0	2	1	0	3
40	0	1	1	1	1	0	4
35	2	3	3	3	7	0	18
25	0	3	6	2	10	0	21
Column Totals	3	14	21	12	36	0	86

Table 33. Washington FOHE bridge pier: 1993–1996 and 1999–2011.

PSL	K	A	B	C	O	Unknown	Row Totals
70	2	0	1	1	0	0	4
60	4	1	2	1	4	0	12
55	1	0	1	1	3	2	8
35	0	1	4	1	2	0	8
30	0	0	0	1	4	0	5
25	1	0	2	1	5	0	9
Column Totals	8	2	10	6	18	2	46

Table 34. New Jersey FOHE Bridge Pier: 2001–2013.

PSL	K	A	B	C	O	Unknown	Row Totals
65	0	0	1	1	2	0	4
55	0	0	1	0	0	0	1
50	0	0	1	0	0	0	1
40	0	0	0	0	1	0	1
35	0	0	0	0	3	0	3
30	0	0	0	0	1	0	1
25	0	0	1	5	8	0	14
20	0	0	0	0	0	0	0
Column Totals	0	0	4	6	15	0	25

Table 35. North Carolina FOHE bridge pier: 2003–2012.

PSL	K	A	B	C	O	Unknown	Row Totals
70	1	1	0	4	1	0	7
65	2	1	1	3	8	0	15
60	0	0	0	1	0	0	1
55	0	0	0	0	3	0	3
45	0	1	4	1	6	0	12
40	0	0	1	0	0	0	1
35	0	0	5	3	4	1	13
Column Totals	3	3	11	12	22	1	52

Table 36. Wyoming FOHE bridge pier: 2008–2013.

PSL	K	A	B	C	O	Unknown	Row Totals
75	1	0	1	0	2	0	4
65	0	0	3	0	6	0	9
40	0	0	0	0	4	1	5
35	0	0	0	0	2	1	3
30	0	0	5	0	2	0	7
20	0	0	1	0	1	0	2
Column Totals	1	0	10	0	17	2	30

4.2.4.4 Step 3: Estimate Unreported Crashes

Step 3 of the EFCCR procedure includes the determination or estimation of the percentage of unreported crashes. These values are added to the field-observed crashes to obtain the full distribution of both reported and unreported crashes. Crash reporting thresholds vary by state, with some states only requiring reports when there is an injury. It has long been recognized that police-reported crash data underreport lower-severity crashes. “These low-severity crashes represent roadside design successes since the vehicle was able to encroach onto the roadside or median without causing an injury” [Ray 2014a]. When the EFCCR approach was developed, it included a step for estimating unreported crashes to account for this bias. The same estimating procedure is used here for the same reasons.

Unreported crashes have been addressed in several research studies, including the FHWA Pole Study [Mak 1980], *NCHRP Report 490* [Ray 2003] and *NCHRP Report 638* [Sicking 2009]. Blincoe estimated that, for all types of highway crashes, nearly half (48%) of all property-damage-only (PDO) crashes and a little over 20% (21.42%) of injury crashes were not reported [Blincoe 2002].

It has been found that the unreported rate is different for different types of roadside objects. For example, 77% of concrete barrier crashes were unreported [Fitzpatrick 1999], while 34% of low-tension cable barrier crashes were unreported [Hammond 2008].

Building on a model developed by Nilsson [Nilsson 1981], Ray et al. estimated the percentage of noninjury crashes (P_{NIC}) by comparing crashes at two speeds [Ray 2014a], as follows:

$$P_{NI2} = 1 - (1 - P_{NI1}) \left[\frac{V_2}{V_1} \right]^2 = 1 - P_{I1} \left[\frac{V_2}{V_1} \right]^2$$

This expression allows the unobservable percentage of noninjury crashes to be estimated based on the number of observed injury crashes. Next, the percentage of unreported and PDO crashes, which is either known or assumed at the base speed of 65 mph, is used to extrapolate to all other speeds. When the estimate produces no negative crash estimates, the estimate is balanced and has reached the maximum-likelihood estimate of total crashes for the dataset [Ray 2014a]. A summary of the total number of reported FOHE unshielded bridge-pier crashes from each dataset is shown in Table 37. The maximum-likelihood estimate of unreported crashes for each dataset resulted in assumed percentage of injury (PI) crashes to total crashes at the 65-mph PSL. PI crashes within each dataset are also shown in Table 37. These values are used to estimate the unreported crashes by comparing the observed PI to the estimated PI and extrapolating to find the corrected percentage of noninjury crashes that include the unreported crashes. The unreported crash counts by dataset and PSL are shown in

Table 37. Total report crashes and estimated injury percentage for each dataset.

State and Hardware Type	Years	Total Reported Crashes	PI
Ohio	2000–2012	86	53
Washington	1993–1996 and 1999–2011	46	52
New Jersey	2001–2013	25	50
North Carolina	2003–2012	52	46
Wyoming	2008–2013	30	33
Combine all datasets		239	37

Table 38. Counts are not estimated when there are no data at a PSL level; therefore, some cells in Table 38 contain no values.

4.2.4.5 Revised Step 4: Determine Probability of a Crash

In this extension of the procedure, rather than calculating an EFCCR in Step 4 for each PSL level within each dataset, $P(KA_{CUSP}|C)$ is determined. Carrigan and Ray discuss the transformation of crash severity to a probability and conclude, based on a review of available literature, that the “risk of an incapacitating or fatal crash (%KA) involving roadside hardware is simply the portion or percentage of all crashes involving that hardware type that result in fatal or severe injuries. The absolute risk when defined this way is also the probability of observing a KA crash given all crash severities” [Carrigan 2016]. $P(KA_{CUSP}|C)$ can therefore be found by summing the total number of KA crashes in the data and dividing by the total number of all crashes of all severities plus the estimated unreported crashes from Step 3, as shown here:

$$P(KA_{CUSP}|C) = \frac{\sum_{PSL=25}^{PSL=75} KA}{\sum_{PSL=25}^{PSL=75} (KABCO + UR)}$$

Where

KA = Number of police-reported severe and fatal injury crashes in each posted speed limit category (PSL_{*i*}),

KABCO = Number of police-reported crashes of all severities in each PSL_{*i*}, and

UR = Estimated number of unreported crashes in each PSL_{*i*}.

The results of this calculation for each posted speed limit level within each dataset and within the combined dataset are shown in Table 39. In some cases, there were no observed crashes at a posted speed limit level; therefore, the calculation could not be performed. In these cases, the cells in the table have no values. In other cases, there are no observed severe or fatal crashes; however, crashes of other severities are observed. In these cases, the probability calculation results in a value of 0, so a 0 is reported in these cells.

4.2.4.6 Revised Step 5: Adjust Probability for Speed

In the EFCCR procedure, the individual EFCCRs are combined into a case-weighted, single, dimensionless value at a baseline speed that can be adjusted up or down for each site-specific analysis. In this extension of the procedure, the speed-weighted probability of a KA crash given a collision at a base PSL of 65 mph [$P(KA_{CUSP}|C)_{65}$] is determined. This is calculated using the case-weighted average $P(KA_{CUSP}|C)$ for each level of PSL in each dataset as follows:

$$P(KA_{CUSP}|C)_{65} = \frac{P(KA_{CUSP}|C) \cdot 65^3}{(PSL)^3}$$

Table 38. Unreported crash count estimates by dataset.

PSL	OH	WA	NJ	NC	WY	Combined Data Analysis
75	–	–	–	–	0.55	0.06
70	–	2.63	–	4.25	–	9.64
65	0.21	–	0.00	0.22	0.09	10.35
60	–	6.06	–	1.55	–	11.03
55	11.89	0.06	1.79	0.00	–	28.17
50	4.38	–	2.38	–	–	10.70
45	4.87	–	–	15.21	–	30.11
40	10.95	–	0.00	4.74	0.00	17.55
35	53.58	31.80	0.00	46.98	0.00	189.04
30	–	4.03	0.00	–	64.13	65.13
25	119.30	43.00	67.12	–	–	322.41
20	–	–	–	–	30.01	26.55
Column Totals	205.18	87.58	71.29	72.95	94.78	720.74

Table 39. Probability of KA crashes [$P(KA_{CUSP}|C)$] by dataset and speed.

PSL	OH	WA	NJ [†]	NC	WY	Combined data analysis
75	–	–	–	–	0.2197	0.2463
70	–	0.3015	–	0.1778	–	0.173
65	0.2271	–	0	0.1971	0	0.1168
60	–	0.2769	–	0	–	0.1051
55	0.1355	0.1241	0	0	–	0.0935
50	0	–	0	–	–	0
45	0	–	–	0.0367	–	0.0222
40	0.0669	–	0	0	0	0.0350
35	0.0698	0.0251	0	0	0	0.0257
30	–	0	0	–	0	0
25	0.0214	0.0192	0	–	–	0.0109
20	–	–	–	–	0	0
$P(KA_{CUSP} C)_{65}$	0.1435	0.1599	0	0.0766	0.0137	0.0656

†No severe or fatal crashes in the data.

The resulting value can be used in the guidelines and adjusted using the site-specific PSL, as follows:

$$P(KA|C)_{PSL_i} = \left[\frac{P(KA_{CUSP}|C)_{65}}{65^3} \right] PSL_i^3$$

The probability of a severe or fatal crash with a bridge pier at a baseline speed of 65 mph, for each dataset, is as follows:

- Ohio: 0.1435
- Washington: 0.1599
- New Jersey: 0 (no observed KA crashes in this dataset)
- North Carolina: 0.0766
- Wyoming: 0.0137
- Combined analysis: 0.0656

Washington State yielded the highest probability (0.1599) for unshielded piers, and (excepting New Jersey) Wyoming yielded the lowest (0.0137). Data from all five states were combined, resulting in a probability of a severe or fatal crash severity of 0.0656 for bridge piers that are unshielded at a base condition speed of 65 mph. It is suggested that the value obtained from the combined analysis be used in the guidelines. Substituting the suggested value of 0.0656 into the formula and simplifying provides this model for use in the guidelines:

$$P(KA_{CUSP}|C)_{PSL_i} = \left[\frac{0.0656}{65^3} \right] PSL_i^3 = 2.3895 \cdot 10^{-7} \cdot PSL_i^3$$

$$P(KA_{CUSP}|C) = 2.3895 \cdot 10^{-7} \cdot PSL_i^3$$

4.2.4.7 Results

As will be shown later in the examples, these procedures estimate the number of crashes with the lead column of a pier system, so impacts with the interior columns must be added to the estimate since fatal and severe injury crashes can occur with these columns as well. RSAPv3 runs show that columns downstream of the leading column experience about one-third the number of collisions as the leading column, so the estimate of total passenger vehicle crashes can be determined from the leading-edge collisions as follows, where n is the number of columns in the pier system:

$$\left[\frac{AF_{PV\ CUSP} \cdot n}{3} \right] + \left[\frac{2 \cdot AF_{PV\ CUSP}}{3} \right] = AF_{PV\ CUSP} \left[\frac{n+2}{3} \right]$$

The annual frequency of severe or fatal passenger vehicle collisions with the unshielded pier component can now be found as follows:

$$AF_{PV\ CUSP} = \sum_{i=1}^m \left[\frac{(n+2)}{3} \right] PVE_i \cdot N_i \cdot P(C|PVE_i) \cdot P(KA_{CUSP}|C)$$

The objective of roadside design is to minimize the consequences of vehicles leaving the road. This has generally been interpreted as attempting to minimize the occurrence of severe and fatal crashes (i.e., KA crashes). NCHRP Project 22-12(03) used a risk of 0.01 of a severe injury or fatal crash occurring during the 30-year design life on a 1,000-ft length of bridge railing as an acceptance value for selecting bridge railings [Ray 2014b]. Converted to an annual per-mile risk, the value used in NCHRP Project 22-12(03) would be a risk of 0.0018 KA

crashes/edge-mile/year. AASHTO SCOBS T7 and the AASHTO Technical Committee on Roadside Safety (TCRS) have been considering the suggestions of NCHRP Project 22-12(03), so there is also some history of support for an annual risk of fatal or severe injury in the range 0.0018 KA crashes/edge-mile/year.

Bridge piers are essentially point hazards, whereas the risk value of 0.0018 KA crashes/edge-mile/year involves a length (e.g., 1 mile). Trajectories in RSAPv3 are generally less than 300 ft, so it could be argued that a point hazard like a bridge pier is actually exposed to traffic 300 ft upstream of the hazard; encroachments that start more than 300 ft upstream of a pier are very unlikely to reach the pier. Using the NCHRP Project 22-12(03) recommendation, this would equate to an annual risk of a fatal or severe crash of 0.01 KA crashes/30 years/1,000 ft of bridge edge = $(0.01 \cdot 300)/(30 \cdot 1,000) = 0.0001$. Interestingly and coincidentally, this value is exactly the value used for the annual risk of bridge collapse in Articles 3.14 and 3.6.5 of the *LRFD Bridge Design Specifications* for critical bridges. It is encouraging that these two entirely independent criteria are the same since that indicates that these two different areas of bridge design have selected consistent thresholds of risk with respect to the possibility of the loss of life in a catastrophic event. The risk criterion suggested for the passenger-vehicle occupant protection procedures is that the annual risk of a fatal or severe injury crash ($AF_{KA\ CUSP}$) must be less than or equal to 0.0001 KA crashes involving an unshielded bridge pier per year.

4.2.5 Shielding Barrier Layout Occupant Protection

Recommendations for barrier placement and layout are provided in Sections 5.6.4 of the RDG [AASHTO 2011]. The suggestions for placement and layout of barriers used for passenger-vehicle occupant protection generally conform to the RDG guidance, with some variations as discussed in the following sections.

4.2.5.1 Shielding Barrier Type

The barrier options for shielding bridge piers to minimize the chance of passenger vehicle occupants being severely or fatally injured in a collision with a bridge pier will only include barriers that meet the MASH crash-testing guidelines [AASHTO 2016]. The FHWA has encouraged states to adopt MASH TL-3 31-in.-tall w-beam guardrails [FHWA 2014b]. A w-beam guardrail is the most commonly used barrier system for occupant protection, and it is the default test level for the National Highway System, so it has been included in this research as the most likely occupant protection alternative,

whereas TL-5 concrete barriers were included for pier protection from heavy-vehicle impacts.

4.2.5.2 Shielding Barrier Layout for Occupant Protection

If the annual frequency of severe or fatal injury passenger vehicle collisions is greater than or equal to 0.0001 for the unshielded pier system, the pier system should be shielded for passenger-vehicle occupant protection. The placement of a shielding barrier for passenger-vehicle occupant protection from pier component impacts should follow the recommendations of Section 5.6.4 of the RDG [AASHTO 2011]. The layout requires determination or selection of the following six dimensions, as shown in RDG Figure 5–39:

1. The shy-line offset distance (L_S) (RDG Table 5–7).
2. The run-out length (L_R) (RDG Table 5–10).
3. The flare rate (a/b), if desired (RDG Table 5–8).
4. The tangent length (L_1), if desired.
5. The barrier offset from the edge of lane (L_2).
6. The lateral extent of the area of concern (L_A).

The user first determines the shy-line offset distance from RDG Table 5–7. Next, the expected barrier deflection distance for a MASH TL-3 barrier should be determined from Table 5–6. The barrier should be placed at least far enough away from the face of the closest pier component to provide the deflection distance in RDG Table 5–6, and ideally this should be beyond the shy-line distance in RDG Table 5–7. If there is insufficient room for both, the deflection distance should be maintained, and the barrier can be placed inside the shy line. This barrier offset distance from edge of the travel lane to the face of the w-beam guardrail is L_2 .

Next, the user should determine if a flared or tangent installation is desired. If the terrain is relatively flat and traversable, a flared installation is often most desirable, but if a flared installation would require extensive site work to make the approach and run-out areas traversable, a tangent installation can be used. The maximum flare rates (a/b) are found in RDG Table 5–8. If the guardrail is inside the shy distance, the column headed “Flare Rate for Barrier Inside Shy Line” should be used, and if it is beyond the shy-line distance, the column headed “B” can be used. The tangent distance (L_1) is the distance upstream that the guardrail will extend before the start of the flare. The run-out length needed for the particular speed limit and traffic volume is then determined from RDG Table 5–10. Once these values are found or selected, RDG Equation 5-1 (flared) or Equation 5-2 (tangent) can be used to find the length-of-need X shown in RDG Figure 5–39.

CHAPTER 5

Verification and Validation

This chapter presents four examples that illustrate the use of the proposed LRFD bridge design procedures and RDG procedures for shielding bridge piers. Please reference Appendix A: Proposed LRFD Bridge Design Pier Protection Specifications and Appendix B: Proposed RDG Occupant Protection Guidelines for the proposed procedures. The examples in the following sections illustrate both procedures.

The processes described in the previous chapters of this report for the *LRFD Bridge Design Specifications* and the RDG were based on extracting portions of the RSAPv3 model and developing simplified statistical models to estimate the various conditional probabilities needed. In order to ensure that the procedure correctly replicates RSAPv3, the example problems were analyzed directly using RSAPv3, and the results have been compared to the LRFD and RDG procedures in the following sections.

5.1 Example #1: Two-Lane Undivided Rural Collector with Three Pier Columns

5.1.1 Introduction

The layout for Example #1 is shown in Figure 36, and the user-supplied input information is shown in Table 40. Example #1 represents a three-column pier system on the right side of the primary direction of an undivided two-lane rural collector with 10,000 vehicles/day, 5% trucks, and a PSL of 45 mph. The three pier columns are parallel to the roadway. The user wishes to evaluate the need for pier protection in order to protect the bridge from collapse. Based on the designer's analysis, the bridge structure is not continuous, and the pier system is not redundant, so the risk assessment model will be used to assess the risk of bridge failure due to a pier collision. All three columns are 2 ft in diameter and spaced 10 ft on center. The designer has calculated that the lateral capacity is 250 kips for each

column, well below the recommended lateral impact capacity of 600 kips.

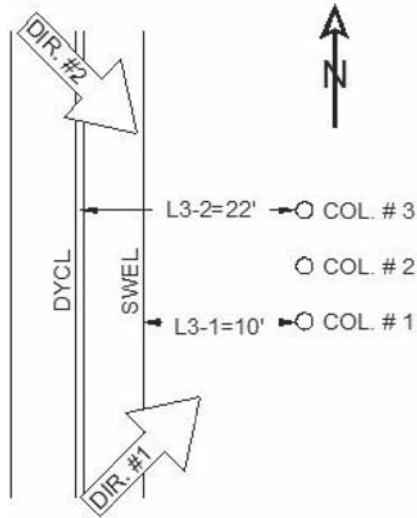
5.1.2 Pier Protection Procedure

5.1.2.1 Find Site-Specific Adjustment Factor: N_i

Direction #1 is arbitrarily defined as the northbound direction, and Direction #2 is the southbound direction. The pier is at risk from a collision from the primary right lane (Direction #1) but is also at risk of a collision from a vehicle crossing the centerline in the opposing direction (Direction #2), so both directions must be considered. Only the leading column in each direction needs to be evaluated since columns further downstream are inaccessible to heavy vehicles (i.e., these columns are essentially shielded by the leading column). Referring to Table 15 and the user-provided information in Table 40, the site-specific adjustments can be calculated; these are shown in Table 41. Since the highway characteristics are the same in each direction, the adjustment factors for each direction are also the same. In this example, the access density and PSL cause an increase in the total encroachment adjustment factor to 3.12.

5.1.2.2 Heavy-Vehicle Base Encroachment Frequency: HVE_i

Next the user must find the heavy-vehicle base encroachment frequency (HVE_i) for each direction of travel. HVE_i is an estimate of the annual number of heavy vehicles that leave the lane in the specified direction of travel and must be calculated for each direction of interest. In Example #1, the user goes to Table 13 (i.e., Appendix A, Table C3.6.5.1-2) with the highway type (undivided), the percentage of trucks (5%), and the two-way traffic volume ($AADT = 10,000$) and looks up the tabulated value. The expected average annual frequency of heavy-vehicle encroachments in each direction is 0.0019, as confirmed in Table 42.



Notes: Col = column, SWEL = solid-white edge line, DYCL = double yellow center line.

Figure 36. Example #1 site layout.

5.1.2.3 Probability of a Collision with an Unshielded Pier Component Given a Heavy-Vehicle Encroachment: $P(C|HVE_i)$

Not all vehicles that leave the roadway will strike the pier system. The probability that an encroaching heavy vehicle will strike the pier system is a function of the offset of the pier component at the leading edge of each direction and the pier component's size. Table 19 (i.e., Appendix A, Table C3.6.5.1-3) lists the probability of a collision with the pier by pier component offset and size. In this example, as shown in Figure 36, the face of Column #1 at the leading edge of the pier system in the primary direction is 10 ft

Table 40. User-input values for Example #1.

Bridge Characteristics	Value	
Nominal resistance of critical pier component: R_{CPC} (kip)	250	
Critical pier component size (ft)	2	
Number of columns in pier system	3	
Pier redundancy?	No	
Superstructure continuity?	No	
Bridge type	Typical	
Site and Traffic Characteristics	Direction #1	Direction #2
Highway type	Undivided	Undivided
Functional classification	Rural Collector	Rural Collector
Two-way AADT (veh/day)	10,000	10,000
PT (%)	5	5
Offset to critical pier component: L_3 (ft)	10	22
Major accesses (points)	2	2
Horizontal curve away from the pier?	NA	NA
Horizontal curve radius	Tangent	Tangent
Lanes in one direction	1	1
Lane width (ft)	12	12
PSL (mph)	45	45
Grade	Flat	Flat

Table 41. Site-specific adjustment factors for Example #1.[†]

Adjustment Factor	Direction #1	Direction #2
Major accesses (f_{ACC})	2.20	2.20
Lane width (f_{LW})	1.00	1.00
Horizontal curve radius (f_{HC})	1.00	1.00
Lanes in one direction (f_{LN})	1.00	1.00
Posted speed limit (f_{PSL})	1.42	1.42
Grade (f_G)	1.00	1.00
Site-specific adjustment factor (N_i)	3.12	3.12

[†]Values are found by taking the user-supplied input data in Table 40 and calculating the appropriate adjustments from Table 15.

Table 42. Heavy-vehicle base encroachment frequency for Example #1.

HVE ₁	HVE ₂
0.0019	0.0019

from the edge of travel as noted by the solid-white edge line (SWEL) of the primary lane. Column #3 is exposed to departures from the opposing lanes (i.e., Direction #2) since it is at the leading edge from that direction. The offset for Direction #2 is the 10-ft offset from the SWEL to the face of Column #3 plus the 12-ft lane width in Direction #1, or 22 ft. Recall from Table 40 that all three columns are 2 ft in diameter. Table 19 indicates a probability of striking an unshielded pier component given an encroachment of 0.1432 for Direction #1 with a 10-ft offset. There is no entry for 22 ft, but interpolating between the value for 20 ft and 25 ft yields 0.0939 (see Table 43). However, interpolation is not necessary since taking the closest offset value would provide a slightly conservative probability.

5.1.2.4 Probability of the Worst-Case Collision Force Exceeding the Critical Pier Component Capacity Given a Collision: $P(Q_{CT} > R_{CPC}|C)$

The next step is to determine the probability that if a collision does occur between the critical pier component and a heavy vehicle, the resulting impact force will exceed the lateral resistance of the pier component. The roadway in this example is an undivided rural collector, which implies a certain distribution of heavy-vehicle mix as described

Table 43. Probability of a collision with an unshielded pier component given a heavy-vehicle encroachment: $P(C|HVE_i)$ for Example #1.

$P(C HVE_1)$	$P(C HVE_2)$
0.1432	0.0939

Table 44. Probability of the worst-case collision force exceeding the critical pier component capacity given a collision: $P(Q_{CT} > R_{CPC}|C)$ for Example #1.

$P(Q_{CT} > R_{CPC} C)_1$	$P(Q_{CT} > R_{CPC} C)_2$
0.3710	0.3710

in Appendix F: Heavy-Vehicle Traffic Mix and Properties. Knowing that the functional classification is a rural collector, the user goes to the upper right section of Table 7 and selects the value corresponding to a 45-mph PSL and a critical pier component lateral resistance of 250 kips to find the value of 0.3710 (see Table 44). This value means that there is a 37% chance of the pier component failing if it is struck by a heavy vehicle on this type of roadway. Since all three piers are the same size, all three have the same probability of failure given a collision.

5.1.2.5 Annual Frequency of Bridge Collapse: AF_{BC}

Now the user is ready to calculate the expected annual frequency of bridge collapse, as follows, from the values previously determined in Table 41 (N_i), Table 42 (HVE_i), Table 43 [$P(C|HVE_i)$], and Table 44 [$P(Q_{CT} > R_{CPC}|C)$]:

$$AF_{BC} = \sum_{i=1}^m N_i \cdot HVE_i \cdot P(C|HVE_i) \cdot P(Q_{CT} > R_{CPC}|C)$$

$$AF_{BC} = [N_1 \cdot HVE_1 \cdot P(C|HVE_1) \cdot P(Q_{CT} > R_{CPC}|C)] \\ + [N_2 \cdot HVE_2 \cdot P(C|HVE_2) \cdot P(Q_{CT} > R_{CPC}|C)]$$

$$AF_{BC} = [3.12 \cdot 0.0019 \cdot 0.1432 \cdot 0.3710] \\ + [3.12 \cdot 0.0019 \cdot 0.0939 \cdot 0.3710]$$

$$AF_{BC} = [0.0003] + [0.0002]$$

$$AF_{BC} = 0.0005$$

The annual expected frequency of collapse of the bridge is, therefore, 0.0005. Another way to view this is that if the agency owned 2,000 bridges that were identical to this one in terms of traffic, geometry, and structural characteristics, one of them would experience an impact that could cause failure each year. While this particular bridge-pier system has a relatively low lateral impact capacity (i.e., 250 kips for a 2-ft-diameter column), and the probability of failure given an impact is relatively high (0.3710), the percentage of trucks is small (5%) and the speed limit is modest (45 mph), resulting in a relatively small chance of a heavy-vehicle

collision. This illustrates that for some bridges that are not designed for the 600-kip lateral impact load, the traffic characteristics at the site may make the chance of a heavy-vehicle collision small and, therefore, it is unnecessary to shield with a barrier.

This particular bridge was defined as a “typical” bridge in Table 40 so, according to Article 3.6.5.1, it does not require shielding and need not be designed for impact loading because the probability of a failure-producing impact is below the 0.0010 threshold (i.e., $0.0005 < 0.0010$). If this bridge were classified as a critical bridge, however, the pier system would require shielding since the expected number of potentially failure-producing impacts would be greater than the critical bridge threshold of 0.0001 (i.e., $0.0005 > 0.0001$).

5.1.3 Occupant Protection Procedure

The previous sections showed that the Example #1 pier system did not require shielding with a barrier because the probability of a truck collision leading to bridge collapse was sufficiently small. Even though the pier system does not need protection to guard against bridge collapse, the site conditions still must be examined to determine if the pier system needs to be shielded to minimize the chance of passenger vehicles striking the pier components and vehicle occupants becoming involved in a severe injury or fatal crash. Evaluating the site for passenger-vehicle occupant protection is the objective of the next several sections.

5.1.3.1 Find Site-Specific Adjustment Factor: N_i

The first step in both the LRFD and RDG procedures is identical, so the values in Table 41 for the site-specific adjustment factors and the procedures for determining them for the LRFD portion of the procedure are the same for this RDG portion of the procedure.

5.1.3.2 Passenger Vehicle Base Encroachment Frequency: PVE_i

Next, the user must find the passenger-vehicle base encroachment frequency (PVE_i) for each direction of travel. PVE_i is an estimate of the annual number of passenger vehicles that will leave the lane in the specified direction of travel and must be determined for each direction of interest. In Example #1, the user goes to Table 24 with the highway type, PT, and the two-way traffic volume and looks up the tabulated value. For an undivided highway with 10,000 vehicles/day and 5% trucks, the expected average annual frequency of passenger vehicle encroachments in each direction is 0.0358, as shown for reference in Table 45.

Table 45. Passenger vehicle base encroachment frequency for Example #1.

PVE ₁	PVE ₂
0.0358	0.0358

5.1.3.3 Probability of a Collision with an Unshielded Pier Component Given a Passenger Vehicle Encroachment: P(C|PVE_i)

The probability that an encroaching passenger vehicle will strike the pier system is a function of the offset of the pier component at the leading edge of each direction and the size of the bridge pier. Table 25 shows the probability of a passenger vehicle collision with the pier column by offset and size. In this example, as shown in Figure 36, the face of Column #1 at the leading edge of the pier system in the primary direction is 10 ft from the SWEL of the lane. Column #3 is the leading edge from the opposing lanes (i.e., Direction #2). The offset for Direction #2 is the 10-ft offset from the SWEL to the face of Column #3 plus the 12-ft lane width of the lane, or 22 ft. Recall from Table 40 that all three columns were 2 ft in diameter. Table 25 indicates that the probability of a passenger vehicle striking an unshielded pier component given an encroachment is 0.1004 for Direction #1 with a 10-ft offset and 0.0722 for Direction #2 with a 22-ft offset.

5.1.3.4 Probability of a Severe or Fatal Injury Given a Crash with an Unshielded Pier Component Occurs: P(KA_{CUSP}|C)

The probability that a crash with an unshielded pier component will result in a severe or fatal injury is found by looking up the appropriate value based on the PSL in Table 26. For this 45-mph roadway, 2.18% of crashes with unshielded bridge-pier components are expected to result in severe or fatal injuries (see Table 47). As shown in Table 26, the percentage of severe and fatal crashes is about three times higher on a 65-mph roadway. The procedure, therefore, accounts for the lower risk of fatal or severe injury on lower-speed roadways.

5.1.3.5 Annual Frequency of Severe Injury or Fatal Crashes with an Unshielded Bridge Pier: AF_{KA CUSP}

Now the user is ready to calculate the expected annual frequency of severe and fatal passenger-vehicle bridge-pier crashes, as follows, from the values determined in Table 41 (*N_i*), Table 45 (PVE_{*i*}), Table 46 [P(C|PVE_{*i*})], and Table 47 [P(KA_{CUSP}|C)]:

Table 46. Probability of a collision with an unshielded pier component given a passenger vehicle encroachment: P(C|PVE_i) for Example #1.

P(C PVE ₁)	P(C PVE ₂)
0.1004	0.0722

$$AF_{KA CUSP} = \sum_{i=1}^m \left[\frac{(n+2)}{3} \right] \cdot N_i \cdot PVE_i \cdot P(C|PVE_i) \cdot P(KA_{CUSP}|C)$$

$$AF_{BC} = \left[\left[\frac{3+2}{3} \right] \cdot 3.12 \cdot 0.0358 \cdot 0.1004 \cdot 0.0218 \right] + \left[\left[\frac{3+2}{3} \right] \cdot 3.12 \cdot 0.0358 \cdot 0.0722 \cdot 0.0218 \right]$$

$$AF_{KA CUSP} = [0.0004] + [0.0003]$$

$$AF_{KA CUSP} = 0.0007$$

The annual expected frequency of severe or fatal injury crashes involving passenger vehicles and this pier system with these traffic and site characteristics is 0.0007. Another way to view this is that if traffic conditions remained the same forever, one severe injury or fatal crash could be expected every 1,429 years. Since the goal is to limit severe injury and fatal crashes to less than 0.0001 per pier system per year, this site requires shielding for occupant protection even though shielding is not required to protect the bridge from collapse.

5.1.4 Shielding Barrier Layout

Since shielding is only required for vehicle occupant protection, a MASH TL-3 crash-tested strong-post w-beam guardrail can be used at the site. Vehicles can approach from either direction on this undivided roadway, so the guardrail will extend in Directions #1 and #2. For purposes of this example, it is assumed that the owner agency prefers a tangent rather than a flared installation.

RDG Table 5-7 recommends a shy-line offset (*L_s*) of 6 ft for a roadway with a 45-mph PSL. The offset to the nearest

Table 47. Probability of a severe or fatal injury given a crash with an unshielded pier component: P(KA_{CUSP}|C) for Example #1.

P(KA _{CUSP} C) ₁	P(KA _{CUSP} C) ₂
0.0218	0.0218

Table 48. Barrier layout parameters from the RDG for Example #1.

RDG Table	Parameter	Direction	
		#1	#2
5-7	L_S Shy-line offset (ft)	6	6
5-9	a/b Flare rate	–	–
5-10(b)	L_R Run-out length (ft)	160	160
	L_1 Tangent length (ft)	–	–
	L_2 Barrier offset (ft)	6	6
	L_A Lateral extent of area of concern (ft)	12	24

pier component is 10 ft from the edge of the lane, and a w-beam guardrail is a little less than 2 ft wide depending on the particular design. RDG Table 5-6 shows that in both finite element simulations and crash tests, MASH TL-3 strong-post w-beam guardrails [i.e., the Midwest Guardrail System (MGS) single w-beam with 6.25-ft post spacing] generally deflect about 3.5 ft, so there is not adequate deflection distance behind the guardrail if it is placed at the edge of the 6-ft shy line ($10 - 2 - 3.5 = 4.5 < 6$). While placing the w-beam inside the shy line is acceptable, a better alternative would be to use the MGS with half-post spacings (i.e., 3.125 ft), which would have a deflection of less than 2 ft. The barrier should, therefore, be placed at the edge of the shy line, 6 ft from the edge of the lane (i.e., $L_S = L_2 = 6$ ft) such that there is at least 3 ft of deflection space.

RDG Table 5-10(b) recommends run-out lengths (L_R) for roadways with traffic volumes of between 5,000 and 10,000 vehicles/day of 130 ft for 40 mph and 190 ft for 50 mph. Interpolating to the site condition of a 45-mph PSL results in a 160-ft run-out length (see Table 48). The usual RDG calculations needed to find the length of need (X) of the guardrail are summarized for both directions in Table 49, recognizing that the lateral extent of the area of concern (L_A) is simply the lateral offset to the face of the pier column ($P_i = 10$ ft) plus the diameter of the pier column ($D_i = 2$ ft). L_A is the distance from the edge of lane to the back face of the pier column, so it is 10 ft plus the 2-ft diameter of the column (12 ft) in Direction #1 and the 12-ft lane width plus the 10-ft lateral offset to the face of the pier plus the 2-ft diameter of the column (24 ft) for Direction #2. RDG Equation 5-2 is used to determine the length of need for a tangent guardrail, as shown in Table 49.

The values in Table 49 show the necessary length of need to shield the pier columns from passenger vehicles according to the RDG. These values are added to the length in front of the pier components themselves, which are spaced 10 ft on center and are 2 ft in diameter (20 ft + 2 ft = 22 ft). The total length of the TL-3 w-beam is therefore 142 ft (80 ft + 22 ft + 40 ft = 142 ft). These distances are measured to the length of need of the guardrail terminal, which is generally at post 3, so the end of the terminal would be another 12.5 ft up- and downstream of this w-beam guardrail. The layout of the guardrail needed to shield vehicle occupants from the pier is shown in Figure 37.

5.1.5 RSAPv3 Comparison

The procedures described in the previous sections were developed by deconstructing the encroachment probability model programed in RSAPv3 into its constituent parts and developing tables and equations for the particular question of pier protection. Since the procedures are based on an encroachment probability approach, the example procedure should result in similar answers obtained using RSAPv3. Table 50 shows that where values from these proposed procedures and RSAPv3 can be checked, there is very good agreement, indicating that the procedures are verified by RSAPv3.

RSAPv3 predicts the number of crashes with each bridge column from all directions, as shown in Table 51. The pier protection procedure only estimates the number of crashes with the pier components at the leading edge of each direction of concern, so impact with the interior columns in this case is neglected. Table 51 shows that each column downstream of the leading column in each direction experiences about one-quarter of the crashes of the leading-edge column. These interior crashes are much less likely to cause pier component failure since the outer columns shield the inner columns. Significantly, of the 18 heavy-vehicle bridge-pier collisions in Table 3 where a pier component either completely failed or was extensively damaged, the impact involved the leading column of the pier system; none of the cases involving failure appeared to have involved an initial collision with an interior pier column.

Table 49. Required length of need (X) for tangent guardrail shielding pier for Example #1.

$X = \frac{L_R(L_A - L_2)}{L_A}$	
Direction #1	Direction #2
$X = \frac{160(12 - 6)}{(12)} = 80$	$X = \frac{160[24 - (6 + 12)]}{(24)} = 40$

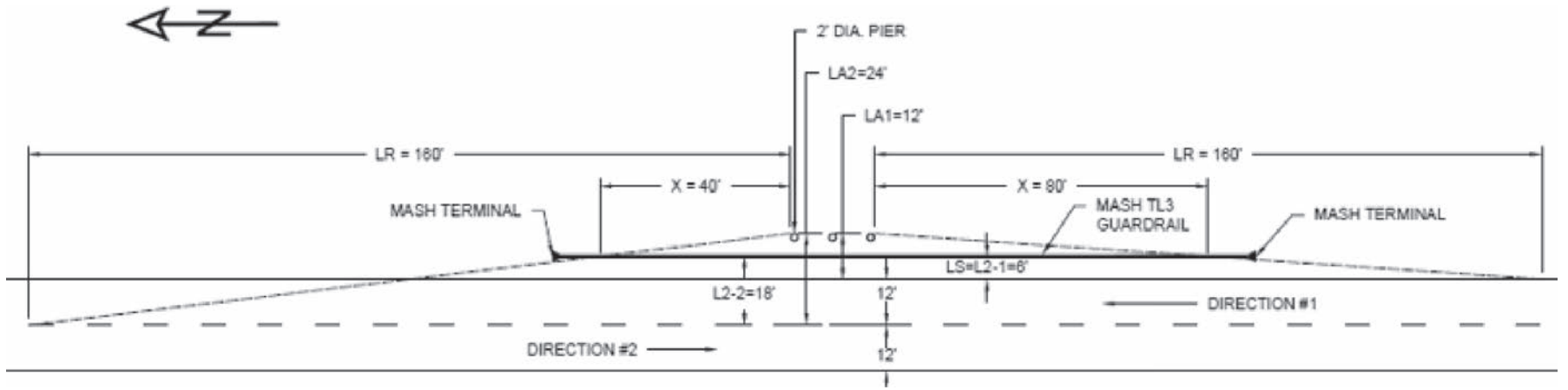


Figure 37. Occupant protection shielding barrier for Example #1.

Table 50. Comparison of RSAPv3 results and procedure results for Example #1.

Parameter	LRFD Procedure Direction		RSAPv3 Direction	
	#1	#2	#1	#2
Site-specific adjustment factor (N_i)	3.1240	3.1240	3.1240	3.1240
Base vehicle encroachment (ENCR)	2.6514	2.6514	2.6514	2.6514
Heavy-vehicle encroachment adjustment factor ($f_{HV\ ENCR}$)	1.00	1.00	1.00	1.00
Annual unshielded pier collisions ($AF_{HV\ CUSP}$)	0.0008	0.0006	0.0008	0.0005
Parameter	RDG Procedure Direction		RSAPv3 Direction	
	#1	#2	#1	#2
Site-specific adjustment factor (N_i)	3.1240	3.1240	3.1240	3.1240
Base vehicle encroachment (ENCR)	2.6514	2.6514	2.6514	2.6514
Annual unshielded pier collisions with the lead column [$N_i\ PVE_i\ P(CIPVE_i)$]	0.0112	0.0081	0.0111	0.0078

RSAPv3 indicates a total of 0.0020 heavy-vehicle collisions per year with this three-column pier, which is 0.0007 heavy-vehicle collisions more than predicted by the LRFD procedure for direct impacts with Column #1 from Direction #1 or Column #3 from Direction #2. As discussed in the previous paragraph, however, column failure is almost exclusively associated with impact with the leading column.

If a more conservative approach were desired, the total number of heavy-vehicle crashes could be estimated using the total number of columns (n), recognizing that interior columns experience one-quarter the impacts of leading-edge columns:

$$\left[\frac{AF_{HV\ CUSP}}{4} \right] (n+3) = \left[\frac{0.0006+0.0008}{4} \right] (3+3) = 0.0021$$

This approach, however, is overly conservative and is not suggested.

The situation for passenger-vehicle occupant protection is somewhat different since passenger vehicles have more maneuverability than heavy vehicles. An interior column impact can result in severe or fatal injury crashes. As shown in Table 51, interior columns experience about one-third the number of the passenger vehicle crashes as the leading-edge column. The estimate of total passenger-vehicle crashes can be determined from the leading-edge collisions as follows, where n is the number of columns in the pier system:

Table 51. Annual pier component collisions from RSAPv3 for Example #1.

Column	Heavy Vehicles		Passenger Vehicles	
	Direction		Direction	
	#1	#2	#1	#2
#3	0.0002	0.0005	0.0043	0.0078
#2	0.0002	0.0002	0.0041	0.0035
#1	0.0008	0.0001	0.0111	0.0036
Total	0.0012	0.0008	0.0195	0.0149
	0.0020		0.0344	

$$\left[\frac{n+2}{3} \right] AF_{PV\ CUSP} = \left[\frac{3+2}{3} \right] (0.0112 + 0.0081) = 0.0322$$

This value is 6% less than the number predicted by RSAPv3.

5.2 Example #2: Four-Lane Divided Rural Primary with Three Pier Columns on a Skew in the Median

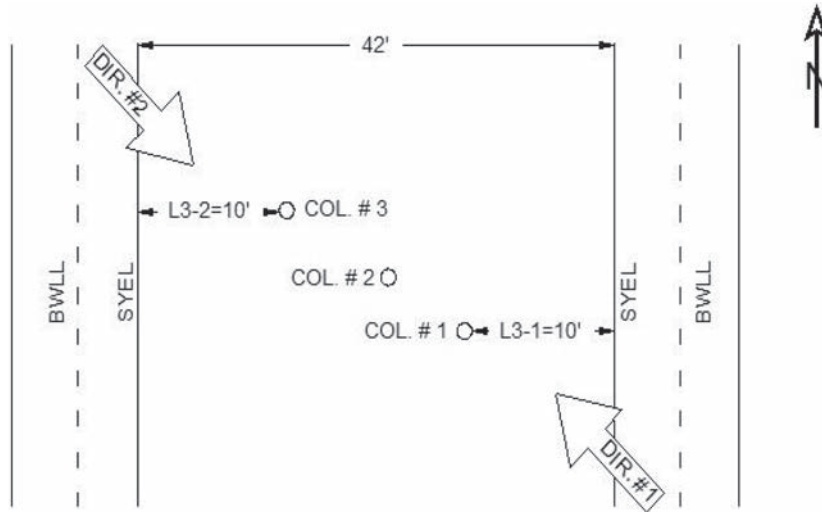
5.2.1 Introduction

The layout for Example #2 is shown in Figure 38, and the user-supplied input information is shown in Table 52. Example #2 represents a three-column pier system located in the center of a 42-ft-wide median of a rural divided Interstate with 50,000 vehicles/day, 25% trucks, and a PSL of 65 mph. The three pier columns are placed in the median on a skew such that the leading pier in each direction is 10 ft from the edge of travel. The user wishes to evaluate the need for pier protection to protect the bridge from collapse. The bridge superstructure is not continuous, and the pier system is not redundant, based on the designer's calculations, so the risk assessment model is used to determine if the pier system should be shielded to minimize the risk of bridge failure due to a pier collision. All three columns are 3 ft in diameter, and the designer has calculated that the lateral capacity of each of the columns is 900 kips.

5.2.2 Pier Protection Procedure

5.2.2.1 Find Site-Specific Adjustment Factor: N_i

Direction #1 is arbitrarily defined as the northbound direction, and Direction #2 is the southbound direction. The pier is at risk of a collision emanating from a northbound left encroachment into the median from the primary lanes (i.e., Direction #1) but is also at risk of a collision from a left



Notes: COL = column, SYEL = solid-yellow edge line, BWLL = broken white lane line.

Figure 38. Example #2 site layout.

encroachment into the median from vehicles traveling in the southbound direction (i.e., Direction #2). Only the leading column in each direction needs to be evaluated since columns further downstream are shielded from heavy-vehicle impacts by the column at the leading edge. The user-provided information in Table 52 can be used in conjunction with Table 15 (i.e., Appendix A, Table C3.6.5.1-1) to calculate the site-specific adjustment, as illustrated in Table 53. All the adjustments are the same except for grade. In the primary direction, the grade is in the uphill direction, and in the opposing direction, the grade is in the downhill direction. In this example, the site-specific adjustment factor in Direction #1 is 1.0 and 1.5 in Direction #2.

Table 52. User-input values for Example #2.

Bridge Characteristics	Value	
Nominal resistance of critical pier component: R_{CPC} (kip)	900	
Critical pier component size (ft)	3	
Number of columns in pier system	3	
Pier redundancy?	No	
Superstructure continuity?	No	
Bridge type	Typical	
Site and Traffic Characteristics	Direction #1	Direction #2
Highway type	Divided	Divided
Functional classification	Rural Primary	Rural Primary
Two-way AADT (veh/day)	50,000	50,000
PT	25	25
Major accesses (points)	0	0
Horizontal curve away from the pier?	NA	NA
Horizontal curve radius	Tangent	Tangent
Lanes in one direction	2	2
Lane width (ft)	12	12
PSL (mph)	65	65
Grade (%)	+4	-4

5.2.2.2 Heavy-Vehicle Base Encroachment Frequency: HVE_i

Next the user must estimate the annual number of heavy vehicles that will leave the lane in each direction of travel (HVE_i). In Example #2, the user goes to Table 13 (i.e., Appendix A, Table C3.6.5.1-2) with the highway type (i.e., divided), the percentage of trucks (25%), and the two-way traffic volume (AADT = 50,000) to find the expected average annual frequency of heavy-vehicle encroachments, which is 0.0065 in each direction, as shown in Table 54.

5.2.2.3 Probability of a Collision with an Unshielded Pier Component Given a Heavy-Vehicle Encroachment: $P(CIHVE_i)$

Larger pier components located closer to the traveled way are more likely to be struck by an errant heavy vehicle, so the probability that an encroaching heavy vehicle will strike the pier system given an encroachment is a function of

Table 53. Site-specific adjustment factors for Example #2.[†]

Adjustment Factor	Direction #1	Direction #2
Major accesses (f_{ACC})	1.00	1.00
Lane width (f_{LW})	1.00	1.00
Horizontal curve radius (f_{HC})	1.00	1.00
Lanes in one direction (f_{LN})	1.00	1.00
PSL (f_{PSL})	1.00	1.00
Grade (f_G)	1.00	1.50
Site-specific adjustment factor (N_i)	1.00	1.50

[†]Values are found by taking the user-supplied input data in Table 52 and calculating the appropriate adjustments from Table 15.

Table 54. Heavy-vehicle base encroachment frequency for Example #2.

HVE ₁	HVE ₂
0.0065	0.0065

the offset of the pier component at the leading edge of each direction and the size of the bridge pier component, as listed in Table 19 (i.e., Appendix A, Table C3.6.5.1-3). In this example, as shown in Figure 38, the face of Column #1 at the leading edge of the pier system in the primary direction (i.e., Direction #1) is 10 ft from the solid-yellow edge line (SYEL). Column #3 is exposed to departures from the opposing lanes (i.e., Direction #2) since it is at the leading edge from that direction. The offset for Direction #2 is also 10 ft from the SYEL to the face of Column #3. Recall from Table 52 that all three columns are 3 ft in diameter, so the probability of striking an unshielded pier component given an encroachment based on Table 19 (i.e., Table C3.6.5.1-3) is 0.1521 for a 10-ft offset, as shown in Table 55.

5.2.2.4 Probability of the Worst-Case Collision Force Exceeding the Critical Pier Component Capacity Given a Collision: $P(Q_{CT} > R_{CPC}|C)$

The next step is to determine the probability that, if a collision does occur between the critical pier component and a heavy vehicle, the resulting impact force will exceed the lateral resistance of the pier component. The roadway in this example is a divided rural primary, which implies a certain distribution of heavy-vehicle mix, as described in Appendix F. Knowing that the functional classification is a rural primary, the user goes to the upper left section of Table 7 (i.e., Appendix A, Table C3.6.5.1-4) and selects the value corresponding to a 65-mph PSL and a critical pier component lateral resistance of 900 kips to find the value of 0.0594. This value means that there is a 5.94% chance of the pier component failing if it is struck by a heavy vehicle on this type of roadway (see Table 56). Notice that since the pier columns are relatively strong (900 kips), the probability of failure given an impact is relatively small (0.0594).

Table 55. Probability of a collision with an unshielded pier component given a heavy-vehicle encroachment: $P(C|HVE_i)$ for Example #2.

$P(C HVE_1)$	$P(C HVE_2)$
0.1521	0.1521

Table 56. Probability of the worst-case collision force exceeding the critical pier component capacity given a collision: $P(Q_{CT} > R_{CPC}|C)$ for Example #2.

$P(Q_{CT} > R_{CPC} C)_1$	$P(Q_{CT} > R_{CPC} C)_2$
0.0594	0.0594

5.2.2.5 Annual Frequency of Bridge Collapse: AF_{BC}

Now the user is ready to calculate the expected annual frequency of bridge collapse, as follows, from the values previously determined in Table 53 (N_i), Table 54 (HVE_{*i*}), Table 55 [$P(C|HVE_i)$], and Table 56 [$P(Q_{CT} > R_{CPC}|C)$]:

$$AF_{BC} = \sum_{i=1}^m N_i \cdot HVE_i \cdot P(C|HVE_i) \cdot P(Q_{CT} > R_{CPC}|C)$$

$$AF_{BC} = [N_1 \cdot HVE_1 \cdot P(C|HVE_1)P(Q_{CT} > R_{CPC}|C)] \\ + [N_2 \cdot HVE_2 \cdot P(C|HVE_2) \cdot P(Q_{CT} > R_{CPC}|C)]$$

$$AF_{BC} = [1.00 \cdot 0.0065 \cdot 0.1521 \cdot 0.0594]$$

$$+ [1.5 \cdot 0.0065 \cdot 0.1521 \cdot 0.0594]$$

$$AF_{BC} = [0.0001] + [0.0001]$$

$$AF_{BC} = 0.0002$$

The annual expected frequency of collapse of the bridge is, therefore, 0.0002. Another way to view this is that if the agency owned 5,000 bridges that were identical to this one in terms of traffic, geometry, and structural characteristics, one of them would experience an impact that could cause failure each year. The columns in this particular bridge-pier system are well over the recommended lateral load capacity of 600 kips, so the probability of failure given an impact even on a high-speed, high-volume Interstate is relatively low (0.0594). This particular bridge was defined as a “typical” in Table 52, so according to Article 3.6.5.1, it does not require shielding to protect it from collapse because the probability of a failure-producing impact is well below the 0.001 threshold.

5.2.3 Occupant Protection Procedure

The previous sections showed that the Example #2 pier system did not require shielding with a barrier because the probability of a failure-inducing truck collision was sufficiently small. Even though the pier system does not need protection to guard against bridge collapse, the site conditions still must be examined to determine if the pier system needs to be shielded to minimize the chance of passenger

vehicles striking the pier components and occupants becoming involved in a severe injury or fatal crash. Evaluating the site for passenger-vehicle occupant protection is the objective of the next several sections.

5.2.3.1 Find Site-Specific Adjustment Factor: N_i

The first steps in both the LRFD and RDG procedures are identical, so the values in Table 53 representing the site characteristic adjustments and the procedures for determining them for the LRFD portion of the procedure are the same for this RDG portion of the procedure.

5.2.3.2 Passenger Vehicle Base Encroachment Frequency: PVE_i

Next, the user must find the passenger-vehicle base encroachment frequency (PVE_i) for each direction of travel. Table 24 shows that for a divided highway with 50,000 vehicles/day and 25% trucks, the expected average annual frequency of passenger vehicle encroachments in each direction is 0.0902, as shown for reference in Table 57.

5.2.3.3 Probability of a Collision with an Unshielded Pier Component Given a Passenger Vehicle Encroachment: $P(C|PVE_i)$

In this example, as shown in Figure 38, the face of Column #1 at the leading edge of the pier system in the primary direction is 10 ft from the SYEL. Column #3 is exposed to departures from the opposing lanes (i.e., Direction #2) since it is at the leading edge from that direction. The offset for Direction #2 is also 10 ft from the SYEL to the face of Column #3. As shown in Table 52, all three columns are 3 ft in diameter, so Table 25 indicates that the probability of a passenger vehicle striking an unshielded pier component given an encroachment is 0.1109 for Direction #1 and 0.1109 for Direction #2. These values are tabulated for reference in Table 58.

5.2.3.4 Probability of a Severe or Fatal Injury Given a Crash with an Unshielded Pier Component Occurs: $P(KA_{CUSP}|C)$

The probability that a crash with an unshielded pier component will result in a severe or fatal injury is found by looking

Table 57. Passenger vehicle base encroachment frequency for Example #2.

PVE_1	PVE_2
0.0902	0.0902

Table 58. Probability of a collision with an unshielded pier component given a passenger vehicle encroachment: $P(C|PVE_i)$ for Example #2.

$P(C PVE_1)$	$P(C PVE_2)$
0.1109	0.1109

up the appropriate values based on the PSL in Table 26. For this 65-mph roadway, 6.56% of the crashes with unshielded bridge piers are expected to result in severe or fatal injuries, as shown in Table 59.

5.2.3.5 Annual Frequency of Severe Injury or Fatal Crash with an Unshielded Bridge Pier: $AF_{KA_{CUSP}}$

Now the user is ready to calculate the expected annual frequency of severe and fatal passenger-vehicle bridge-pier crashes, as follows, from the values previously determined in Table 53 (N_i), Table 57 (PVE_i), Table 58 [$P(C|PVE_i)$], and Table 59 [$P(KA_{CUSP}|C)$]:

$$AF_{KA_{CUSP}} = \sum_{i=1}^m \left[\frac{(n+2)}{3} \right] \cdot N_i \cdot PVE_i \cdot P(C|PVE_i) \cdot P(KA_{CUSP}|C)$$

$$AF_{BC} = \left[\left[\frac{(3+2)}{3} \right] \cdot 1.00 \cdot 0.0902 \cdot 0.1109 \cdot 0.0656 \right] + \left[\left[\frac{(3+2)}{3} \right] \cdot 1.50 \cdot 0.0902 \cdot 0.1109 \cdot 0.0656 \right]$$

$$AF_{KA_{CUSP}} = [0.0011] + [0.0016]$$

$$AF_{KA_{CUSP}} = 0.0027$$

The annual expected frequency of severe or fatal injury crashes involving passenger vehicles and this pier system with these traffic and site characteristics is 0.0027. Another way to view this is that, if traffic conditions remained the same forever, one severe injury or fatal crash could be expected every 370 years. Since the goal is to limit annual severe injury and fatal crashes to less than 0.0001 per pier system per year, this site requires shielding with a MASH TL-3 w-beam guardrail

Table 59. Probability of a severe or fatal injury given a crash with an unshielded pier component: $P(KA_{CUSP}|C)$ for Example #2.

$P(KA_{CUSP} C)_1$	$P(KA_{CUSP} C)_2$
0.0656	0.0656

for occupant protection even though shielding is not required to protect the bridge from collapse.

5.2.4 Shielding Barrier Layout

Shielding is only required for vehicle occupant protection in Example #2, so a MASH TL-3 strong-post w-beam guardrail will be used. Vehicles can enter the median from either direction on this divided highway, so the guardrail will extend in Directions #1 and #2, as shown in Figure 39. For purposes of this example, it is assumed that the owner agency prefers to use a flared guardrail in this median situation.

RDG Table 5-7 recommends a shy-line offset (L_s) of 8.5 ft for a roadway with a 65-mph PSL. RDG Table 5-6 recommends about 3.5 ft of lateral space from the back of a MASH TL-3 w-beam barrier (i.e., MGS single w-beam at 6.25-ft post spacing) to the face of the hazard, and the barrier itself is about 2 ft wide, so the offset from the lane edge to the guardrail will be at least $10 - 2 - 3.5 = 4.5$ ft, which is inside the shy-line distance. The user could use the MGS at half-post spacing, but it is also acceptable to place the barrier inside the shy line, especially in a median situation, as noted by the RDG. In this case, the designer can be satisfied with a 4.5-ft shoulder with the guardrail at the edge of shoulder since it is a median application, so the barrier offset used in $L_2 = 4.5$ ft.

The lateral extent of area of concern (L_A) is the distance from SYEL to the back face of the farthest pier column from the road. The face of Column #1 is 10 ft from the edge of the left primary lane, and Column #3 is $42 - 10 = 32$ ft from the left edge of the primary lane, so L_A is 32 ft. Since the arrangement is symmetrical, L_A is also 32 ft in Direction #2.

RDG Table 5-9 indicates that the maximum flare rate for a rigid barrier inside the shy-line distance on a 65-mph roadway is 28:1. A tangent length in front of the columns of 24 ft is used.

Interpolating from RDG Table 5-10(b) for a design speed of 65 mph results in a run-out length (L_R) of 330 ft for a roadway with 50,000 vehicles/day. The values needed to use RDG Equation 5-1 to determine the length of need for a flared guardrail are shown in Table 60, and the calculation is shown in Table 61. The left column of Table 61 shows that a length of need of 246 ft is needed to shield the farthest column from the traveled lanes, so the 246 ft is measured from the face of Column #3 in Direction #1. Column #1 is closer to the traveled lanes, so the right column of Table 61 is used to make sure the length of need for Column #1 falls within that calculated for Column #3. Since Column #1 requires a length of need of 172 ft, and that is included within the length of need for Column #3, the arrangement shown in Figure 39 is sufficient. Direction #2 is a mirror image, so those values are not repeated.

The values in Table 61 show the necessary length of need to shield the pier columns from passenger vehicles according

to the RDG. Column #3 in Direction #1 requires a longer length of MASH TL-3 w-beam than Column #1 in Direction #1; therefore, the 246-ft length governs. Both directions are symmetric; therefore, Direction #2 was not calculated. The MASH TL-3 w-beam guardrail needed to shield vehicle occupants from the pier system in Example #2 should extend 246 ft upstream of Column #3 in Direction #1 and 246 ft upstream of Column #1 in Direction #2.

5.2.5 RSAPv3 Comparison

Table 62 compares the number of collisions from these suggested procedures to the values determined in an RSAPv3 simulation of the Example #2 conditions. As shown in Table 62, the suggested procedures are similar and slightly conservative to the values found from RSAPv3, indicating that the simplified suggested procedures are verified by RSAPv3.

As discussed for Example #1, the procedures are based on estimating the number of collisions with the leading column of the pier system. As shown in Table 63, the procedures accurately predict the number of crashes with the leading columns in Direction #1 and #2 for both heavy vehicles and passenger vehicles.

The pier protection procedures are based on the heavy-vehicle crashes with the leading column, but the passenger-vehicle occupant protection procedures use an estimate of collisions with all the columns in the pier group as follows:

$$\left[\frac{n+2}{3} \right]_{AF_{PV_{CUSP}}} = \left[\frac{3+2}{3} \right] (0.0100 + 0.0150) = 0.0417$$

In this example, the columns are at a 34-degree skew from the direction of the roadway. Table 63 shows that the passenger-vehicle occupant protection procedures underpredict the total number of passenger-vehicle pier column collisions by less than 2% even though the columns are arranged in a skew across the median. This illustrates that the interior columns need not be directly in a parallel line behind the lead columns for shielding to occur.

5.3 Example #3: Six-Lane Divided Urban Primary with Four Pier Columns Offset in the Median

5.3.1 Introduction

The layout for Example #3 is shown in Figure 40, and the user-supplied input information is shown in Table 64. Example #3 represents a four-column pier system located offset toward the opposing side in a 47.5-ft-wide median of a six-lane divided urban Interstate with 80,000 vehicles/day, 20% trucks, and a PSL of 55 mph. The roadway curves to the right

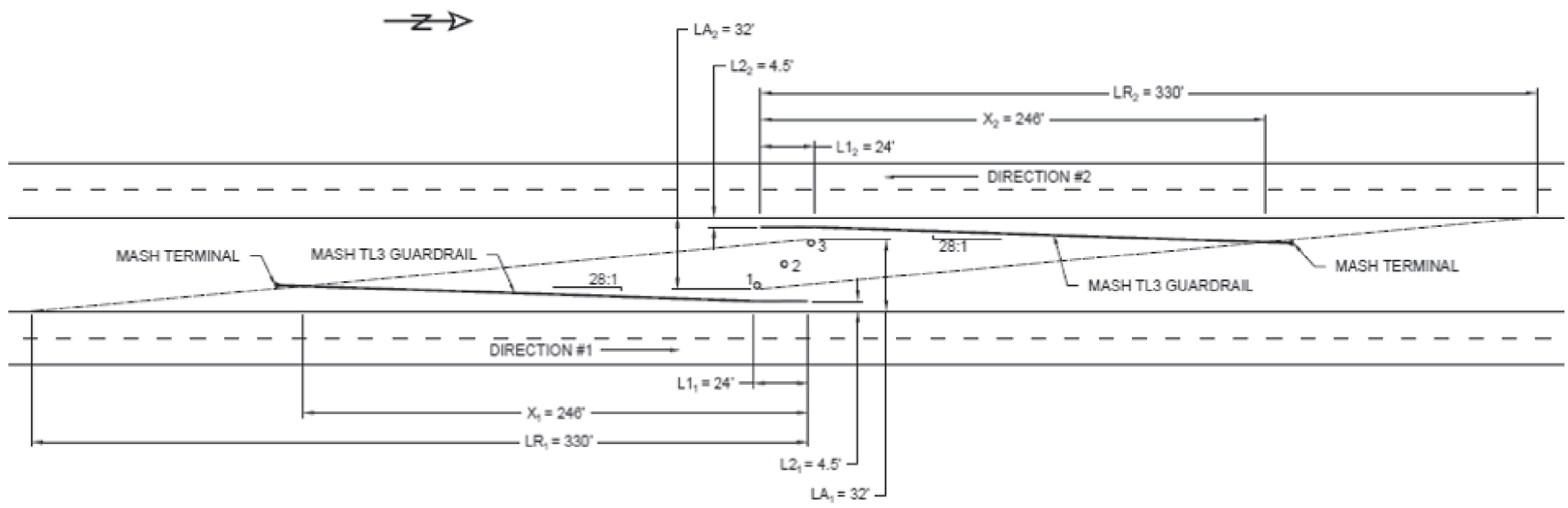


Figure 39. Occupant protection shielding barrier for Example #2.

Table 60. Barrier layout parameters from the RDG for Example #2.

RDG Table	Parameter		Direction #1	Direction #1
			Column #3	Column #1
5-7	L_S	Shy-line offset (ft)	8.5	8.5
5-9	a/b	Flare rate	28:1	28:1
5-10(b)	L_R	Run-out length (ft)	330	330
	L_1	Tangent length (ft)	24	3
	L_2	Barrier offset (ft)	4.5	4.5
	L_A	Lateral extent of area of concern (ft)	32	13

Table 61. Required length of need for flared guardrail shielding pier for Example #2.

$X = \frac{(L_A + \left\lceil \frac{b}{a} \right\rceil L_1 - L_2)}{\left\lceil \frac{b}{a} \right\rceil + \left\lceil \frac{L_A}{L_R} \right\rceil}$	
Direction #1: Column #3 $X = \frac{(32 + \left\lceil \frac{1}{28} \right\rceil 24 - 4.5)}{\left\lceil \frac{1}{28} \right\rceil + \left\lceil \frac{32}{330} \right\rceil} = 246$	Direction #1: Column #1 $X = \frac{(13 + \left\lceil \frac{1}{28} \right\rceil 3 - 4.5)}{\left\lceil \frac{1}{28} \right\rceil + \left\lceil \frac{13}{330} \right\rceil} = 172$

Table 62. Comparison of RSAPv3 results and procedure results for Example #2.

Parameter	LRFD Procedure Direction		RSAPv3 Direction	
	#1	#2	#1	#2
Site-specific adjustment factor (N_i)	1.00	1.50	1.00	1.50
Base vehicle encroachment (ENCR)	8.4673	8.4673	8.4673	8.4673
Heavy-vehicle encroachment adjustment factor ($f_{HV\ ENCR}$)	0.2168	0.2168	0.2168	0.2168
Annual unshielded pier collisions ($AF_{HV\ CUSP}$)	0.0010	0.0015	0.0009	0.0013
Parameter	RDG Procedure Direction		RSAPv3 Direction	
	#1	#2	#1	#2
Site-specific adjustment factor (N_i)	1.00	1.50	1.00	1.50
Base vehicle encroachment (ENCR)	8.4673	8.4673	8.4673	8.4673
Annual unshielded pier collisions with the lead column ($N_i\ PVE_i\ P(CIPVE_i)$)	0.0100	0.0150	0.0095	0.0141

in the primary direction. The four pier columns are placed in the median tangent to the traveled way but 25 ft from the primary left edge and 20 ft from the opposing left edge. The bridge superstructure is not continuous, and the pier system is not redundant based on the designer's calculations, so the risk assessment model is used to determine if the pier system

should be shielded to minimize the risk of bridge failure due to a pier collision. All four columns are 2.5 ft in diameter, and the designer has calculated the lateral capacity of each of the columns is 500 kips.

Table 63. Annual pier component collisions from RSAPv3 for Example #2.

Column	Heavy Vehicles Direction		Passenger Vehicles Direction	
	#1	#2	#1	#2
	#3	0.0002	0.0013	0.0031
#2	0.0004	0.0006	0.0045	0.0066
#1	0.0009	0.0003	0.0095	0.0046
Total	0.0015	0.0022	0.0171	0.0253
	0.0037		0.0424	

5.3.2 Pier Protection Procedure

5.3.2.1 Find Site-Specific Adjustment Factor: N_i

Direction #1 is arbitrarily defined as the northbound direction, and Direction #2 is the southbound direction. The pier system is at risk of a collision emanating from a left encroachment into the median from either the primary lanes (i.e., Direction #1) or the opposing lanes (i.e., Direction #2). Only the leading column in each direction needs to be evaluated since columns further downstream are shielded by the column at the leading edge. The user-provided information

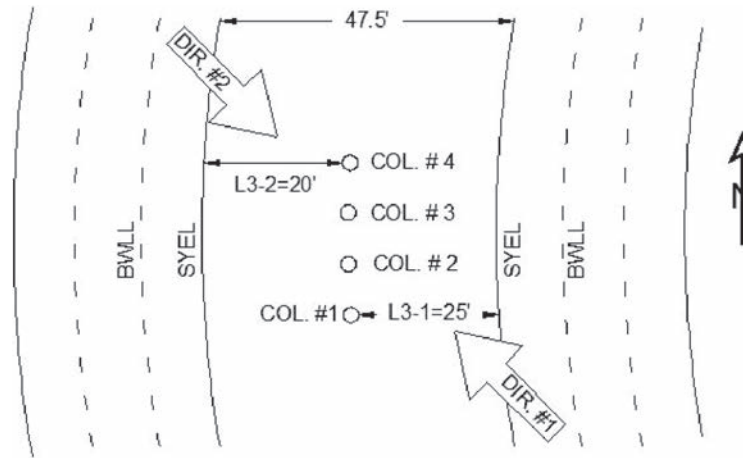


Figure 40. Example #3 site layout.

in Table 64 can be used in conjunction with Table 15 (i.e., Appendix A, Table C3.6.5.1-1) to calculate the site-specific adjustment, as illustrated in Table 65.

In Direction #1, the horizontal curve is away from the pier columns, so the adjustment is 1.27. This indicates that vehicles will tend to continue straight on a curve and potentially exit toward the pier columns. In Direction #2, the horizontal curve is toward the columns, so the adjustment is 1.09, which is smaller because vehicles are less likely to exit the roadway.

The number of lanes is accounted for in the “lanes in one direction” adjustment. For divided highways with two lanes in each direction, the adjustment is 1. For this highway, with three lanes in each direction, the adjustment for the number of lanes is 0.91. This highway has 11-ft-wide lanes rather than the more standard 12-ft-wide lanes, so the adjustment for lane width is 1.03, indicating a slight increase in the encroachment rate due to more constricted lanes.

Table 64. User-input values for Example #3.

Bridge Characteristics	Value	
Nominal resistance of critical pier component: R_{CPC} (kip)	500	
Critical pier component size (ft)	2.5	
Number of columns in pier system	4	
Pier redundancy?	No	
Superstructure continuity?	No	
Bridge type	Typical	
Site and Traffic Characteristics	Direction #1	Direction #2
Highway type	Divided	Divided
Functional classification	Urban Primary	Urban Primary
Two-way AADT (veh/day)	80,000	80,000
PT	20	20
Offset to critical pier component: L_3 (ft)	25	20
Major accesses (points)	0	0
Horizontal curve away from the pier?	Yes	No
Horizontal curve radius (ft)	2,000	2,000
Lanes in one direction	3	3
Lane width (ft)	11	11
PSL (mph)	55	55
Grade	Flat	Flat

The resulting site-specific adjustments are 1.40 in Direction #1 and 1.21 in Direction #2, indicating that there will be somewhat more departures from Direction #1, largely due to the horizontal curvature.

5.3.2.2 Heavy-Vehicle Base Encroachment Frequency: HVE_i

Next the user must estimate the annual number of heavy vehicles that will leave the lane in each direction of travel (HVE_i). In Example #3, the user goes to Table 13 (i.e., Appendix A, Table C3.6.5.1-2) with the highway type (i.e., divided), the percentage of trucks (20%), and the two-way traffic volume (AADT = 80,000) to find that the expected average annual frequency of heavy-vehicle encroachments is 0.0103 in each direction, as shown in Table 66.

5.3.2.3 Probability of a Collision with an Unshielded Pier Component Given a Heavy-Vehicle Encroachment: $P(CIHVE_i)$

In this example, as shown in Figure 40, the face of Column #1 at the leading edge of the pier system in Direction #1 is 25 ft from the SYEL. Column #4 is exposed to

Table 65. Site-specific adjustment factors for Example #3.[†]

Adjustment Factor	Direction #1	Direction #2
Major accesses (f_{ACC})	1.00	1.00
Lane width (f_{LW})	1.03	1.03
Horizontal curve radius (f_{HC})	1.27	1.09
Lanes in one direction (f_{LN})	0.91	0.91
PSL (f_{PSL})	1.18	1.18
Grade (f_G)	1.00	1.00
Site-specific adjustment factor (N_i)	1.40	1.21

[†]Values are found by taking the user-supplied input data in Table 64 and calculating the appropriate adjustments from Table 15.

Table 66. Heavy-vehicle base encroachment frequency for Example #3.

HVE ₁	HVE ₂
0.0103	0.0103

departures from Direction #2 since it is at the leading edge from that direction. The offset for Direction #2 is the 20-ft offset from the SYEL to the face of Column #4. All four columns are 2.5 ft in diameter, as shown in Table 64, so the probability of striking an unshielded pier component given an encroachment based on interpolation from Table 19 (i.e., Appendix A, Table C3.6.5.1-3) is 0.0870 for a 25-ft offset in Direction #1 and 0.1042 for a 20-ft offset in Direction #2, as shown in Table 67.

5.3.2.4 Probability of the Worst-Case Collision Force Exceeding the Critical Pier Component Capacity Given a Collision: $P(Q_{CT} > R_{CPC}|C)$

The roadway in this example is a divided urban Interstate, which implies a particular heavy-vehicle mix such as more single-unit trucks, as described in Appendix F. Knowing that the functional classification is an urban Interstate, the user goes to the lower left section of Table 7 (i.e., Appendix A, Table C3.6.5.1-4) and selects the value corresponding to a 55-mph PSL and a critical pier component lateral resistance of 500 kips to find the value of 0.6562, as listed in Table 68. There is a high chance (i.e., 65.62%) of one of these pier columns failing if it is struck by a heavy vehicle on this type of roadway with these traffic conditions. Since all the piers are the same size, all four have the same probability of failure given a collision.

5.3.2.5 Annual Frequency of Bridge Collapse: AF_{BC}

The user is now ready to calculate the expected annual frequency of bridge collapse, as follows, from the values previously determined in Table 65 (N_i), Table 66 (HVE_{*i*}), Table 67 [$P(C|HVE_i)$], and Table 68 [$P(Q_{CT} > R_{CPC}|C)$]:

Table 67. Probability of a collision with an unshielded pier component given a heavy-vehicle encroachment: $P(C|HVE_i)$ for Example #3.

$P(C HVE_1)$	$P(C HVE_2)$
0.0870	0.1042

Table 68. Probability of the worst-case collision force exceeding the critical pier component capacity given a collision: $P(Q_{CT} > R_{CPC}|C)$ for Example #3.

$P(Q_{CT} > R_{CPC} C)_1$	$P(Q_{CT} > R_{CPC} C)_2$
0.6562	0.6562

$$AF_{BC} = \sum_{i=1}^m N_i \cdot HVE_i \cdot P(C|HVE_i) \cdot P(Q_{CT} > R_{CPC}|C)$$

$$AF_{BC} = [N_1 \cdot HVE_1 \cdot P(C|HVE_1) \cdot P(Q_{CT} > R_{CPC}|C)] \\ + [N_2 \cdot HVE_2 \cdot P(C|HVE_2) \cdot P(Q_{CT} > R_{CPC}|C)]$$

$$AF_{BC} = [1.40 \cdot 0.0103 \cdot 0.0870 \cdot 0.6562] \\ + [1.21 \cdot 0.0103 \cdot 0.1042 \cdot 0.6562]$$

$$AF_{BC} = [0.0008] + [0.0009]$$

$$AF_{BC} = 0.0017$$

The annual expected frequency of collapse of this bridge under these traffic conditions is 0.0017. If the agency owned 588 bridges that were identical to this one in terms of traffic, geometry, and structural characteristics, one of them could experience an impact that could cause failure each year. The columns in this particular bridge-pier system have a lateral resistance of 500 kips, which is under the recommended lateral load capacity of 600 kips, so the probability of failure given an impact on this high-volume urban Interstate is relatively high (i.e., 0.6562). This particular bridge was defined as a “typical” bridge in Table 64 so, according to proposed Article 3.6.5.1, it requires shielding because the probability of a failure-producing impact is above the 0.001 threshold.

The user could elect to shield the pier system in Direction #2 and not in Direction #1 because the annual frequency of bridge collapse in that case would be just less than 0.001. If Direction #2 were shielded, then the annual frequency of bridge collapse would be entirely due to Direction #1 traffic, where $AF_{BC1} = 0.0008 < 0.0010$. In this case, such a strategy is probably not wise since each direction is close to the critical value by itself. This example does illustrate, however, that all directions need not be shielded as long as the annual frequency of bridge collapse for the entire pier system is less than the critical value.

5.3.3 Occupant Protection Procedure

The previous section showed that the pier system in Example #3 requires shielding with a barrier because the

probability of a failure-inducing truck collision was sufficiently high. There is, therefore, no need to check the RDG occupant protection procedure because a MASH TL-5 concrete barrier is already needed to shield the pier system from heavy-vehicle impacts.

5.3.4 Shielding Barrier Layout

Since shielding is required for pier system protection from heavy-vehicle impacts, a MASH TL-5 rigid concrete barrier will be used in this example. Since vehicles can enter the median from either direction on this six-lane divided highway, the rigid concrete barrier will extend upstream of Column #1 in the primary direction and upstream of Column #4 in the opposing direction, as shown in Figure 41. For the purpose of this example, it is assumed that the owner agency prefers to use flared barriers in this median situation.

A longitudinal barrier layout procedure is provided in RDG Section 5.6.4. RDG Table 5-7 recommends a shy-line offset (L_s) of 7.0 ft for a roadway with a 55-mph PSL. The barrier will be installed at the edge of the 6-ft median shoulder, so there will be 19 ft from the traffic face of the barrier to the face of the pier columns from Direction #1 and 14 ft from Direction #2. This is much more than the 3.25 ft minimum clearance suggested by the proposed LRFD Bridge Specifications procedure shown in Article 3.6.5.1, so the clearance is more than adequate. The suggested flare rate for a rigid barrier just inside the shy line on a 55-mph roadway is given in RDG Table 5-9 as 24:1. Interpolating RDG Table 5-10(b) for a design speed of 55 mph results in a run-out length (L_R) of 265 for a roadway with more than 10,000 vehicles/day. The RDG barrier layout dimensions for this example are shown in Table 69.

The lateral extent of area of concern (L_A) is the distance from the SYEL to the back face of the pier column, so in Direction #1 it is the 25-ft offset from the primary left lane to the face of the pier plus the 2.5-ft diameter of the column, or 27.5 ft. In Direction #2, L_A is the 20-ft offset from the left lane edge to the face of the pier plus the 2.5-ft column diameter, or 22.5 ft. RDG Equation 5-1 is used to determine the length of need for a flared guardrail, as shown in Table 70.

The values in Table 70 show the necessary length of need to shield the pier columns from heavy vehicles according to Section 5.6.4 of the RDG. The rigid MASH TL-5 barrier needed to protect the pier columns from potentially failure-causing impacts should extend 187 ft upstream of Column #1 in Direction #1 and 176 ft upstream of Column #4 in Direction #2, as shown in Figure 41. Both lengths are greater than the minimum 60 ft length of need. Additionally, the MASH TL-5 barrier must extend across the front of the columns, parallel to the road in both directions. The approach ends of these rigid MASH TL-5 barriers must be shielded with

either an appropriate guardrail and guardrail terminal or a crash cushion.

5.3.5 RSAPv3 Comparison

Table 71 shows the comparison values for the pier protection and RSAPv3 results. The pier protection procedure results are similar though slightly conservative values compared to RSAPv3 for this four-column pier system.

Even though the passenger-vehicle occupant protection procedure was not used in this example, these values were calculated to allow for a comparison with RSAPv3. Table 71 shows the comparison values between the occupant protection procedures and RSAPv3. The values agree with the RDG procedure being somewhat conservative in comparison to the RSAPv3 estimates.

While the passenger-vehicle occupant protection procedures were not required in this example since a shielding barrier was already required for pier protection, it is nonetheless interesting to determine if the number of predicted passenger-vehicle crashes with all the pier columns compares favorably with RSAPv3 (see Table 72). The passenger-vehicle protection procedures estimate a total of 0.0712 passenger vehicle crashes, whereas RSAPv3 predicts 0.0650, meaning the procedures under predict by about 6%.

$$\left[\frac{n+2}{3} \right]_{AF_{PV\ CUSP}} = \left[\frac{4+2}{3} \right] (0.0152 + 0.0152) = 0.0608$$

5.4 Example #4: Six-Lane Rural Primary with Two Columns in a Gore of an Off-Ramp

5.4.1 Introduction

Example #4 is a two-column pier system located in the gore of an off-ramp of a six-lane divided highway. The layout for Example #4 is shown in Figure 42, and the user-supplied input information is shown in Table 73. The median of the divided highway is not traversable, so there is no likelihood of a vehicle crossing over the median and striking the piers. The pier columns may be struck, however, by vehicles leaving the left side of the off-ramp (i.e., Direction #1) or leaving the right edge of the mainline (i.e., Direction #2). As shown in Table 73, the off-ramp is a one-way, one-lane roadway with a traffic volume of 5,000 vehicles per day, 5% of which are trucks. In contrast, the mainline divided highway has 60,000 vehicles/day and 25% trucks. The face of Column #1 is 12 ft from the left edge of the one-way ramp, and Column #2 is 14 ft from the right edge of the mainline highway. The bridge superstructure is not continuous, and the pier system is not redundant, based on the designer's

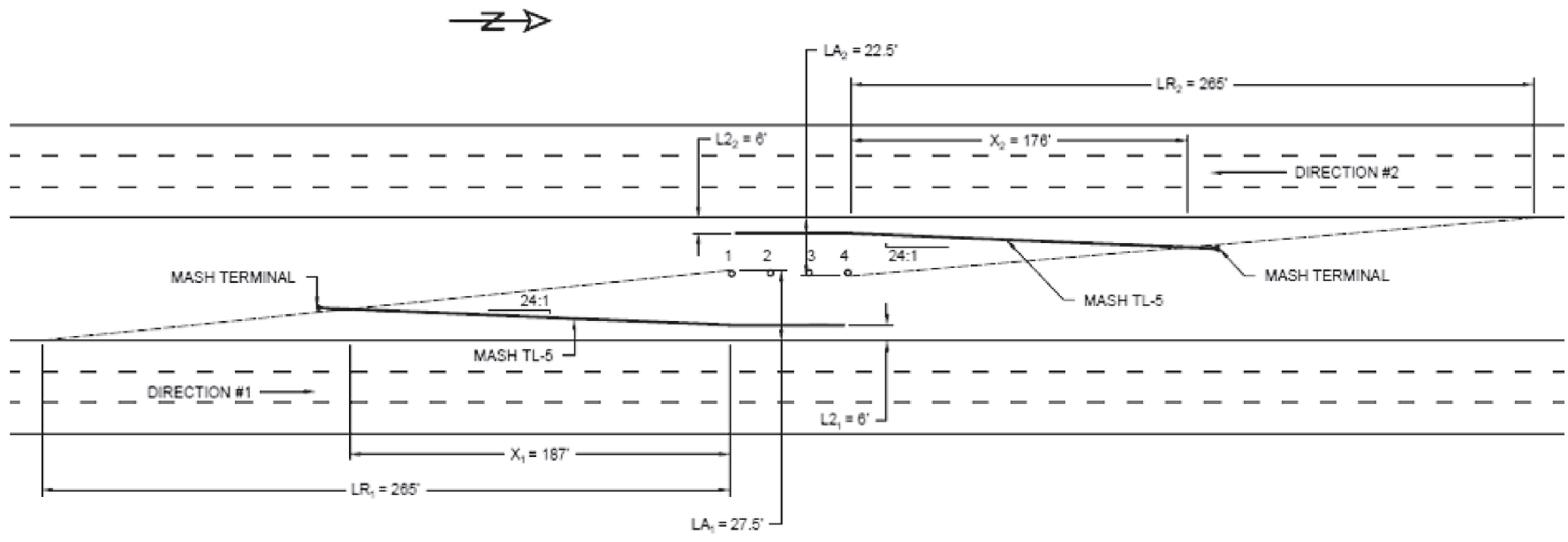


Figure 41. Pier protection shielding barrier for Example #3.

Table 69. Barrier layout parameters from the RDG for Example #3.

RDG Table	Parameter	Direction	
		#1	#2
5-7	L_S Shy-line offset (ft)	7	7
5-9	a/b Flare rate	24:1	24:1
5-10(b)	L_R Run-out length (ft)	265	265
	L_1 Tangent length (ft)	0	0
	L_2 Barrier offset (ft)	6	6
	L_A Lateral extent of area of concern (ft)	27.5	22.5

calculations, so the risk assessment model is used to determine if the pier system should be shielded to minimize the risk of bridge failure due to a pier collision. Both columns are small, 2-ft-diameter circular columns, and the designer has determined that the lateral capacity of each is only 250 kips.

5.4.2 Pier Protection Procedure

5.4.2.1 Find Site-Specific Adjustment Factor: N_i

Direction #1 is arbitrarily defined as the one-way off-ramp, and Direction #2 is the northbound mainline of the divided highway. As discussed previously, there is no need to include another direction for the opposing lanes of the divided highway since the median is not traversable. The user-provided information in Table 73 can be used in conjunction with

Table 15 (i.e., Appendix A, Table C3.6.5.1-1) to calculate the site-specific adjustment factors listed in Table 74. The adjustments are quite different for the two different directions since one direction is a one-way, low-speed, low-volume ramp, and the other is a high-speed, high-volume, six-lane highway. This example shows that the adjustments for each direction can be very different if the geometric and traffic characteristics are substantially different for the different potential impact directions. This allows the user to assess pier systems where the pier system is a risk from multiple direction with very different site and traffic characteristics.

5.4.2.2 Heavy-Vehicle Base Encroachment Frequency: HVE_i

The user estimates the annual number of heavy vehicles that encroach in each direction in Example #4 using Table 13 (i.e., Appendix A, Table C3.6.5.1-2). Direction #1 is a one-way ramp with a traffic volume of 5,000 vehicles/day. As stated in the note to Table 13, the encroachments for one-way roads are estimated by doubling the AADT of the one-way road and using the entries in Table 13 for divided highways. Entering Table 13 with an AADT of $2 \cdot 5,000 = 10,000$ vehicles and 5% trucks results in 0.0042 expected heavy-vehicle encroachments per edge in Direction #1, the one-way ramp. Direction #2 is the primary right edge of the six-lane mainline

Table 70. Required length of need for flared rigid barrier shielding pier for Example #3.

$X = \frac{(L_A + \frac{b}{a})L_1 - L_2}{\frac{b}{a} + \frac{L_A}{L_R}}$	
Direction #1	Direction #2
$X = \frac{(27.5 + \frac{1}{24})0 - 6}{\frac{1}{24} + \frac{27.5}{265}} = 187$	$X = \frac{(22.5 + \frac{1}{24})0 - 6}{\frac{1}{24} + \frac{22.5}{265}} = 176$

Table 71. Comparison of RSAPv3 results and procedure results for Example #3.

Parameter	LRFD Procedure Direction		RSAPv3 Direction	
	#1	#2	#1	#2
Site-specific adjustment factor (N_i)	1.40	1.21	1.40	1.21
Base vehicle encroachment (ENCR)	13.5477	13.5477	13.5477	13.5477
Heavy-vehicle encroachment adjustment factor ($f_{HV\ ENCR}$)	0.2682	0.2682	0.2682	0.2682
Annual unshielded pier collisions ($AF_{HV\ CUSP}$)	0.0013	0.0013	0.0011	0.0012
Parameter	RDG Procedure Direction		RSAPv3 Direction	
	#1	#2	#1	#2
Site-specific adjustment factor (N_i)	1.40	1.21	1.40	1.21
Base vehicle encroachment (ENCR)	13.5477	13.5477	13.5477	13.5477
Annual unshielded pier collisions with the lead column ($N_i PVE_i P(CIPVE_i)$)	0.0153	0.0152	0.0139	0.0138

Table 72. Annual pier component collisions from RSAPv3 for Example #3.

Column	Heavy Vehicles		Passenger Vehicles	
	Direction		Direction	
	#1	#2	#1	#2
#4	0.0003	0.0012	0.0066	0.0138
#3	0.0004	0.0003	0.0063	0.0060
#2	0.0003	0.0003	0.0066	0.0059
#1	0.0011	0.0003	0.0139	0.0059
Total	0.0021	0.0021	0.0334	0.0316
	0.0042		0.0650	

divided highway so the user enters the divided highway portion of Table 13 with an AADT of 60,000 vehicles/day and 25% trucks to find that 0.0078 heavy-vehicle encroachments can be expected annually, as shown for reference in Table 75.

5.4.2.3 Probability of a Collision with an Unshielded Pier Component Given a Heavy-Vehicle Encroachment: $P(C|HVE_i)$

In this example, as shown in Figure 42, the distance to the face of Column #1 from the edge of the one-way ramp (i.e., Direction #1) is 12 ft, and the distance from the right edge of the primary lanes of the mainline divided highway to

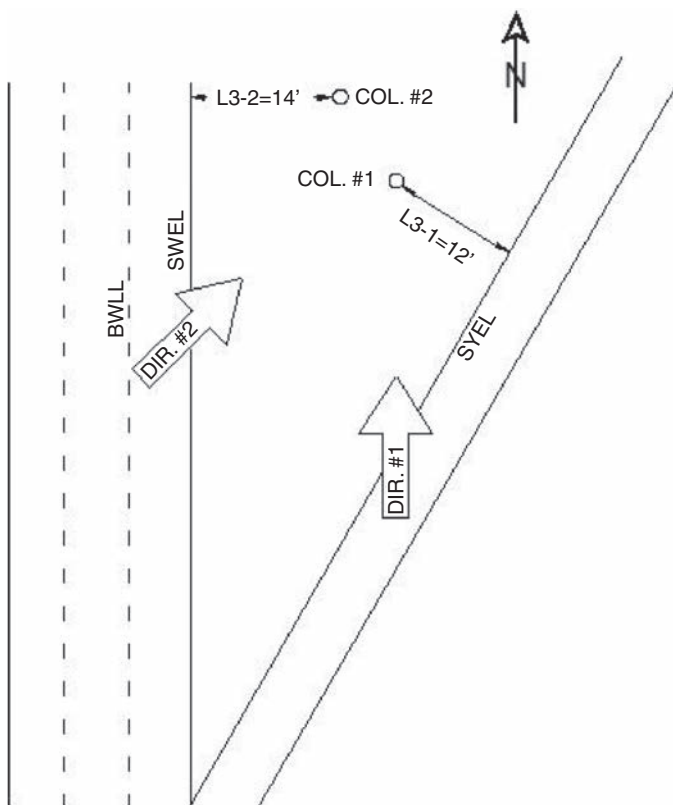


Figure 42. Example #4 site layout.

Table 73. User-input values for Example #4.

Bridge Characteristics	Value	
Nominal resistance of critical pier component: R_{CPC} (kip)	250	
Critical pier component size (ft)	2	
Number of columns in pier system	2	
Pier redundancy?	No	
Superstructure continuity?	No	
Bridge type	Typical	
Site and Traffic Characteristics	Direction #1	Direction #2
Highway type	One-way ramp	Divided
Functional classification	Rural primary	Rural primary
Two-way AADT (veh/day)	5,000 (one-way)	60,000
PT	5	25
Offset to critical pier component: L_3 (ft)	12	14
Major accesses (points)	0	1
Horizontal curve away from the pier?	Yes	NA
Horizontal curve radius (ft)	4,500	Tangent
Lanes in one direction	1	3
Lane width (ft)	12	12
PSL (mph)	30	65
Grade (%)	-5	Flat

Column #2 is 14 ft. Both columns are 2 ft in diameter with a lateral impact capacity of 250 kips, as shown in Table 73, so the probability of striking an unshielded pier component given an encroachment based on Table 19 (i.e., Appendix A, Table C3.6.5.1-3) is 0.1337 for a 12-ft offset in Direction #1 and 0.1247 for a 14-ft offset in Direction #2, as shown in Table 67. Table 19 only lists offsets of 10 and 15 ft, so these values were found using the equation at the bottom of Table 19, but the user could also interpolate the listed values and get essentially the same results.

5.4.2.4 Probability of the Worst-Case Collision Force Exceeding the Critical Pier Component Capacity Given a Collision: $P(Q_{CT} > R_{CPC}|C)$

The roadway in this example is a one-way off-ramp in Direction #1 and a divided rural primary highway in Direction #2. Each functional class and highway type implies a particular heavy-vehicle mix. Knowing that the functional classification is rural divided, the user goes to the upper left

Table 74. Site-specific adjustment factors for Example #4.[†]

Adjustment Factor	Direction #1	Direction #2
Major accesses (f_{ACC})	1.00	2.00
Lane width (f_{LW})	1.00	1.00
Horizontal curve radius (f_{HC})	1.11	1.00
Lanes in one direction (f_{LN})	1.00	0.91
PSL (f_{PSL})	1.18	1.00
Grade (f_G)	1.75	1.00
Site-specific adjustment factor (N_i)	2.29	1.82

[†] Values are found by taking the user-supplied input data in Table 73 and calculating the appropriate adjustments from Table 15.

Table 75. Heavy-vehicle base encroachment frequency for Example #4.

HVE ₁	HVE ₂
0.0042	0.0078

section of Table 7 (i.e., Appendix A, Table C3.6.5.1-4). Similar to determining the AADT, one-way facilities are assumed to have the same vehicle mix characteristics as divided roadways so the user goes to Table 7 with the 30-mph PSL (i.e., less than or equal to 45 mph) of the one-way ramp to find that the probability of exceeding the 250-kip lateral capacity given that an impact occurs in Direction #1 is 0.8058. In Direction #2 on the mainline, the user goes to Table 7 with the 65-mph PSL to find that the probability of exceeding the 250-kip lateral capacity if an impact occurs is 0.9824, as listed for reference in Table 77. There is an extremely high chance of one of these pier columns failing if it is struck by a heavy vehicle from either direction due to the combination of the small lateral load capacity, the high speed and volume on the mainline, and the geometry on the ramp (e.g., curvature, grade).

5.4.2.5 Annual Frequency of Bridge Collapse: AF_{BC}

The user is now ready to calculate the expected annual frequency of bridge collapse, as follows, from the values previously determined in Table 74 (N_i), Table 75 (HVE_{*i*}), Table 76 [$P(C|HVE_i)$], and Table 77 [$P(Q_{CT} > R_{CPC}|C)$]:

$$AF_{BC} = \sum_{i=1}^m N_i \cdot HVE_i \cdot P(C|HVE_i) \cdot P(Q_{CT} > R_{CPC}|C)$$

$$AF_{BC} = [N_1 \cdot HVE_1 \cdot P(C|HVE_1) P(Q_{CT} > R_{CPC}|C)] \\ + [N_2 \cdot HVE_2 \cdot P(C|HVE_2) \cdot P(Q_{CT} > R_{CPC}|C)]$$

$$AF_{BC} = [2.29 \cdot 0.0042 \cdot 0.1337 \cdot 0.8058] \\ + [1.82 \cdot 0.0078 \cdot 0.1247 \cdot 0.9824]$$

$$AF_{BC} = [0.0010] + [0.0017]$$

$$AF_{BC} = 0.0028$$

Table 76. Probability of a collision with an unshielded pier component given a heavy-vehicle encroachment: $P(C|HVE_i)$ for Example #4.

$P(C HVE_1)$	$P(C HVE_2)$
0.1337	0.1247

Table 77. Probability of the worst-case collision force exceeding the critical pier component capacity given a collision: $P(Q_{CT} > R_{CPC}|C)$ for Example #4.

$P(Q_{CT} > R_{CPC} C)_1$	$P(Q_{CT} > R_{CPC} C)_2$
0.8058	0.9824

The annual expected frequency of collapse of this bridge under these traffic conditions is 0.0028. This expected risk is almost three times higher than the critical risk of 0.001 for a typical bridge, so this pier system should be either shielded to protect the piers, or the pier columns could be redesigned so they are stronger.

If this pier system was being contemplated for new construction, the designer could increase the lateral strength of the pier columns to 800 kips. In so doing, the probability of exceeding the impact load would decrease from 0.8058 to essentially 0 in Direction #1 and from 0.9824 to 0.2706 in Direction #2. The annual frequency of bridge collapse would then be 0.0005, which is less than the critical value of 0.001. On the other hand, if this bridge were already built and being evaluated for bridge collapse risk, then shielding the pier system would likely be the only feasible solution.

5.4.3 Occupant Protection Procedure

The previous sections showed that the pier system in Example #4 requires shielding with a barrier because the probability of a failure-inducing truck collision is almost three times higher than the critical value of 0.001. A MASH TL-5 rigid concrete barrier would, therefore, be required to protect the pier system from heavy-vehicle impacts. Since the pier system must be shielded for pier protection reasons, there is no need to check for occupant protection from pier collisions since a barrier is already needed.

5.4.4 Shielding Barrier Layout

Since shielding is required for pier component protection from heavy-vehicle collisions, a MASH TL-5 rigid concrete barrier would be used at the site. Since heavy vehicles are a risk in both directions, a shielding barrier should be used on the ramp approach as well as the approach on the mainline of the divided highway, as shown in Figure 43. For purposes of this example, it is assumed that the owner agency prefers to use a flared barrier in this ramp situation.

RDG Table 5-7 recommends a shy-line offset (L_s) of 4 ft for the 30-mph ramp, as shown in Table 78. On the ramp (i.e., Direction #1), the face of the pier is 12 ft from the left edge of the lane, and the pier protection procedures suggest

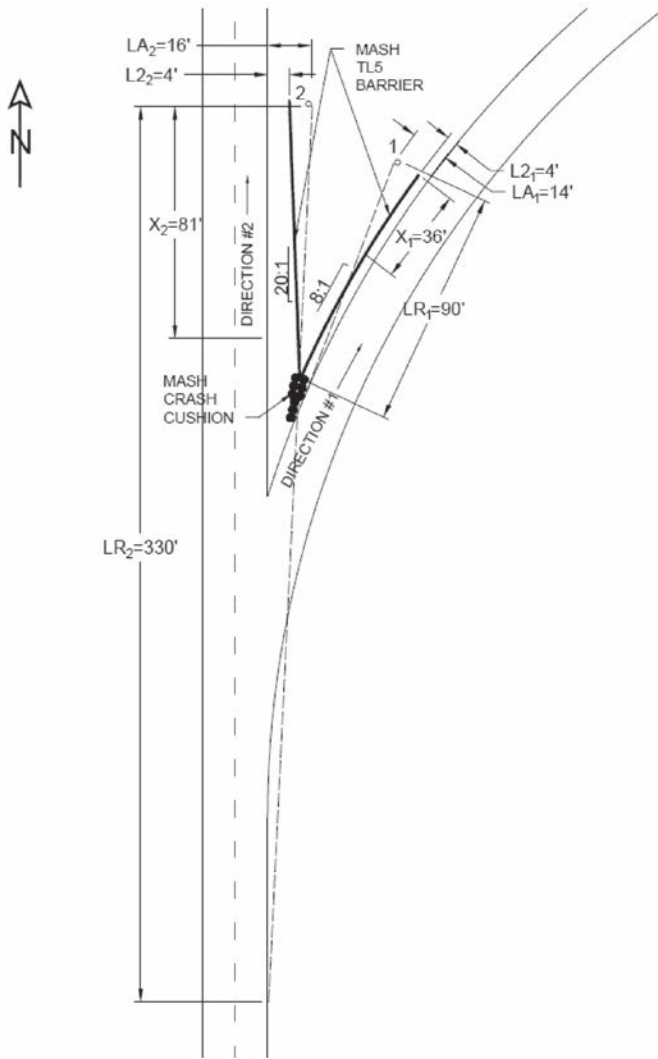


Figure 43. Pier protection shielding barrier for Example #4.

3.25 ft of space from the back of the barrier to the face of the pier. A typical single-faced section of rigid concrete barrier is about 18 in. wide, so there is sufficient room to place the barrier at the edge of the 4-ft shy line. The RDG recommends an 8:1 flare rate for rigid barriers at or beyond the shy line on 30-mph roads, as shown in Table 78. The run-out length for

Table 78. Barrier layout parameters from the RDG for Example #4.

RDG Table	Parameter	Direction	
		#1	#2
5-7	L_S Shy-line offset (ft)	4	7
5-9	a/b Flare rate	8:1	20:1
5-10(b)	L_R Run-out length (ft)	90	330
	L_1 Tangent length (ft)	0	0
	L_A Lateral extent of area of concern (ft)	14	16

30-mph roadways with 5,000–10,000 vehicles per day is 90 ft, as also shown in Table 78. Table 79 shows that the shielding barrier should extend 36 ft upstream of Column #1 on the one-way ramp.

RDG Table 5-7 recommends a shy-line offset (L_S) of 7 ft for the 65-mph mainline divided highway, as shown in Table 78. The face of the pier is 14 ft from the right edge of the mainline highway, and the pier protection procedures suggest 3.25 ft of space from the back of the barrier to the face of the pier. A typical single-faced section of rigid concrete barrier is about 18 in. wide, so there is sufficient room to place the barrier at the edge of an 8-ft shoulder, which would be just beyond the 7-ft shy line. The RDG recommends a 20:1 flare rate for rigid barriers at or beyond the shy line on 65-mph roads, as shown in Table 78. The run-out length for 65-mph roadways with more than 10,000 vehicles/day is 330 ft, as is also shown in Table 78. Table 79 shows that the shielding barrier should extend 81 ft upstream of Column #2 on the mainline of the divided highway.

In this case, the length of Direction #1 was calculated to require a length of need of 36 ft using the RDG procedure. This barrier, however, is being provided for pier protection. The minimum 60-ft upstream length recommended by the LRFD procedures should therefore be provided. Additionally, the ends of the two barriers are fairly close to one another and the intersecting roadways. The designer could, if this were new construction, provide stronger pier components. The design could also extend the barrier in Directions #1 and #2 to intersect and terminate both with a single crash cushion placed in front of the end of the rigid concrete barrier. This is shown in Figure 43.

Table 79. Required length of need for tangent guardrail shielding pier for Example #4.

$X = \frac{(L_A + \frac{b}{a})L_1 - L_2}{\frac{b}{a} + \frac{L_A}{L_R}}$	
<p>Direction #1</p> $X = \frac{(14 + \frac{1}{8})0 - 4}{\frac{1}{8} + \frac{14}{90}} = 35.6 \rightarrow 36$	<p>Direction #2</p> $X = \frac{(16 + \frac{1}{20})0 - 8}{\frac{1}{20} + \frac{16}{330}} = 81 \rightarrow 85$

Table 80. Comparison of RSAPv3 results and procedure results for Example #4.

Parameter	LRFD Procedure Direction		RSAPv3 Direction	
	#1	#2	#1	#2
Site-specific adjustment factor (N_i)	2.29	1.82	2.30	1.82
Base vehicle encroachment (ENCR)	5.8435	10.1608	5.8435	10.1608
Heavy-vehicle encroachment adjustment factor ($f_{HV\ ENCR}$)	1.0000	0.2168	1.0000	0.2168
Annual unshielded pier collisions ($AF_{HV\ CUSP}$)	0.0010	0.0017	0.0011	0.0017
Parameter	RDG Procedure Direction		RSAPv3 Direction	
	#1	#2	#1	#2
Site-specific adjustment factor (N_i)	2.29	1.82	2.30	1.82
Base vehicle encroachment (ENCR)	5.8435	10.1608	5.8435	10.1608
Annual unshielded pier collisions with the lead column ($N_i\ PVE_i\ P(CIPVE_i)$)	0.0218	0.0208	0.0164	0.0168

5.4.5 RSAPv3 Comparison

RSAPv3 is not able to analyze intersecting roadways, so this example was analyzed using two RSAPv3 simulations—one for each direction. Table 80 shows the comparison values for the LRFD pier protection procedure and RSAPv3 results. The pier protection procedure results are essentially identical to the RSAPv3 estimates for this two-column pier system.

Even though the passenger-vehicle occupant protection procedure was not used in this example, Table 80 also shows the comparison values between the occupant protection procedures and RSAPv3. The values for the RDG procedure somewhat overpredict compared to the RSAPv3 estimates.

While the passenger-vehicle occupant protection procedures were not required in this example since a shielding barrier was already required for pier protection, the number of predicted passenger-vehicle crashes with all the pier columns compares favorably with RSAPv3. The passenger-

Table 81. Annual pier component collisions from RSAPv3 for Example #4.

Column	Heavy Vehicles Direction		Passenger Vehicles Direction	
	#1	#2	#1	#2
	#2	0.0011	0.0004	0.0164
#1	0.0010	0.0017	0.0114	0.0168
Total	0.0021		0.0278	
	0.0042		0.0516	

vehicle protection procedures estimate a total of 0.0568, calculated as follows:

$$\left[\frac{n+2}{3} \right] AF_{PV\ CUSP} = \left[\frac{2+2}{3} \right] (0.0218 + 0.0208) = 0.0568$$

RSAPv3 predicts 0.0516 (see Table 81), meaning that the RDG procedures overpredict by almost 10%. This is conservative but not unreasonably so.

CHAPTER 6

Implementation Strategy

In addition to this report, the products developed in this research are presented in Appendix A: Proposed LRFD Bridge Design Pier Protection Specifications and Appendix B: Proposed RDG Occupant Protection Guidelines. These research products have been prepared with the goal of implementation in mind. Dekelbab et al. suggest “a formula for successful product implementation multiplies three components: effective products, effective implementation, and enabling contexts” [Dekelbab 2017]. These products have been presented in a format that can readily be adopted by AASHTO into the *LRFD Bridge Design Specifications* and RDG. The research team has presented the results of this research to the relevant AASHTO committees and stakeholders. During these presentations, the draft products were evaluated for their technical effectiveness, ease of use, and relevance to real field situations. Stakeholders were informed of the background, development, and potential use of the guidelines. Additionally, some panel members provided draft versions of the research products to their DOTs for early evaluation and assessment, and the comments received from these early adopters have been integrated into the final products such that implementation has already begun. The following sections summarize an implementation plan for the research products.

6.1 Products

This research project developed the following two proposed guidelines:

- Proposed LRFD Bridge Design Pier Protection Specifications (Appendix A), and
- Proposed Preliminary RDG Occupant Protection Guidelines (Appendix B).

Full implementation will necessitate adoption of Appendix A into the *LRFD Bridge Design Specifications* by the AASHTO Committee on Bridges and Structures (COBS) and adoption of Appendix B into the RDG by the AASHTO Committee on Design (COD) Technical Committee on Roadside Safety (TCRS).

6.2 Audience

The primary audience for the guidelines produced in this project is bridge engineers, highway designers, roadside safety researchers, and policy makers. In particular, the AASHTO COBS may use the guidelines presented in Appendix A to update Article 3.6.5 of the *LRFD Bridge Design Specifications*, and the AASHTO TCRS may use the guidelines in Appendix B to update the identified sections of the RDG. These AASHTO documents are expected to be used in turn to update state bridge design and roadway design manuals and policies.

6.3 Impediments

One possible impediment to successful implementation could be the mindset of designers, which would need to shift from the current warrant-based policies to risk-based guidelines. There is a general movement toward risk-based evaluation processes that will help implementation, but there is still significant inertia with respect to methods of assessing pier protection.

6.4 Leadership

The leadership of the AASHTO COBS and TCRS will be essential to the implementation of this research by the states in their bridge and roadway design policies.

6.5 Activities

Continued presentations of these research products at AASHTO COBS, AASHTO COD TCRS, and Transportation Research Board meetings is suggested to inform these AASHTO groups and the profession on the availability of these new guidelines. Regional workshops may be considered to provide further background and target DOT personnel and consultants who will be implementing designs with these guidelines in state bridge design and roadway design manuals. Finally, after use of the guidelines, a summary of

pilot projects may be considered at an upcoming technical meeting to demonstrate the use of the guidelines by early adopters.

6.6 Criteria

This project will have been successful if the guidelines included in Appendix A and Appendix B are incorporated

into the *LRFD Bridge Design Specifications* and RDG and, subsequently, into the design and evaluation procedures of the states.

This implementation plan will result in improved pier protection guidelines that better target scarce funding toward the most effective countermeasures and most at-risk structures and drivers such that the safety of the motoring public is enhanced.

CHAPTER 7

Conclusion

The preceding chapters have presented bridge pier protection guidelines proposed for inclusion in both the *AASHTO LRFD Bridge Design Specifications* and the RDG. Procedures, background regarding the development of those procedures, example problems, and comparisons to RSAPv3 have been presented.

In the LRFD Bridge Design pier protection procedures, the user proceeds by looking up site-specific values in four tables and then inserting these values into a short calculation to determine the annual frequency of bridge collapse. If that value is less than 0.001 for a typical bridge or 0.0001 for a critical bridge, the pier system need not be shielded. These acceptance criteria values can be modified by AASHTO or adopting states should they want to make the criteria either more or less conservative.

The proposed LRFD pier protection guidelines describe what types of pier systems need to be evaluated for shielding and also provide lateral capacity suggestions. If a shielding barrier is required, it must be a MASH crash-tested TL-5 rigid concrete barrier positioned on the site according to RDG Section 5.6.4. Additionally, a minimum 60-ft TL-5 rigid concrete barrier should be provided in advance of the leading

pier component. Reference has been made to the RDG to ensure conflict between publications is not created. The 60-ft minimum is suggested to ensure that, regardless of how the length-of-need calculations are presented in the RDG in the future, the LRFD will include the minimum barrier necessary to redirect a heavy vehicle.

Similarly, for the passenger-vehicle occupant protection procedures, the user proceeds by looking up site-specific values in three tables, then uses those values in a short calculation to determine the annual number of severe and fatal injury crashes. If that value is less than 0.0001 severe or fatal injury crashes per year, then the pier system need not be shielded for occupant protection. These criteria can be modified by AASHTO or adopting states should they want to make the criteria either more or less conservative. If a shielding barrier is required for passenger-vehicle occupant protection, a MASH crash-tested TL-3 w-beam guardrail positioned on the site according to RDG Section 5.6.4 is suggested.

Four example problems were presented that illustrate the application of both the LRFD and RDG procedures and compare the results to RSAPv3 simulations. The results of the procedures compare closely with the RSAPv3 estimates.

References

- AASHTO 1977. American Association of State Highway and Transportation Officials, “Guide for Selecting, Locating, and Designing Traffic Barriers,” Washington, D.C., 1977.
- AASHTO 1989a. Technical Committee for Roadside Safety, *AASHTO Roadside Design Guide*, American Association of State Highway and Transportation Officials, Washington, D.C., 1989.
- AASHTO 1989b. AASHTO, “Guide Specifications for Bridge Railings,” American Association of State Highway and Transportation Officials, Washington, D.C., 1989.
- AASHTO 1992. AASHTO, *Standard Specifications for Highway Bridges*, American Association of State Highway and Transportation Officials, Washington, D.C., 1992.
- AASHTO 1994a. Task Force 13, “SBC01a-c” AASHTO-ARTBA-AGC Joint Committee Subcommittee on New Highway Materials Task Force 13 Report, <http://guides.roadsafellc.com/>, accessed February 10, 2016, dated 1994.
- AASHTO 1994b. AASHTO, *AASHTO LRFD Bridge Design Specifications*, 1st Edition. American Association of State Highway and Transportation Officials, Washington, D.C., 1994.
- AASHTO 1998. AASHTO, *AASHTO LRFD Bridge Design Specifications*, 2nd Edition. American Association of State Highway and Transportation Officials, Washington, D.C., 1998.
- AASHTO 2002a. Task Force for Roadside Safety, *Roadside Design Guide*, American Association of State Highway and Transportation Officials, Washington, D.C., 2002.
- AASHTO 2002b. AASHTO, *Standard Specifications for Highway Bridges*, 17th Edition. American Association of State Highway and Transportation Officials, Washington, D.C., 2002.
- AASHTO 2006. Task Force for Roadside Safety, *Roadside Design Guide*, 3rd Edition, American Association of State Highway and Transportation Officials, Washington D.C., 2006.
- AASHTO 2007. AASHTO, *AASHTO LRFD Bridge Design Specifications*, 4th Edition. American Association of State Highway and Transportation Officials, Washington, D.C., 2007.
- AASHTO 2009. Technical Committee for Roadside Safety, *Manual for Assessing Safety Hardware*, American Association of State Highway and Transportation Officials, Washington, D.C., 2009.
- AASHTO 2010. AASHTO, *AASHTO LRFD Bridge Design Specifications*, 5th Edition. American Association of State Highway and Transportation Officials, Washington, D.C., 2010.
- AASHTO 2011. Technical Committee for Roadside Safety, *Roadside Design Guide*, American Association of State Highway and Transportation Officials, Washington, D.C., 2011.
- AASHTO 2012. AASHTO, *AASHTO LRFD Bridge Design Specifications*, 6th Edition. American Association of State Highway and Transportation Officials, Washington, D.C., 2012.
- AASHTO 2016. AASHTO, Technical Committee for Roadside Safety, *Manual for Assessing Safety Hardware*, 2nd Edition, American Association of State Highway and Transportation Officials, Washington, D.C., 2016.
- AASHTO 2017. AASHTO, *AASHTO LRFD Bridge Design Specifications*, 8th Edition, American Association of State Highway and Transportation Officials, Washington, D.C., 2017.
- Alberson 1996. Alberson, D.C., R. A. Zimmer, and W. L. Menges, *NCHRP Report 350: Compliance Test 5-12 of the 1.07-m Vertical Wall Bridge Railing*, Report No. FHWA-RD-96-199, Office of Safety and Traffic Operations R&D, Federal Highway Administration, McLean, Virginia, May 1996.
- Blakley 2012. Derrick Blakley, “A Look at Recent Megabus Problems: Coincidence or Pattern?” CBS Chicago, August 9, 2012, <http://chicago.cbslocal.com/2012/08/09/a-look-at-recent-megabus-problems-coincidence-or-pattern>.
- Blincoe 2002. L. Blincoe, A. Seay, E. Zaloshnja, T. Miller, E. Romano, S. Luchter, and R. Spicer, “The Economic Impact of Motor Vehicle Crashes, 2000,” National Highway Traffic Safety Administration, Report No. DOT HS 809 446, Washington, D.C., 2002.
- Bullard 2010. Bullard, D. L., Bligh, R. P., Menges, W. L., “MASH TL-4 Testing and Evaluation of the New Jersey Safety Shape Bridge Rail,” National Cooperative Highway Research Program, TTI-RF Project 476460, 2010.
- Buth 1982. Butth, C. E., Campise, W. L., “Full-Scale Crash Tests of High-Performance Median Barrier,” Federal Highway Administration and the New Jersey Turnpike Authority, Contract DOT-FH-11-9485 (prepared by Texas Transportation Institute, College Station, Texas), 1982.
- Buth 1989. Butth, C. E., Kaderka, D. L., “Evaluation of L. B. Foster Precast Concrete Bolt-Down Barrier System,” Test Report 7118-1, Texas Transportation Institute, College Station, Texas, 1989.
- Buth 1993a. Butth, C. E., Hirsch, T. J., Menges, W. L., “Volume I – Testing of New Bridge Rail and Transition Designs,” Federal Highway Administration, Washington, D.C., (prepared by Texas Transportation Institute, College Station, Texas), 1993.
- Buth 1993b. Butth, C. E., T. J. Hirsch, and W. L. Menges, “Testing of New Bridge Rail and Transition Designs,” Report No. FHWA-RD-93-068, Vol. XI Appendix J: 42-in. (1.07-m) F-Shape Bridge Railing, Turner-Fairbank Highway Research Center, Federal Highway Administration, McLean, Virginia, 1993.

- Buth 2010. Buth, C. E., W. F. Williams, M. S. Brackin, D. Lord, S. R. Geedipally, and A. Y. Abu-Odeh, "Analysis of Large Truck Collisions with Bridge Piers: Phase 1. Report of Guidelines for Designing Bridge Piers and Abutments for Vehicle Collisions," Research Report. Texas Transportation Institute, College Station, TX, <http://ntl.bts.gov/lib/33000/33100/33107/9-4973-1.pdf>, 2010.
- Buth 2011. Buth, C. E., W. F. Williams, M. S. Brackin, D. Lord, S. R. Geedipally, and A. Y. Abu-Odeh, "Collision Loads on Bridge Piers: Phase 2. Report of Guidelines for Designing Bridge Piers and Abutments for Vehicle Collisions," Research Report. Texas Transportation Institute, College Station, TX, <http://texashistory.unt.edu/ark:/67531/metaph303536/m1/3>, 2011.
- Campise 1985. Campise, W. L. and C. E. Buth, "Performance Limits of Longitudinal Barrier Systems, Volume III – Appendix B: Details of Full-Scale Crash Tests on Longitudinal Barriers," Federal Highway Administration, U.S. Department of Transportation, Washington, D.C. (prepared by Texas Transportation Institute, College Station, Texas), May 1985.
- Carrigan 2014. C. E. Carrigan, M. H. Ray and T. O. Johnson, *Transportation Research Record 2437: Understanding Heavy Vehicle Encroachment Frequency*, Transportation Research Board of the National Academies, Washington, D.C., 2014.
- Carrigan 2016. C. E. Carrigan and M. H. Ray, "Practitioner's Guide to the Analysis of In-Service Performance Evaluation Data," TRB 95th Annual Meeting Compendium of Papers, Transportation Research Board, Washington, D.C., 2016.
- Carrigan 2017. Carrigan, C. E. and M. H. Ray, NCHRP Project 17-54, "Consideration of Roadside Features in the *Highway Safety Manual*," Roadsafe LLC, Canton, ME, (in progress).
- Cooper 1980. Cooper, P., Analysis of Roadside Encroachments—Single Vehicle Run-Off-Road Accident Data Analysis for Five Provinces, Interim Report, B.C. Research Council, Vancouver, British Columbia, Canada., 1980.
- Dekelbab 2017. Dekelbab, W., Hedges, C., and Sundstrom, L. "Active Implementation at the National Cooperative Highway Research Program," *TR News*, Number 310, July–August 2017, <http://onlinepubs.trb.org/onlinepubs/trnews/trnews310.pdf>.
- Dobrovoly 2017. Dobrovoly, C. S., N. Schulz, S. Moran, T. Skinner, R. Bligh, W. Williams, NCHRP Project 20-07/Task 395, "MASH Equivalency of NCHRP Report 350-Approved Bridge Railings," contractor's final report, <http://apps.trb.org/cmsfeed/trbnetprojectdisplay.asp?projectid=4214>, November 2017.
- El-Tawil 2004. El-Tawil, S., "Vehicle Collision with Bridge Piers," FDOT Contract BC-355-6, University of Michigan, April 1, 2004, http://www.dot.state.fl.us/structures/structuresresearchcenter/Final%20Reports/BC355_06.pdf, accessed November 7, 2012.
- FDOT 2013a. Florida Department of Transportation Pier Protection Barrier, Index No. 411, revision dated January 1, 2012, <http://www.dot.state.fl.us/rddesign/DS/13/IDx/00411.pdf>, accessed April 12, 2013.
- FDOT 2013b. Florida Department of Transportation Concrete Barrier Wall, index No. 410, Revision Undated, <http://www.dot.state.fl.us/rddesign/DS/13/IDx/00410.pdf>, accessed April 12, 2013.
- FHWA 2013. Federal Highway Administration, U.S. Department of Transportation, "State Department of Transportation LRFD Implementation Plan Initial Draft," <http://www.fhwa.dot.gov/bridge/lrfd/plan.cfm> accessed January 2013.
- FHWA 2014a. Federal Highway Administration, "VTRIS W-Table web site," <https://fhwaapps.fhwa.dot.gov/vtris-wp/about.aspx>, accessed March 10, 2014.
- FHWA 2014b. Federal Highway Administration, "W-Beam Guardrail," http://safety.fhwa.dot.gov/roadway_dept/policy_guide/road_hardware/ctrmeasures/wbeam/ accessed January 18, 2016, dated October 15, 2014.
- Fitzpatrick 1999. Fitzpatrick, M. S., K. L. Hancock, and M. H. Ray, "Videolog Assessment of the Vehicle Collision Frequency with Concrete Median Barriers on an Urban Highway in Connecticut," Roadside Safety Features, *Transportation Research Record: Journal of the Transportation Research Board*, No. 1690, TRB, National Research Council, Washington, D.C., 1999.
- Ghosn 2014. Ghosn, M., J. Yang, D. Beal, and B. Sivakumar. *NCHRP Report 776: Bridge System Safety and Redundancy*. Transportation Research Board of the National Academies, Washington, D.C., 2014.
- Hammond 2008. Hammond, P. and J. Batiste, "Cable Median Barrier: Reassessment and Recommendations Update." Washington State Department of Transportation, Olympia, WA, 2008.
- Hardwick 2012. Hardwick, R., "WB-I-30 Closed at Dolphin in Dallas," June 11, 2012, <https://www.nbcdfw.com/news/local/I-30-Closed-At-Dolphin-Rd—158372185.html>.
- Harwood 2003. Harwood, D. W., D. J., Torbic, K. R., Richard, W. D., Glauz, and L. Eleferiadou, *NCHRP Report 505: Review of Truck Characteristics as Factors in Roadway Design*, Transportation Research Board of the National Academies, Washington, D.C., 2003.
- HCM 2016. *Highway Capacity Manual: A Guide for Multimodal Mobility Analysis*, 6th ed. Transportation Research Board, Washington, D.C., 2016.
- Hirsch 1984. Hirsch, T. J., W. L. Fairbanks, and C. E. Buth, "Concrete Safety Shape with Metal Rail on Top to Redirect 80,000 lb Trucks," Report No. FHWA/TX-83, Texas State Department of Highways and Public Transportation, Austin, Texas, 1984.
- Hirsch 1985. Hirsch, T. J., and Fairbanks, W. L., Bridge Rail to Contain and Redirect 80,000-lb Tank Trucks, Transportation Research Record No. 1024, Transportation Research Board, National Research Council, Washington, D.C., 1985.
- IDOT 2013. *Iowa Department of Transportation Design Manual*, Warrants for Specific Obstacles, <http://www.iowadot.gov/design/dmanual/08A-04.pdf>, accessed April 23, 2013, dated April 17, 2013.
- Liu 2001. Liu, W. D., A. Neuenhoffer, M. Ghosn, and F. Moses, *NCHRP Report 458: Redundancy in Highway Bridge Substructures*, TRB, National Research Council, Washington, D.C., 2001.
- Mak 1980. Mak, K. K. and R. L. Mason, Accident Analysis – Breakaway and Nonbreakaway Poles Including Sign and Light Standards Along Highways, Volume 1: Executive Summary, U.S. Department of Transportation, National Highway Traffic Safety Administration, Federal Highway Administration, Washington, D.C., August 1980.
- Mak 1990. Mak, K. K., W. L. Campise, "Test and Evaluation of Ontario 'Tall Wall' Barrier with an 80,000-Pound Tractor-Trailer," Project No. 4221-9089-534, Ontario Ministry of Transportation, Ontario, September 1990.
- Mak 2010. Mak, K. K., D. L. Sicking, and B. A. Coon, *NCHRP Report 665: Identification of Vehicular Impact Conditions Associated with Serious Ran-off-Road Crashes*, Transportation Research Board of the National Academies, Washington, D.C., 2010.
- McDonald 2009. McDonald, T. J., I. Nlenanya, and Z. Hans, "Analysis of Safety Benefits for Shielding of Bridge Piers," Institute for Transportation, Iowa State University, InTrans Project 08-322, <http://www.intrans.iastate.edu/reports/bridge-pier-shielding.pdf>, accessed November 12, 2012, dated June 2009.
- Michie 1981. Michie, J. D., NCHRP Report 230: Recommended Procedures for the Safety Performance Evaluation of Highway Appurtenances, TRB, National Research Council, Washington, D.C., 1981.
- Miele 2010. Miele, C., C. Plaxico, D. Stephens, and S. Simunovic, Enhanced Finite Element Analysis Crash Model of Tractor-Trailers

- (Phase C), National Transportation Research Center, Inc., Knoxville, TN, September 2010.
- Miller 1988. Miller, T. R., C. P. Brinkman, and S. Luchter; “Crash Costs and Safety Investment,” Proceedings of the 32nd Annual Conference, Association for the Advancement of Automotive Medicine, Des Plaines, IL, 1988.
- MNDOT 2003. Minnesota Department of Transportation, “Quick Response Re-opens I-90 after Heavy Truck Buckles Bridge Pier,” Mn/DOT Newsline, www.newsline.dot.state.mn.us/archive/03/jun/11.html, June 11, 2003.
- MNDOT 2007a. Minnesota Department of Transportation, Bridge Office Memo (2007-01) to Bridge Design Engineers, from K. Western, <http://www.dot.state.mn.us/bridge/manuals/LRFD/pdf/memo/Memo2007-01.pdf>, accessed October 16, 2013, dated July 23, 2007.
- MNDOT 2007b. “Memo to Designers (2007-01): Bridge Office Substructure Protection Policy,” Memorandum, Minnesota Department of Transportation, Oakdale, MN, July 23, 2007.
- MNDOT 2013. *Minnesota DOT Bridge Design Manual*, <http://www.dot.state.mn.us/bridge/manuals/LRFD/pdf/section11-6302010.pdf>, accessed October 15, 2013, dated 2013.
- MNDOT 2016. *Bridge Design Manual*, Minnesota Department of Transportation, <http://www.dot.state.mn.us/bridge/pdf/lrfdmanual/section11.pdf>, 2016.
- MwRSF 2010. “Evaluation of Rollover and Injury Rates for Vertical and Safety Shape Bridge Rails in Iowa,” ongoing study.
- Nilsson 1981. Nilsson, G., “The Effect of Speed Limits on Traffic Accidents in Sweden,” Proceedings of the International Symposium on the Effects of Speed Limits on Traffic Accidents and Transport Energy Use, Organization for Economic Cooperation and Development, 1981.
- NJDOT 2012. New Jersey Department of Transportation, “Roadway Information and Traffic Monitoring System Program,” Vehicle Classification, <http://www.state.nj.us/transportation/refdata/roadway/pdf/TravelActivityVehTypeByRegion.pdf>, Accessed online March 10, 2014.
- NJDOT 2013. *New Jersey Department of Transportation Roadside Design Manual*, <http://www.state.nj.us/transportation/eng/documents/RDM/sec8.shtm>, accessed April 10, 2013, dated 2013.
- NTSB 1973. “Greyhound Bus Collision with Concrete Overpass Support Column on I-880, San Juan Overpass, Sacramento, California,” National Transportation Safety Board, Washington, D.C., November 3, 1973.
- NTSB 1993. “Tractor-Semitrailer Collision with Bridge Columns on Interstate 65, Evergreen, Alabama,” National Transportation Safety Board, Washington, D.C., May 19, 1993.
- NTSB 2011. NTSB, Safety Recommendation H-11-13 through 17, National Transportation Safety Board, Washington, D.C., <https://www.nts.gov/safety/safety-recs/reclatters/H-11-013-017.pdf>, accessed September 2018, dated September 2, 2011.
- NYDOT 2013. New York State Department of Transportation, *Highway Design Manual*, Chapter 10, https://www.dot.ny.gov/divisions/engineering/design/dqab/hdm/hdm-repository/rev_64_HDM_Ch10.pdf, accessed April 23, 2013, dated 2013.
- ODOT 2007. *Bridge Design Manual*, Ohio Department of Transportation, (http://www.dot.state.oh.us/Divisions/Engineering/Structures/standard/Bridges/BDM/BDM2007_01-17-14.pdf, http://www.dot.state.oh.us/Divisions/Engineering/Structures/standard/Bridges/BDM/BDM2007_01-18-13.pdf, accessed April 23, 2013, dated 2007.
- ODOT 2013. *Ohio Department of Transportation Bridge Design Manual*, Section 900, http://www.dot.state.oh.us/Divisions/Engineering/Structures/standard/Bridges/BDM/BDM2007_01-18-13.pdf, accessed April 23, 2013, dated 2013.
- ODOT 2014. Piers. <https://www.dot.state.oh.us/Divisions/Engineering/Structures/bridge%20operations%20and%20maintenance/PreventiveMaintenanceManual/BPMM/piers/piers.htm>.
- R Core Team 2016. R Core Team. R: A Language and Environment for Statistical Computing. R Foundation for Statistical Computing, Vienna, Austria. URL <https://www.R-project.org/>, 2016.
- Ray 2003. Ray, M. H., J. Weir, and J. Hopp, *NCHRP Report 490: In-Service Performance of Traffic Barriers*, Transportation Research Board of the National Academies, Washington, D.C., 2003.
- Ray 2012. Ray, M. H., C. E. Carrigan, C. A. Plaxico, and T. O. Johnson, *Engineer’s Manual: Roadside Safety Analysis Program (RSAP) Update*, <http://rsap.roadsafellc.com/RSAPv3EngineersManual.pdf>, Roadsafe LLC, Canton, ME, December 2012.
- Ray 2014a. Ray, M. H., C. E. Carrigan, and C. A. Plaxico, “Method for Modeling Crash Severity with Observable Crash Data.” *Transportation Research Record: Journal of the Transportation Research Board*, No 2437, Transportation Research Board of the National Academies, pp. 1–9, Washington, D.C., 2014.
- Ray 2014b. Ray M. H. and C. E. Carrigan, NCHRP Project 22-12(03), “Recommended Guidelines for the Selection of Test Levels 2 Through 5 Bridge Rails,” RoadSafe LLC, Canton, ME, <https://apps.trb.org/cmsfeed/TRBNetProjectDisplay.asp?ProjectID=2899>, February 2014.
- Ray 2016. Ray, M. H., C. A. Plaxico, and C. E. Carrigan, RSAPv3, release 160909BP: Originally documented in *Roadside Safety Analysis Program (RSAP) Engineer’s Manual*, Roadsafe LLC, rsap.roadsafellc.com, accessed October 25, 2012.
- Ray 2017a. Ray, M. H., C. E. Carrigan, and C. A. Plaxico, *Transportation Research Circular E-C220: Heavy Vehicle Encroachment Trajectories*, pp. 820–830, Transportation Research Board, Washington, D.C., 2017. <http://onlinepubs.trb.org/onlinepubs/circulars/ec220.pdf>.
- Ray 2017b. Ray, M. H. and C. E. Carrigan, NCHRP Project 15-65, “Development of Safety Performance Based Guidelines for the Roadside Design Guide,” Transportation Research Board, Washington, D.C., 2017. <http://apps.trb.org/cmsfeed/TRBNetProjectDisplay.asp?ProjectID=4198>.
- Rosenbaugh 2007. Rosenbaugh, S. K., D. L. Sicking, and R. K. Faller, “Development of a TL-5 Vertical Faced Concrete Median Barrier Incorporating Head Ejection Criteria,” Report No. TRP-03-194-07, Midwest Roadside Safety Facility, Lincoln, Nebraska, 2007.
- Rosenbaugh 2016. Rosenbaugh, S. K., J. D. Schmidt, E. M. Regier, and R. K. Faller, “Development of the Manitoba Constrained-Width, Tall Wall Barrier,” Draft Technical Report, Research Project No. 2015-17-TE, performed by the Midwest Roadside Safety Facility, Lincoln, Nebraska (9/2/2016).
- Ross 1993. Ross, H. E., D. L. Sicking, R. A. Zimmer, and J. D. Michie. *NCHRP Report 350: Recommended Procedures for the Safety Performance Evaluation of Highway Features*. TRB, National Research Council, Washington, D.C., 1993.
- SDDOT 2013. *South Dakota Department of Transportation Roadway Design Manual*, Chapter 10, Roadside Safety, www.sddot.com/business/design/forms/roaddesign, accessed April 23, 2013, dated 2013.
- Sheikh 2011. Sheikh, N. M., R. P. Bligh, and W. L. Menges, “Determination of Minimum Height and Lateral Design Load for MASH Test Level 4 Bridge Rails,” Texas Department of Transportation, Report No. FHWA/TX-12/9-1002-5, December 2011.
- Sheikh 2017. Sheikh, N., R. Carhuayano, M. Zdenek, and D. Riggs, “MASH Test Level 5 Steel Bridge Rail for Suspension Bridges,” Paper No. 17-06870, presented at the 95th Annual Meeting of the Transportation Research Board, Washington, D.C., 2017.

- Sicking 2009. Sicking, D. L., K. A. Lechtenberg, and S. Peterson, *NCHRP Report 638: Guidelines for Guardrail Implementation*, Transportation Research Board of the National Academies, Washington, D.C., 2009.
- Stone 2012. Stone, J., “Megabus Crashes into Bridge on I-55 Between St. Louis and Chicago, More Than 20 Emergency Vehicles on the Scene,” *International Business Times*, August 2, 2012, http://s1.ibtimes.com/sites/www.ibtimes.com/files/styles/v2_article_large/public/2012/08/02/293060-megabus-crash-via-kmovnewsfeed.jpg.
- TXDOT 2013. *Bridge Design Manual*, Texas Department of Transportation, pp. 4–12, <http://onlinemanuals.txdot.gov/txdotmanuals/lrf/lrf.pdf>.
- Venables 2002. Venables, W. N. and B. D. Ripley, *Modern Applied Statistics with S*. Fourth Edition. Springer, New York. ISBN 0-387-95457-0, 2002.
- WIDOT 2013a. *Wisconsin Department of Transportation Bridge Design Manual*, Chapter 13, http://on.dot.wi.gov/dtid_bos/extranet/structures/LRFD/BridgeManual/Ch-13.pdf, accessed April 11, 2013, dated 2013.
- WIDOT 2013b. *Facilities Development Manual*, Chapter 11: Design, Section 35: Structures, Wisconsin Department of Transportation, <http://roadwaystandards.dot.wi.gov/standards/fdm/11-35.pdf>, accessed April 11, 2013, dated 2013.
- Williams 2017. Williams, W. F., J. Ries, R. Bligh, and W. Odell, “Design and Full-Scale Testing of Aesthetic TXDOT Type T224 Bridge Rail for MASH TL-5 Application,” Paper No. 17-06469, presented at the 95th Annual Meeting of the Transportation Research Board, Washington, D.C., 2017.
- WLWT 2008. WLWT5 News, “Interstate Overpass Crash Could Cause Months of Detours,” www.wlwt.com/article/interstate-overpass-crash-could-cause-months-of-detours/3498673, May 21, 2008.
-

Appendices

The following appendices can be found at the NCHRP Project 12-90 web page (<https://apps.trb.org/cmsfeed/TRBNetProjectDisplay.asp?ProjectID=3170>).

Appendix A: Proposed LRFD Bridge Design Pier Protection Specifications

Appendix B: Proposed RDG Occupant Protection Guidelines

Appendix C: Survey of Practice

Appendix D: Lateral Impact Loads on Pier Columns

Appendix E: Nominal Resistance to Lateral Impact Loads on Pier Columns

Appendix F: Heavy-Vehicle Traffic Mix and Properties

Abbreviations and acronyms used without definitions in TRB publications:

A4A	Airlines for America
AAAAE	American Association of Airport Executives
AASHO	American Association of State Highway Officials
AASHTO	American Association of State Highway and Transportation Officials
ACI-NA	Airports Council International-North America
ACRP	Airport Cooperative Research Program
ADA	Americans with Disabilities Act
APTA	American Public Transportation Association
ASCE	American Society of Civil Engineers
ASME	American Society of Mechanical Engineers
ASTM	American Society for Testing and Materials
ATA	American Trucking Associations
CTAA	Community Transportation Association of America
CTBSSP	Commercial Truck and Bus Safety Synthesis Program
DHS	Department of Homeland Security
DOE	Department of Energy
EPA	Environmental Protection Agency
FAA	Federal Aviation Administration
FAST	Fixing America's Surface Transportation Act (2015)
FHWA	Federal Highway Administration
FMCSA	Federal Motor Carrier Safety Administration
FRA	Federal Railroad Administration
FTA	Federal Transit Administration
HMCRP	Hazardous Materials Cooperative Research Program
IEEE	Institute of Electrical and Electronics Engineers
ISTEA	Intermodal Surface Transportation Efficiency Act of 1991
ITE	Institute of Transportation Engineers
MAP-21	Moving Ahead for Progress in the 21st Century Act (2012)
NASA	National Aeronautics and Space Administration
NASAO	National Association of State Aviation Officials
NCFRP	National Cooperative Freight Research Program
NCHRP	National Cooperative Highway Research Program
NHTSA	National Highway Traffic Safety Administration
NTSB	National Transportation Safety Board
PHMSA	Pipeline and Hazardous Materials Safety Administration
RITA	Research and Innovative Technology Administration
SAE	Society of Automotive Engineers
SAFETEA-LU	Safe, Accountable, Flexible, Efficient Transportation Equity Act: A Legacy for Users (2005)
TCRP	Transit Cooperative Research Program
TDC	Transit Development Corporation
TEA-21	Transportation Equity Act for the 21st Century (1998)
TRB	Transportation Research Board
TSA	Transportation Security Administration
U.S.DOT	United States Department of Transportation

TRANSPORTATION RESEARCH BOARD
500 Fifth Street, NW
Washington, DC 20001

ADDRESS SERVICE REQUESTED

The National Academies of
SCIENCES • ENGINEERING • MEDICINE

The nation turns to the National Academies of Sciences, Engineering, and Medicine for independent, objective advice on issues that affect people's lives worldwide.

www.national-academies.org

ISBN 978-0-309-47995-0



NON-PROFIT ORG.
U.S. POSTAGE
PAID
COLUMBIA, MD
PERMIT NO. 88